PRODUCTION AND CHARACTERIZATION OF

MONOCLONAL ANTIBODIES AGAINST HUMAN LDL

AND THE ROLE OF MM-LDL IN ATHEROSCLEROSIS

PROGRESSION

Kanokwan Lowhalidanon

A Thesis submitted in Partial Fulfillment of the Requirements for the

Degree of Doctor of Philosophy in Biochemistry

Suranaree University of Technology

Academic Year 2018

การผลิตและคุณลักษณะของโมโนโคลนอลแอนติบอดีต่อ LDL ของมนุษย์ และบทบาทของ mm-LDL ต่อกลไกการเกิดภาวะหลอดเลือดแดงแข็ง

นางสาวกนกวรรณ เลาหลิดานนท์

วิทยานิพนธ์นี้เป็นส่วนหนึ่งของการศึกษาตามหลักสูตรปริญญาวิทยาศาสตรดุษฎีบัณฑิต
สาขาวิชาชีวเคมี
มหาวิทยาลัยเทคโนโลยีสุรนารี
ปีการศึกษา 2561

PRODUCTION AND CHARACTERIZATION OF MONOCLONAL ANTIBODIES AGAINST HUMAN LDL AND THE ROLE OF MM-LDL IN ATHEROSCLEROSIS PROGRESSION

Suranaree University of Technology has approved this thesis submitted in partial fulfillment of the requirements for the Degree of Doctor of Philosophy.

Thesis Examining Committee

_____

(Asst. Prof. Dr. Chutima Talabnin)

Chairperson

_____

(Asst. Prof. Dr. Panida Khunkaewla)

Member (Thesis Advisor)

_____

(Asst. Prof. Dr. Saengduen Moonsom)

Member

_____

(Assoc. Prof. Dr. Griangsak Eumkeb)

Member

_____
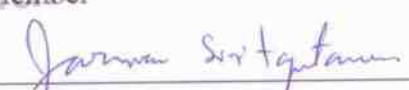
(Assoc. Prof. Dr. Jaruwan Siritapetawee)

Member

_____   _____

(Assoc. Prof. Flt. Lt. Dr. Kontorn Chamniprasart)   (Assoc. Prof. Dr. Worawat Meevasana)

Vice Rector for Academic Affairs   Dean of Institute of Science

and Internationalization

กนกวรรณ เลาหลิดานนท์ : การผลิตและคุณลักษณะของโมโนโคลนอลแอนติบอดีต่อ LDL ของมนุษย์ และบทบาทของ mm-LDL ต่อกลไกการเกิดภาวะหลอดเลือดแดงแข็ง (PRODUCTION AND CHARACTERIZATION OF MONOCLONAL ANTIBODIES AGAINST HUMAN LDL AND THE ROLE OF MM-LDL IN ATHEROSCLEROSIS PROGRESSION). อาจารย์ที่ปรึกษา : ผู้ช่วยศาสตราจารย์ ดร.พนิดา ขันแก้วหล้า, 180 หน้า.

ภาวะหลอดเลือดแดงแข็ง LDL mm-LDL โมโนโคลนอลแอนติบอดี การตรวจวัดปริมาณ LDL ใน น้ำเลือดแบบตรง เมทริกเมทัลโลโปรติเนส โฟมเซลล์

ระดับของ LDL ที่สูงเป็นหนึ่งในปัจจัยเสี่ยงหลักของพยาธิสภาพการเกิดภาวะหลอดเลือด แดงแข็ง วิธีทั่วไปที่ใช้ในการตรวจวัดระดับ LDL ในน้ำเลือดในโรงพยาบาล คือ การคำนวณจาก สมการของ Friedewald อย่างไรก็ตาม วิธีนี้มีข้อจำกัดโดยขึ้นกับระดับของไตรกลีเซอไรด์ในกระแส เลือด ดังนั้น เทคนิคจำนวนมากจึงถูกพัฒนาขึ้นเพื่อแก้ปัญหาข้อจำกัดนี้ การศึกษานี้ โมโนโคลนอล แอนติบอดี ที่จำเพาะต่อ LDL ของมนุษย์ จำนวน 7 โคลน ถูกผลิตขึ้นโดยเทคนิคไฮบริโดมา มาตรฐาน และพบว่าโมโนโคลนอลแอนติบอดีเหล่านี้จับอย่างจำเพาะเจาะจงกับ อะโพลิโพโปรตีน ชนิดบี 100 (apoB-100) ที่ปรากฏบนอนุภาคของ LDL จากโคลนเหล่านี้ โมโนโคลนอลแอนติบอดี 2 โคลน ที่จับกับตำแหน่งบนแอนติเจนที่จำเพาะต่างกัน คือ โคลน hLDL-E8 (IgG$_1$) และ hLDL-2D8 (IgG$_{2b}$) ถูกเลือกสำหรับการพัฒนาเทคนิคตรวจวัดระดับ LDL แบบตรงบนพื้นฐานของเทคนิค แซนด์วิช ELISA เนื่องจาก apoB-100 ไม่ได้ปรากฏบนอนุภาคของ LDL เพียงอย่างเดียว ดังนั้น LDL จะถูกทำให้ตกตะกอนโดยสารเฮพาริน/ซิเตรต ก่อนการหาปริมาณ เพื่อเปรียบเทียบระดับของ LDL ที่ได้จากเทคนิคที่พัฒนาขึ้น กับระดับของ LDL ที่ได้จากโรงพยาบาล ตัวอย่างน้ำเลือดแบบสุ่ม จำนวน 208 ตัวอย่างจากโรงพยาบาลมหาวิทยาลัยเทคโนโลยีสุรนารีถูกนำมาตรวจสอบหาปริมาณ พบว่า ค่าเฉลี่ยที่ได้จากเทคนิคที่พัฒนาขึ้น คือ 126.6±43.1 มิลลิกรัมต่อเดซิลิตร (ช่วง 90.0 ถึง 258.0 มิลลิกรัมต่อเดซิลิตร) ในขณะที่ค่าเฉลี่ยที่ได้จากโรงพยาบาลมหาวิทยาลัยเทคโนโลยีสุรนารี คือ 123.2±42.3 มิลลิกรัมต่อเดซิลิตร (ช่วง 34.0 ถึง 236.0 มิลลิกรัมต่อเดซิลิตร) การวิเคราะห์การ ถดถอยเชิงเส้นแสดงความเกี่ยวเนื่องสหสัมพันธ์ที่สูงระหว่างเทคนิคที่พัฒนาขึ้นและจาก โรงพยาบาลมหาวิทยาลัยเทคโนโลยีสุรนารี (สัมประสิทธิ์สหสัมพันธ์ = 0.8491 ค่าความน่าจะเป็น <0.0001) เป็นที่น่าสังเกตว่า ระดับของไตรกลีเซอไรด์ไม่มีอิทธิพลต่อการหาปริมาณของ LDL โดย เทคนิคที่พัฒนาขึ้น ดังนั้น เราได้นำเสนอเทคนิคทางเลือกสำหรับตรวจวัดปริมาณ LDL ในน้ำเลือด

แบบตรง โดยใช้โมโนโคลนอลแอนติบอดีที่พัฒนาขึ้นเอง แต่อย่างไรก็ตาม เทคนิคที่ง่ายและ
เหมาะสมสำหรับการทดสอบประจำในห้องปฏิบัติการ จำเป็นที่จะต้องถูกปรับปรุงให้ดีขึ้น

      LDL สามารถถูกออกซิไดซ์อย่างเป็นขั้นตอน LDL ที่ถูกเปลี่ยนแปลงเพียงเล็กน้อย (mm-LDL) เฉพาะส่วนของไขมันที่ถูกออกซิไดซ์ และ LDL ที่ถูกออกซิไดซ์อย่างสมบูรณ์ (ox-LDL) ทั้ง
ส่วนของไขมันและโปรตีนถูกออกซิไดซ์ การศึกษาจำนวนมากรายงานว่า ox-LDL เกี่ยวข้องกับการ
เกิดภาวะหลอดเลือดแดงแข็ง แต่มีการศึกษาเพียงเล็กน้อยที่กล่าวถึงบทบาทของ mm-LDL ใน
กระบวนการนี้ ในการศึกษานี้ ได้ศึกษาผลกระทบของ LDL ต่างชนิดกันต่อการแสดงออกของเมท
ริกเมทัลโลโปรติเนส (MMP) โดยใช้แมโครฟาจที่ได้จากการกระตุ้นเซลล์ชนิด THP1 และ U937
ด้วย phorbal-12-myristate 13-acetate (PMA) โฟมเซลล์ถูกเหนี่ยวนำให้เกิดขึ้นโดยการเลี้ยงแมโคร
ฟาจร่วมกันระหว่าง LDL หรือ mm-LDL หรือ ox-LDL ที่ความเข้มข้นต่างๆ หยดไขมันภายใน
เซลล์ของโฟมเซลล์ถูกทำให้มองเห็นโดยการย้อมสีชนิด Oil Red O และดูใต้กล้องจุลทรรศน์ชนิด
หัวกลับ การวิเคราะห์ MMPs โดยใช้เทคนิคการตรวจสารพันธุกรรมด้วยเครื่องตรวจสารพันธุกรรม
ในสภาพจริง แสดงให้เห็นว่าการแสดงออกของ MMP-1, 2, 9, 12, 14, และ 16 ในระดับ mRNA ถูก
ทำให้เพิ่มขึ้นเมื่อระดับของการออกซิเดชันของ LDL เพิ่มมากขึ้น การวิเคราะห์ด้วยเทคนิคเจลาติน
ไซโมกราฟี แสดงให้เห็นว่า รูปออกฤทธิ์ของ MMP-2 จะเพิ่มขึ้น เมื่อระดับของการออกซิเดชันของ
LDL เพิ่มมากขึ้น ในขณะที่การออกฤทธิ์ของ MMP-9 จะลดลงเมื่อระยะเวลาในการบ่มระหว่าง
LDL กับแมโครฟาจเพิ่มมากขึ้น ผลการทดลองในเบื้องต้นนี้บ่งชี้ให้เห็นว่า mm-LDL สามารถ
เหนี่ยวนำการเกิดโฟมเซลล์และการแสดงออกของ MMPs แม้ว่าผลที่เกิดขึ้นจะไม่ชัดเจนเท่า LDL
ที่ถูกออกซิไดซ์อย่างสมบูรณ์

สาขาวิชาเคมี   ลายมือชื่อนักศึกษา _กนกวรรณ เลาหลัคฐานนท์_

ปีการศึกษา 2561   ลายมือชื่ออาจารย์ที่ปรึกษา

KANOKWAN LOWHALIDANON : PRODUCTION AND
CHARACTERIZATION OF MONOCLONAL ANTIBODIES AGAINST
HUMAN LDL AND THE ROLE OF MM-LDL IN ATHEROSCLEROSIS
PROGRESSION. THESIS ADVISOR : ASST. PROF. PANIDA
KHUNKAEWLA, Ph.D. 180 PP.

ATHEROSCLEROSIS, LDL, MM-LDL, MONOCLONAL ANTIBODY, DIRECT
PLASMA LDL MEASUREMENT, MMP, FOAM CELLS

High level of low density lipoprotein (LDL) is one of the major risk factors in
the pathogenesis of atherosclerosis. The most common approach for determination of
plasma LDL level in hospital is Friedewald equation. Nonetheless, some limitations
of this method are found, especially high plasma triglyceride level. Thus several
methods have been developed to overcome these limitations. This study, seven
specific monoclonal antibodies (mAbs) against human LDL were generated by
standard hybridoma technique and specific to apolipoprotein B-100 (apoB-100)
presented on LDL particle. Among these clones, 2 distinct epitope binding mAbs,
hLDL-E8 (IgG_1) and hLDL-2D8 (IgG_{2b}), were selected for developing of direct LDL
measurement using sandwich ELISA. As apoB-100 is not presented only in LDL
particle, therefore the LDL was precipitated by heparin/citrate pH 5.04 prior to
quantification. To compare the LDL level obtained by the developed method and
from the hospital, 208 randomized samples from Suranaree University of Technology
(SUT) hospital were examined. The mean value obtained from the developed method
was 126.6±43.1 mg/dl (range 90.0 to 258.0 mg/dl) while the value obtained from the

SUT hospital was 123.2±42.3 mg/dl (range 34.0 to 236.0 mg/dl). Linear regression analysis showed high correlation among assessment by the developing method and from SUT hospital ($r = 0.8491$, p-value < 0.0001). Notably, triglyceride level has no influence on LDL quantification by the developed method. Thus, we prepared an alternative method for direct plasma LDL measurement using in-house mAbs. Nonetheless, the technique is needed to be improved to suit with routine laboratory test.

LDL can be oxidized in a stepwise manner. Minimally modified low density lipoprotein (mm-LDL), which only lipid part is oxidized and fully oxidized-LDL (ox-LDL) which both lipid and protein parts are oxidized. Several studies reported that the ox-LDL is involved in the atherosclerosis progression but a few studies regarding the role of the mm-LDL on this process has been reported. This study, effect of different LDLs on expression of matrix metalloproteinases (MMPs) was studied using macrophages derived from phorbal-12-myristate 13-acetate (PMA) activated THP1 and U937 cells as the study model. These primary results suggested that foam cells were induced by co-cultivation of the generated macrophages with various concentrations of LDL, or mm-LDL, or ox-LDL. MMPs analysis using RT-PCR revealed that mRNA level of MMP-1, 2, 9, 12, 14, and 16 were increased once the degree of oxidation increased. Gelatin zymography showed that active form of MMP-2 was increased when the oxidation degree was increased whereas MMP-9 activity was decreased when increase the incubation time of LDL and macrophages.

School of Chemistry

Academic Year 2018

Student's signature ___Kanokwan Louhalidanon___

Advisor's signature _____

ACKNOWLEDGEMENTS

Kanokwan Lowhalidanon

CONTENTS

CONTENTS (Continued)

CONTENTS (Continued)

CONTENTS (Continued)

CONTENTS (Continued)

CONTENTS (Continued)

LIST OF TABLES

LIST OF FIGURES

LIST OF FIGURES (Continued)

LIST OF FIGURES (Continued)

LIST OF FIGURES (Continued)

LIST OF FIGURES (Continued)

LIST OF ABBREVIATIONS

Ab	Antibody
ACAT1	Acetyl-CoA Acethyl Transferase 1
Apo	Apolipoprotein
CD	Cluster of differentiation
CHD	Coronary heart disease
CM	Chylomicron
dl	deciliter
DNA	Deoxyribonucleic acid
ELISA	Enzyme-linked immunosorbent assay
ER	Endoplasmic reticulum
g	gram
FBS	Fetal Bovine Serum
h	hour
HAT	Hypoxanthine Aminopterin Thymidine
HDL	High density lipoprotein
HG	Hinge region
HGPRT	Hypoxanthine-guanine phosphoribosyl transferase
HT	Hypoxanthine Thymidine
IDL	Intermediate density lipoprotein
Ig	Immunoglobulin

LIST OF ABBREVIATIONS (Continued)

IL	Interleukin
kDa	kilo Dalton
kg	kilogram
L	liter
LDL	Low density lipoprotein
mAb	monoclonal antibody
MDA	Malondialdehyde
mg	milligram
min	minute
mm-LDL	Minimally modified low density lipoprotein
MMPs	Matrix metalloproteinases
MT-MMPs	Membrane type matrix metalloproteinases
NCEP ATP	The National Cholesterol Education Program Adult Treatment Panel
nm	nanometer
ox-LDL	Fully oxidized low density lipoprotein
pAb	polyclonal antibody
PCR	Polymerase chain reaction
PEG	Polyethyleneglycol
PMA	Phorbol 12-myristate 13-acetate
Pro	Pro-domain
RNA	Ribonucleic acid

LIST OF ABBREVIATIONS (Continued)

ROS   Reactive oxygen species

RT-PCR   Real time polymerase chain reaction

SP   Signal peptide

SRs   Scavenger receptors

TBA   Thiobarbituric acid

TBARS   Thiobarbituric acid reactive substance

TG   Triglyceride

TIMPs   Tissue inhibitor of matrix metalloproteinases

TLR   Toll-like receptor

TM   Transmembrane domain

TNF   Tumor necrosis factor

VLDL   Very low density lipoprotein

CHAPTER I

INTRODUCTION

1.1 Statement and significance of research

Atherosclerosis is one of the leading causes of mortality worldwide. High concentration of low density lipoprotein (LDL) cholesterol is deliberated as one of the major risk factors for the pathogenesis of atherosclerosis that lead to hypertension, coronary heart disease (CHD), stroke, and death by resulting in cholesterol-burdened and activated macrophages, a hallmark of atherosclerotic plaques. The reference method for quantitative estimation of LDL in circulation is β-quantification. Nevertheless, this method requires ultracentrifugation, needs large sample volume, time-consuming, and expensive. Thus, this method does not suit for laboratory routine. Consequently, an inexpensive method and easy approach for estimation of LDL concentration, called Friedewald method, was established and named according to inventor (William T. Friedewald, 1972). Nowadays, this calculation method is widely used by many laboratories throughout the world to determine plasma LDL level.

The Friedewald equation estimates LDL level from measurement of total cholesterol, triglyceride, and high density lipoprotein (HDL) cholesterol. However, if triglyceride level is higher than 400 mg/dl, this calculated concentration of LDL is not accurate. Several studies have tried to modify this formula to overcome this limitation (Richard K. D. Ephraim, 2018). Still, these modifications were complicate and not accurate.

To figure out this limitation, several direct LDL measurement procedures have been developed such as homogenous methods capable of full automation which are different in details and procedures depend on manufacturers. The first objective of this study is to develop the direct plasma or serum LDL measurement method using immunologically-based technique as an alternative method and can be developed for self-evaluation of LDL level in blood samples in the future.

For the study of progression of atherosclerosis, circulating LDL particles invade the arterial wall where they undergo some modifications such as oxidation. The uptake of oxidized-LDL by intimal macrophages via scavenger receptors leads to development of foam cells and atherosclerotic plaque. LDL was considered to be oxidized in the stepwise manner. At the initial phase of oxidation, only lipid part of LDL was oxidized. It is known as minimally modified LDL (mm-LDL). Mm-LDL was also found in the atherosclerotic lesion but the effect to atherosclerosis progression is not fully understood. While at the advanced stages of atherosclerosis, full oxidation of LDL, both lipid and protein parts, was found. It has been reported that during atherosclerotic plaque formation, the extracellular matrixes around the fibrous cap, adjacent core, and shoulder region of atherosclerotic plaque are degraded by proteolytic property of matrix metalloproteinases (MMPs). Several MMPs were found at the atherosclerotic lesions and play an important role on plaque stabilization and destabilization of atherosclerotic progression. However, clear mechanism and the specific type of MMP are not yet revealed. As a consequence, the second objective of this study is to investigate the effect of mm-LDL and fully ox-LDL on expression by PMA-activated macrophages derived foam cells.

1.2 Objectives

1.2.1 To produce and characterize the biochemical properties of mAbs against human LDL

1.2.2 To develop the direct plasma LDL measurement method using our self-generated mAbs against human LDL

1.2.3 To apply our self-generated mAbs against human LDL to distinguish between mm-LDL and ox-LDL

1.2.4 To study the effect of mm-LDL on MMPs expression of macrophage-derived foam cells

1.3 Literature review

1.3.1 Lipid transport

There are 2 main sources of lipids obtained in our body. The first source are lipids absorbed from dietary food called exogenous lipid and the second source are lipids which synthesized in the body, mainly by liver, called endogenous lipid. Both absorbed and newly synthesized lipids will be transported to various tissues in the body via blood circulation. However, lipids are insoluble in water, therefore they will be transported through the circulation via soluble complexes of proteins (apolipoproteins) and several types of lipids, called lipoprotein particles.

Exogenous pathway, dietary lipids are packed into lipoprotein particles named chylomicrons. Chylomicrons are formed in the epithelial intestine for transportation of dietary lipids, mostly triacylglycerol. During transportation along the capillaries, free fatty acids are transferred to adipose and muscle tissues by the help of lipoprotein lipase located at the vascular endothelial cells. Remain particles called

chylomicron remnants will be then taken up by the liver. Endogenous pathway starts in the liver with formation of very low density lipoprotein (VLDL) cholesterol, which delivers newly synthesized lipids from liver to adipose and muscle tissues. During transportation, VLDL are hydrolyzed into intermediate density lipoprotein (IDL) cholesterol and then returned to the liver so that they may be repackaged as LDL and then taken from the circulation by peripheral tissues. The main function of LDL is delivering of cholesterol to the peripheral tissues and liver. Excess cholesterol in extrahepatic tissues are transported back to the liver by high density lipoprotein (HDL) cholesterol which synthesized in the liver and intestine or from metabolic transformation of other lipoproteins in circulation (David L. Nelson, 2008). Transportation of lipid by endogenous and exogenous pathways is shown in Figure 1.1.
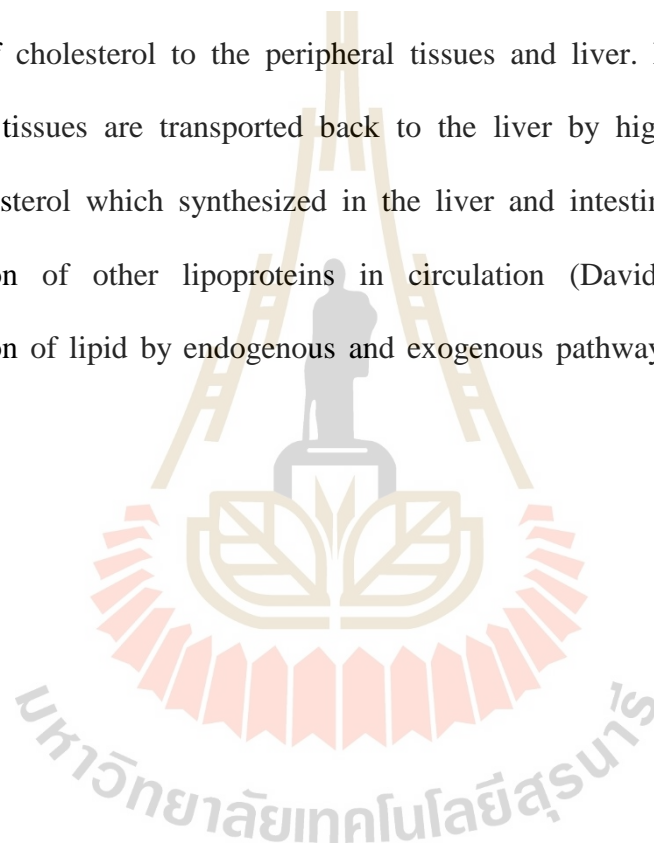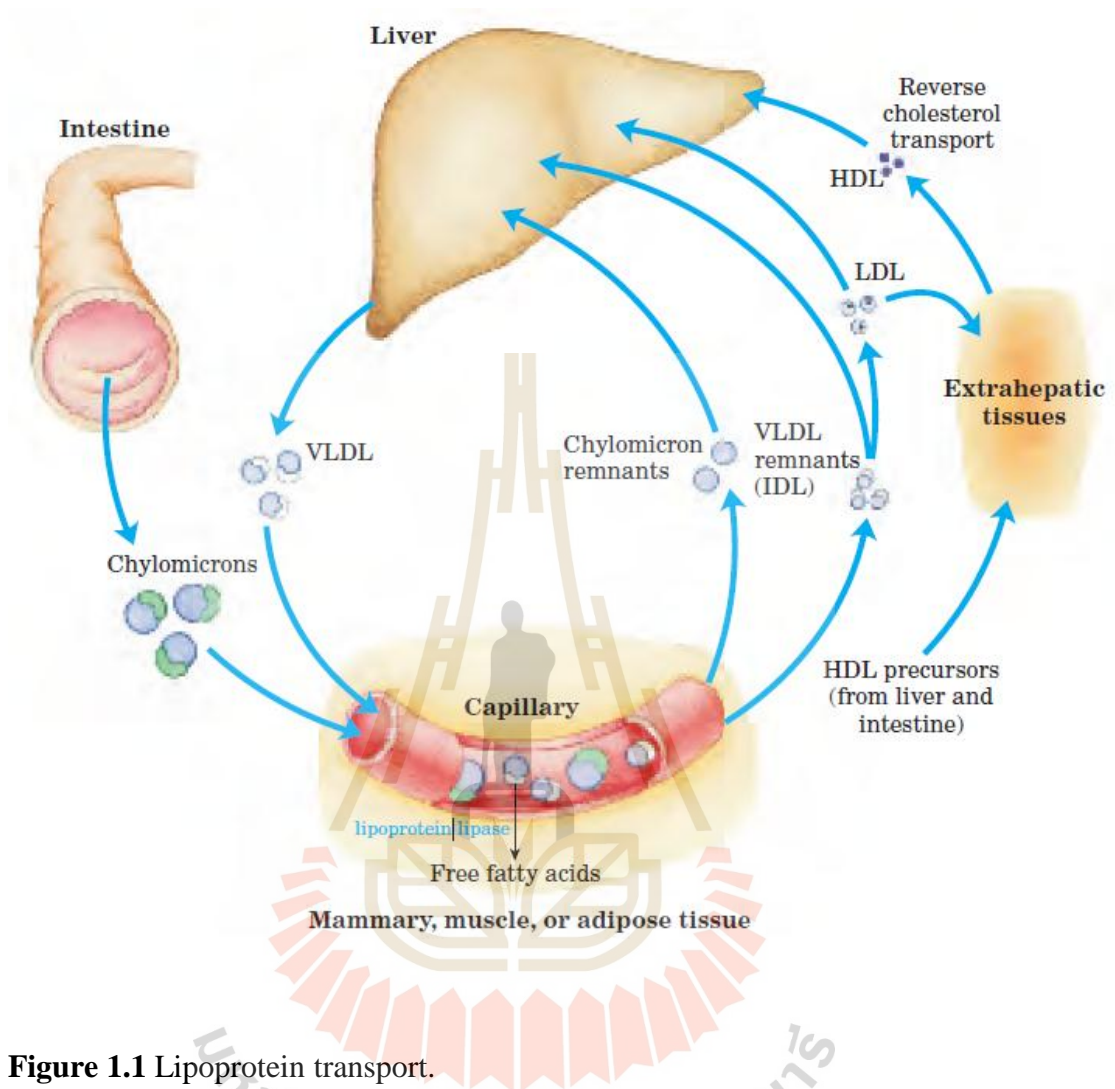
Figure 1.1 Lipoprotein transport.

Lipids are transported in blood circulation via soluble complexes of proteins called lipoproteins that consist of exogenous and endogenous pathway. Exogenous pathway starts with the incorporation of dietary lipids into chylomicrons in the intestine and endogenous pathway starts with the formation of VLDL in the liver (David L. Nelson, 2008).

1.3.2 Lipoproteins

The general structure of lipoproteins consists of a central hydrophobic core containing non-polar lipids, cholesteryl ester and triacylglycerol surrounded by more polar lipids, free cholesterol, phospholipids, and apolipoproteins as shown in Figure 1.2.
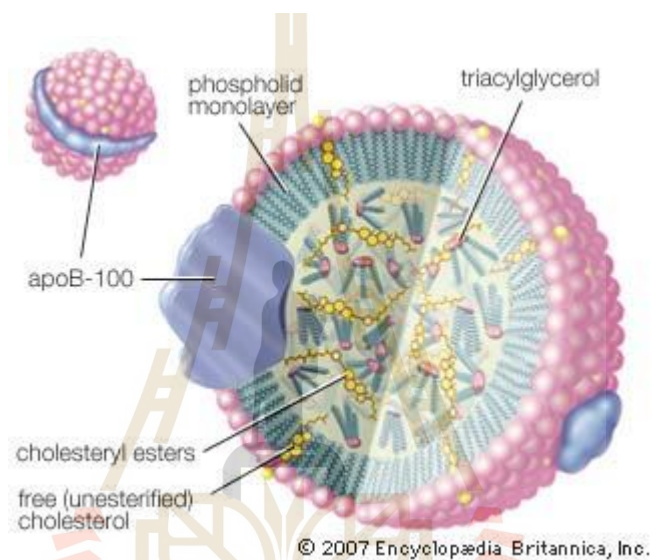
Figure 1.2 General structure of lipoprotein.

Structure of each lipoprotein particle consists of core of hydrophobic lipids, triacylglycerol, and cholesteryl ester, surrounded by shell of more polar lipids and apolipoproteins.

Plasma lipoproteins can be classified into different types based on size, lipid composition, and apolipoproteins; chylomicron (CM), very low density lipoprotein (VLDL), intermediate density lipoprotein (IDL), low density lipoprotein (LDL), and high density lipoprotein (HDL). CM and VLDL have the highest content of triacylglycerol and 1-10% apolipoproteins by weight. While LDL and HDL contain mostly cholesterol and 20-50% of apolipoproteins by weight (Dennis Vance, 2002) (Figure 1.3).
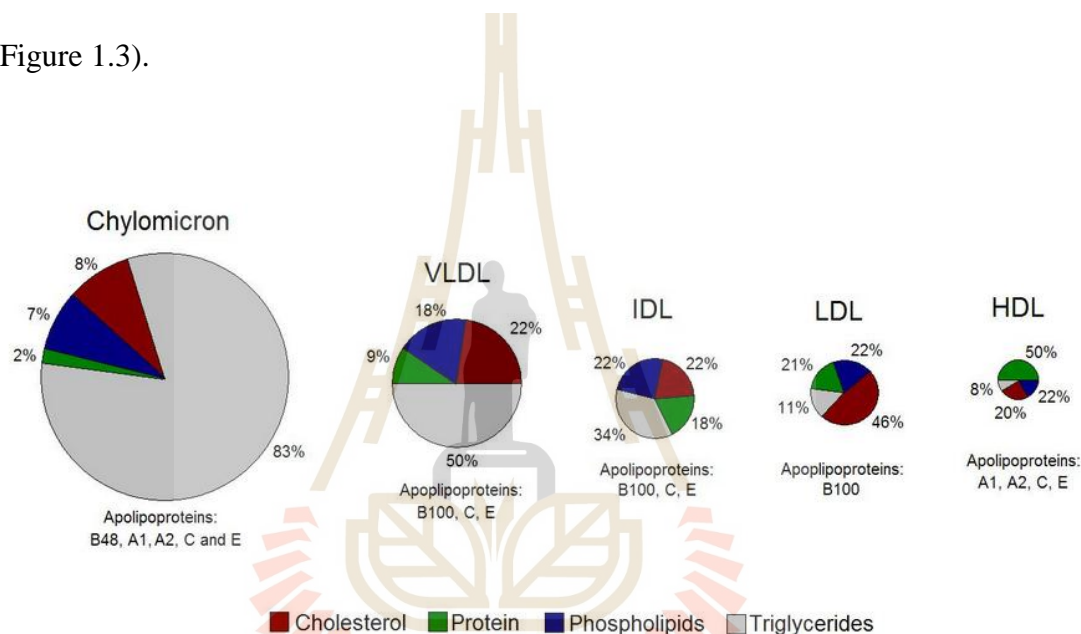
Figure 1.3 Composition of different types of lipoproteins. (Barrington, 2013)

CM is a large triacylglycerol rich particle synthesized in the intestine involved in the transportation of dietary triacylglycerol to muscle and adipose tissues. This particle contains apolipoproteins A1, A2, B-48, C, and E. ApoB-48 is the main structural protein found in this particle. Removing of triacylglycerol by lipoprotein lipase during transport through capillaries results in reducing the size of chylomicron. This small chylomicron is named as chylomicron remnant and will be taken up by the liver.

VLDL is also triacylglycerol rich particle that is synthesized in the liver. These particles contain apoB-100, C, and E. The endogenous lipoprotein pathway begins in the liver with the formation of VLDL. The triglycerides carried in VLDL are metabolized in muscle and adipose tissue by lipoprotein lipase leading to the releasing of free fatty acids and the formation of IDL.

IDL is the particle result in the removal of triacylglycerol from VLDL. IDL is cholesterol enriched particle contains apolipoprotein B-100, C, and E.

LDL is cholesterol enriched particle derived from VLDL and IDL. LDL carries the majority of the cholesterol in the circulation. The predominant apolipoprotein is B-100.

HDL is cholesterol and phospholipids enriched particle contain apo A1, A2, C, and E which apoA1 is a core structural protein. These particles play an important role in reverse cholesterol transport from peripheral tissues to the liver, which is one potential mechanism by which HDL may be anti-atherogenic (Kenneth R Feingold, 2018).

1.3.3 Apolipoproteins

Apolipoproteins are proteins that play a crucial role in lipoprotein metabolism. These molecules assemble in lipoprotein particles, which have 4 major functions including 1) serving a structural role, 2) acting as ligands for lipoprotein receptors, 3) guiding the formation of lipoproteins, and 4) serving as activators or inhibitors of enzymes involved in the metabolism of lipoproteins (Kenneth R Feingold, 2018). These proteins are classified into 2 broad types: non-exchangeable and exchangeable (or soluble) apolipoproteins. ApoB-100 and apoB-48 are non-exchangeable apolipoproteins. They are very large and water-insoluble protein that are stay together with lipid at the liver or intestinal cells, their site of synthesis. They bound to the same lipoproteins through various metabolic transformations in plasma. In contrast, apoA1, A2, C, and E are exchangeable apolipoproteins, they are smaller and more water soluble than non-exchangeable apolipoproteins in their delipidated state. They can transfer between lipoprotein particles and can acquire lipid during in the circulation (Dennis Vance, 2002).

ApoB belongs to non-exchangeable apolipoprotein which is the principal apolipoprotein component of LDL, VLDL, and CM. This protein in human is encoded by APOB gene. It has a very large size and insoluble in water. There are 2 types of apoB, apoB-100 and apoB-48. ApoB-100 is synthesized in the liver and found as primary component of VLDL, IDL, and LDL. The molecular weight of apo B-100 is about 512 kDa. Concentration of apoB-100 found in human plasma is about 1.0 g/L depends on gender and age. Full length of apoB-100 is a ligand for LDL receptor in various cells throughout the body (Dennis Vance, 2002). Moreover, due to gene editing in the intestine, certain amino acid sequence at C-terminal of apoB-

100 is eliminated. As the result, shorten amino acid residue apolipoprotein is synthesized and named as apoB-48. Both apoB-48 and apoB-100 share a common N-terminal sequence, but apoB-48 cannot bind to the LDL receptor due to lacking of the LDL binding region (Kenneth R Feingold, 2018). ApoB-48 is a unique protein that found to incorporate into chylomicrons for transportation of dietary lipid from the small intestine.

ApoE belongs to exchangeable apolipoprotein group. It is synthesized in many tissues, but liver and intestine are the primary source of circulating apoE. This apolipoprotein has molecular weight about 34 kDa and its concentration found in human plasma is about 25 mg/L. ApoE has been reported as a heparin binding glycoprotein. ApoE exhibits a genetic polymorphism with 3 common alleles, apoE2, apoE3, and apoE4, which show high variation among various ethnic groups (Kenneth R Feingold, 2018). These proteins are found in CM, VLDL, IDL, and HDL. ApoE is important for facilitating receptor-mediated uptake of large lipoproteins. It plays a role as the primary carrier of lipid in the brain that important for functional neurophysiology. Therefore, it is related with both cardiovascular and neurological disease such as Alzheimer's disease (Chia-Chen Liu, 2013).

In most laboratories, the reagent used for apoB precipitation is a combination of heparin and polyvalent anion or divalent cation such as a combination of heparin and manganese chloride or phosphotungstic acid or magnesium chloride. These methods are widely used because they are rapid, inexpensive, and as precise as the traditional method of lipoprotein separation by ultracentrifugation (Joyce Corey Gibson, 1984). Since apoE is heparin binding glycoprotein, LDL is not only apoB containing lipoproteins but also VLDL will be precipitated by this precipitation

procedure. It has been reported that only LDL can be precipitated by heparin in the absence of additional divalent cations by reducing the pH of plasma to 5.11. Under these conditions, VLDL and HDL were remained in the solution (Heinrich Wieland, 1983).

ApoA1, A2, C, and E belong to exchangeable apolipoprotein, which have a smaller size and more hydrophilic than apoB. ApoA1 and apoA2 are in human encoded by APOA1 and APOA2 gene, respectively. ApoA1 is synthesized in the liver and intestine, while apoA2 is synthesized only in the liver. ApoA1 is the major protein component of HDL particle, whereas apoA2 is the second most abundant protein of HDL. ApoA has molecular weight about 28 kDa and found in human plasma about 1.3 g/L. This protein is necessary for reverse excess cholesterol and transport to the liver for degradation. Low plasma apoA1 level is associated with increasing the risk of cardiovascular disease (Dennis Vance, 2002).

1.3.4 Determination of LDL in routine laboratory

Increasing of plasma LDL level is one of major risk factors in the pathogenesis of atherosclerosis that lead to hypertension, coronary heart disease, stroke, and death. Atherosclerosis is one of the leading causes of mortality worldwide. As a result, LDL is the main target for diagnosis and treatment of hyperlipidemia. Beta quantification is the gold standard method for LDL measurement. The principal of this technique is separation of LDL according to density of 1.006 kg/l using ultracentrifugation before measurement (Masakazu Nakamuraa, 2014). Nevertheless, this technique is not convenient in routine laboratory because complication, time-consuming, and expert technician is required. The National Cholesterol Education Program Adult Treatment Panel III (NCEP ATP III) guidelines for hyperlipidemia

suggests that calculated LDL using Friedewald equation should be the primary target for coronary heart disease reduction.

Nowadays, the most common approach to determine plasma LDL level in clinical laboratory is Friedewald calculation, which was calculated from total cholesterol, triglyceride, and HDL measurement as in the following equation (William T. Friedewald, 1972).

LDL (mg/dl) = Total cholesterol (mg/dl) − ((Triglyceride (mg/dl) / 5) + HDL (mg/dl))

In plasma, HDL level is normally low and quite stable while triglyceride is varied depends on dietary and individual metabolism, mainly come from CM and VLDL. Many evidences report that calculated LDL level is not accurate if triglyceride level is higher than 400 mg/dl. Several studies have tried to modify this formula to overcome this limitation. However, these modifications are complicate and not really accurate. Nonetheless, Friedewald calculation is still used in clinical laboratory because it is less expensive and more convenient than the complicated and time-consuming standard technique; beta quantification.

To overcome the limitations of Friedewald equation, several direct LDL measurements have been developed such as homogenous methods capable of fully automation, which are different in details and techniques depend on manufacturers, selective chemical precipitation, and immunoseparation that include antibodies against apoA1 and apoE to remove HDL and VLDL before LDL was directly measured in the filtrate.

1.3.5 Low density lipoprotein (LDL) oxidation

LDL can be oxidized into different degrees in stepwise manner as shown in Figure 1.4. In the initial phase of modification, the lipid components react with oxidizing agents resulting in radical chain reactions that produce many types of oxidation products, usually on lipid part of LDL. The generated product of this phase is named as minimally modified low density lipoprotein (mm-LDL). In the next step, apoB is directly attacked by the generated lipid oxidation products. The oxidative changes of amino acid side chains and the cleavage of peptide bonds are occurred (Hiroyuki Itabe, 2011). The products of this protein modification is then named as fully oxidized-LDL (ox-LDL) (Shutong Yao, 2012).

Roles of mm-LDL and ox-LDL in atherosclerosis are not completely understood. Nevertheless, the involvement of these modified LDL has been proposed during the 3 major stages of atherogenesis as illustrated in Figure 1.5. Early stage of atherogenesis, mm-LDL may be transferred between the vessel wall and circulation, which maybe further modified to ox-LDL in the advanced stage of atherosclerosis. Advanced lesion is the second step of atherogenesis, which many macrophages and foam cells were found at the atherosclerotic lesions. Ox-LDL is then taken up by macrophages and further processed in lysosomes. Some of ox-LDL is completely degraded but some resisted to proteolytic processing. Therefore, partially degraded ox-LDL particles can be observed in the atherosclerotic lesions. Final stage is plaque rupture, which ox-LDL and partially degraded ox-LDL are rapidly released from the lesions into the circulation leads to increasing of plasma ox-LDL and atherothrombosis (Hiroyuki Itabe, 2011).

Some reports revealed that mm-LDL can induce intimal foam cell formation. This mechanism is driven by endoplasmic reticulum stress, a cross-point to link cellular processes with multiple risk factors that exist in all stages of atherosclerosis. However, the mechanism remains unclear (Shutong Yao, 2012).
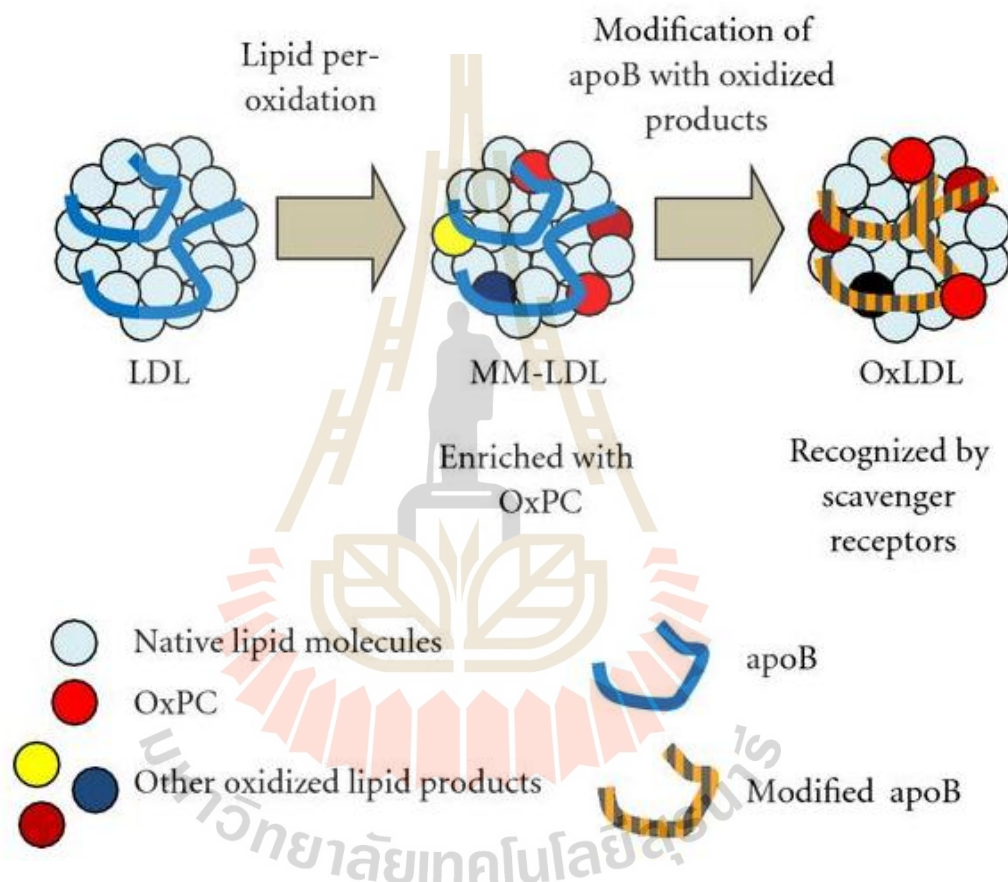
Figure 1.4 Difference between mm-LDL and ox-LDL.

LDL oxidation occurred in a stepwise manner. Minimally modified low density lipoprotein (mm-LDL) is the oxidized-LDL that only lipid part has been modified in the early stage of oxidation whereas fully oxidized-LDL (ox-LDL) is the oxidized-LDL that both lipid and protein parts were modified (Hiroyuki Itabe, 2011).
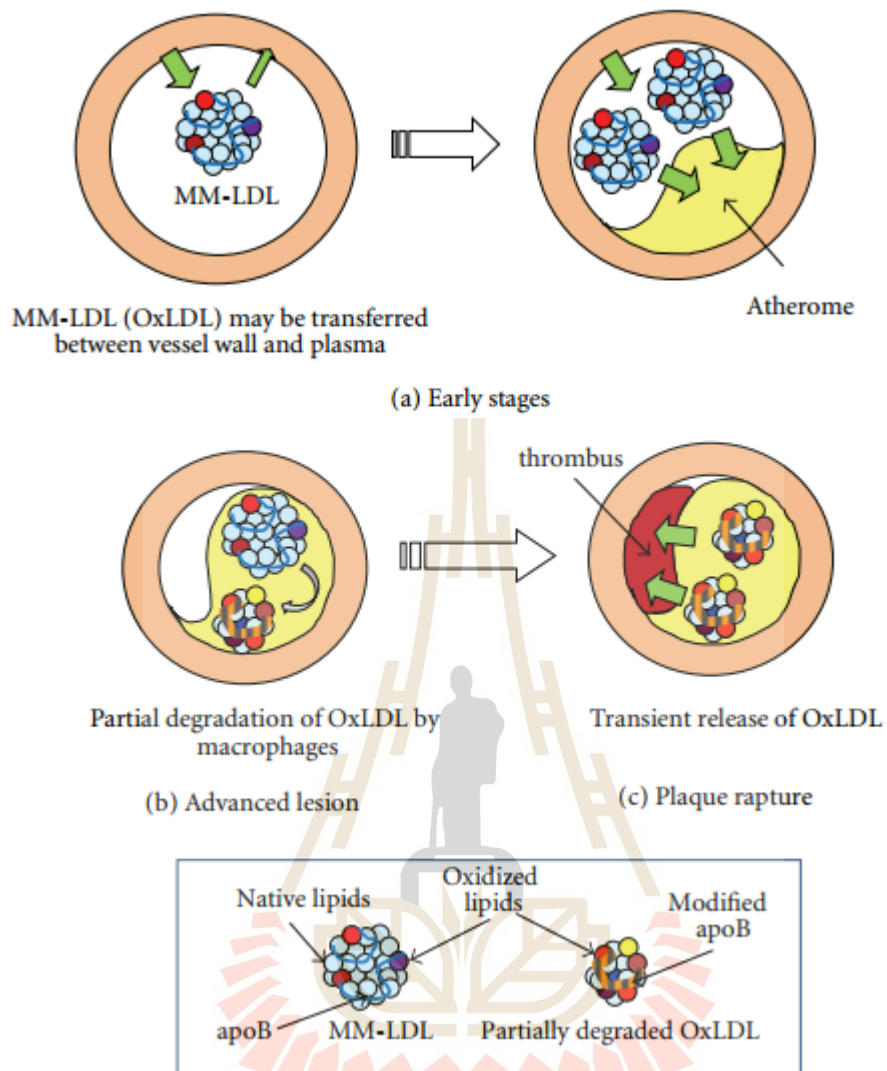
Figure 1.5 Possible roles of mm-LDL and ox-LDL in *vivo*.

In the early stage of atherosclerosis, mm-LDL may be transferred between the vessel wall and circulation. Mm-LDL could be further modified to ox-LDL in the advanced stage of atherosclerosis (Hiroyuki Itabe, 2011).

1.3.6 Generation of oxidized-LDL

The most common approach to generate ox-LDL in the laboratory is the incubation of LDL fractions with micromolar concentration of copper (II) sulfate. Copper acts as oxidizing agent that can participate in electron transfer reactions with the consequent production of oxidant species capable of oxidizing cell components. Copper can catalyze the formation of the highly reactive hydroxyl radicals from hydrogen peroxide and decompose lipid peroxides to peroxyl and alkoxyl radicals, which favor the propagation of lipid peroxidation (Ghaffari, 2010).

The copper ion induces lipid peroxidation chain reactions, and subsequently, the chemical modification of apoB protein side chains with reactive lipid peroxidation products, such as 4-hydroxynonenal (4-HNE), acrolein, and malondialdehyde (MDA). MDA can be measured as Thiobarbituric Acid Reactive Substances (TBARS). TBARS assay is a commonly used and convenient method for determining the relative lipid peroxide content of sample sets, including serum, plasma, urine, cell lysates, and cell culture supernatant. Lipid that is unsaturated is likely to form peroxide and the most reactive in the TBARS assay. Free MDA is typically low and require acid treatment of proteins for MDA release and breakdown of peroxides by heat and acid to facilitate color development in the TBARS reaction (www.rndsystems.com/rnd_page_objectname_tbars_parameter_kit_measuring_oxidative_stress.aspx).
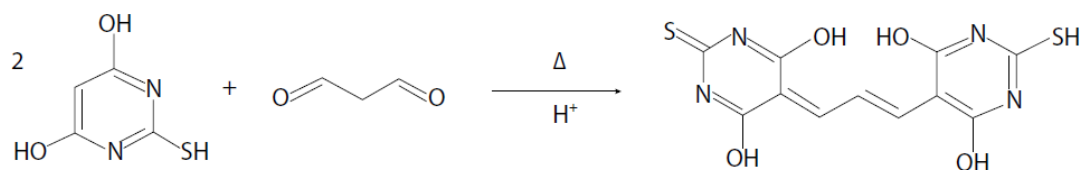
Figure 1.6 Reaction scheme of TBARS assay.

In the presence of acid and heat, 2 molecules of thiobarbituric acid (TBA) react with MDA to produce colored end product that can be easily quantified by measuring the absorbance value at wavelength 532 nm (Ghaffari, 2010).

1.3.7 Antibody

Antibody (Ab) can be divided into 2 major types according to their number of the producing cells and the binding epitopes, polyclonal antibody (pAb) and monoclonal antibody (mAb). Polyclonal antibodies are the pool of antibodies that are produced and secreted by different clone of plasma cells. The producing antibodies bind to different epitopes of an antigen. MAb is antibody that comes from a single clone of plasma cell and bind to a single epitope on an antigen. MAb producing plasma cells was firstly discovered in multiple myeloma patients. The mAb was found to produce in a large amount in the blood and urine of patients. In 1975, well known mAb generating technique called hybridoma technique had been developed by Kohler and Milstein (Kohler, 1975). The principal behind this technique is based on the fact that each B lymphocyte produces a single specific antibody, hybridoma technique was developed for immortalizing individual antibody-secreting cells from an immunized animal by producing hybridoma cells. The specific antibody produced by the hybridoma cell is referred as a monoclonal antibody. MAb is

homogeneous in specificity, affinity, and isotype. Each mAb specifically binds to a single antigen determinant on the immunogen.

1.3.8 Biochemical structure of antibody

The basic structure of an antibody is showed in Figure 1.7. General structure of antibody composed of 2 light chains and 2 heavy chains. Each chain composed of variable region (V) and constant region (C). The V region composed of a heavy chain (V_H) and the adjoining V region of a light chain (V_L) from an antigen-binding site. The constant region of light chains (C_H) has 2 amino acid sequences named kappa and lambda. The C_H has 1 of 5 basic amino acid sequences i.e. α, δ, ϵ, γ, or μ. These sequences determine the isotype of antibody molecules. Based on the isotype of the heavy chain constant region, human antibody can be classified into 5 isotypes; IgG, IgA, IgM, IgD, and IgE.

Among the immunoglobulin isotypes, IgG is the most abundant found in human circulation. Furthermore, IgG consists of 4 subtypes: IgG_1, IgG_2, IgG_3, and IgG_4. Major differences among these subtypes are their amino acid sequences and the number of disulfide bonds between the heavy chains (Janeway, 1999).
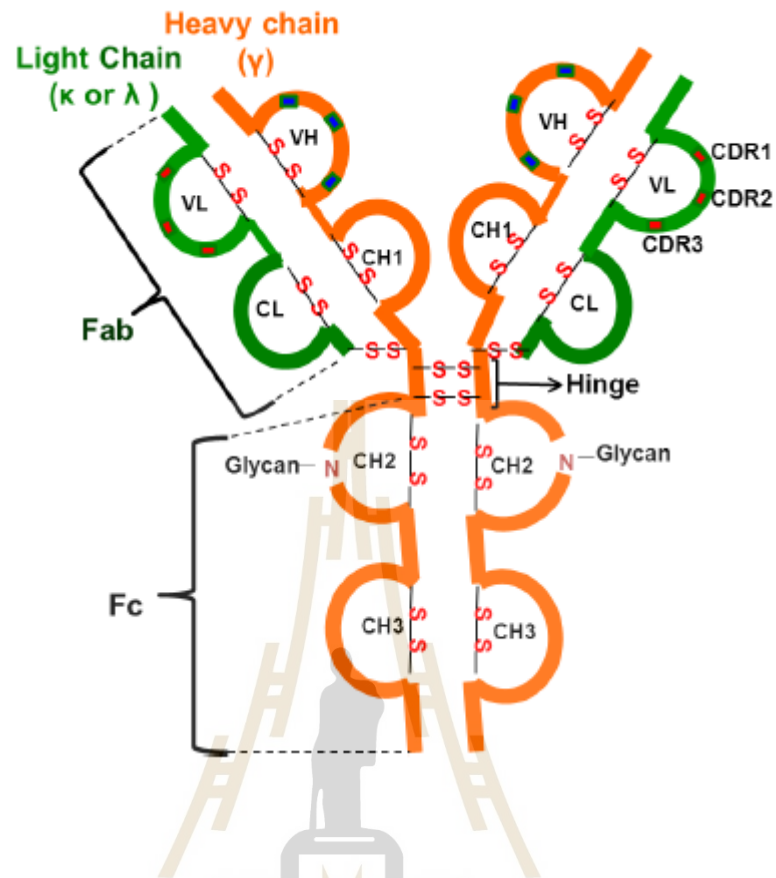
Figure 1.7 Structure of human IgG molecule.

Green parts are light chains and orange parts are heavy chains. V indicates

variable regions. C indicates constant regions. V_L and C_L are domains of the

light (L) chain. V_H, C_{H1}, C_{H2}, and C_{H3} are domains of the heavy (H) chain

(Wang, 2012).

1.3.9 Antigen-antibody interaction

Antibody can recognize antigen of almost every kind of biological molecules, including simple intermediate metabolites, sugars, lipids, hormones, as well as macromolecules such as complex of carbohydrates, phospholipids, nucleic acids, and proteins. For proteins, the formation of some antigenic determinants depends on the primary structure, and the formation of other antigenic determinants reflects tertiary structure, or conformation. Binding epitopes formed by several adjacent amino acid residues are called linear determinants. The antigen binding site of an antibody can accommodate a linear determinant made up of about 6 amino acids. If linear determinants appear on the external surface or in a region of extended conformation in the native folded protein, they may be accessible to antibody. Moreover, linear determinants may be inaccessible in the native conformation and appear only when the protein is denatured. Antibodies that are specific for certain linear determinants and for conformational determinants can be used to determine whether the specific protein is denatured or in its native conformation, respectively. Some proteins have been modified by adding of some functional groups or deleting some amino acid residues such as glycosylation, phosphorylation, ubiquitination, acetylation, and proteolysis. Thus, altering of the protein structure can generate new epitopes. Such epitopes are called neo-antigenic determinants, and they may be recognized by specific antibodies too. Different types of antigenic determinants are shown in Figure 1.8.

Antigen-antibody interactions occur at the binding cleft, which has a rough size of about 3x1x1 nm (the size of 5 or 6 sugar units). Several evidences showed that antigens may bind to larger, or even separate parts of the variable region.

Binding depends on a close-dimensional fit, allowing weak intermolecular forces to overcome repulsion between molecules as shown in Figure 1.9 (Playfair, 2012).
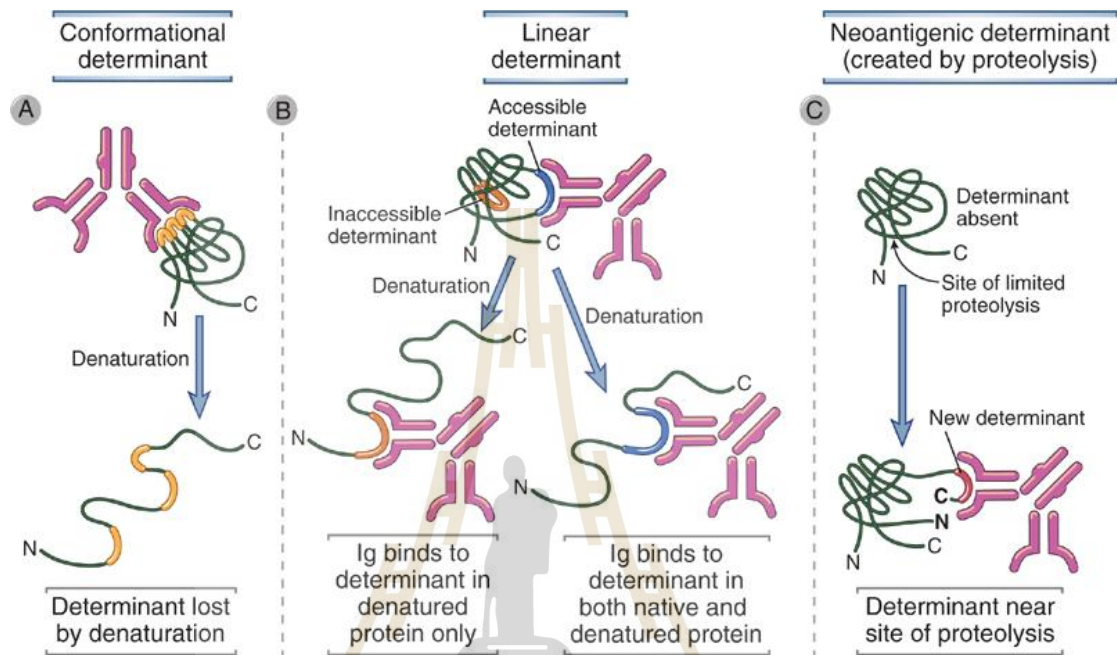
Figure 1.8 Nature of antigenic determinants.

Antigenic determinants (shown in yellow, orange, and blue) depend on protein folding (conformation), as well as on primary structure. (A) Conformational determinant; antigenic determinant that the Ab can bind only on unfolding native protein. (B) Linear determinant; antigenic determinants that are accessible in both native and denatured proteins. (B). Neo-antigenic determinants, which arised from post-synthetic modifications such as peptide bond cleavage (Abbas, 2011).
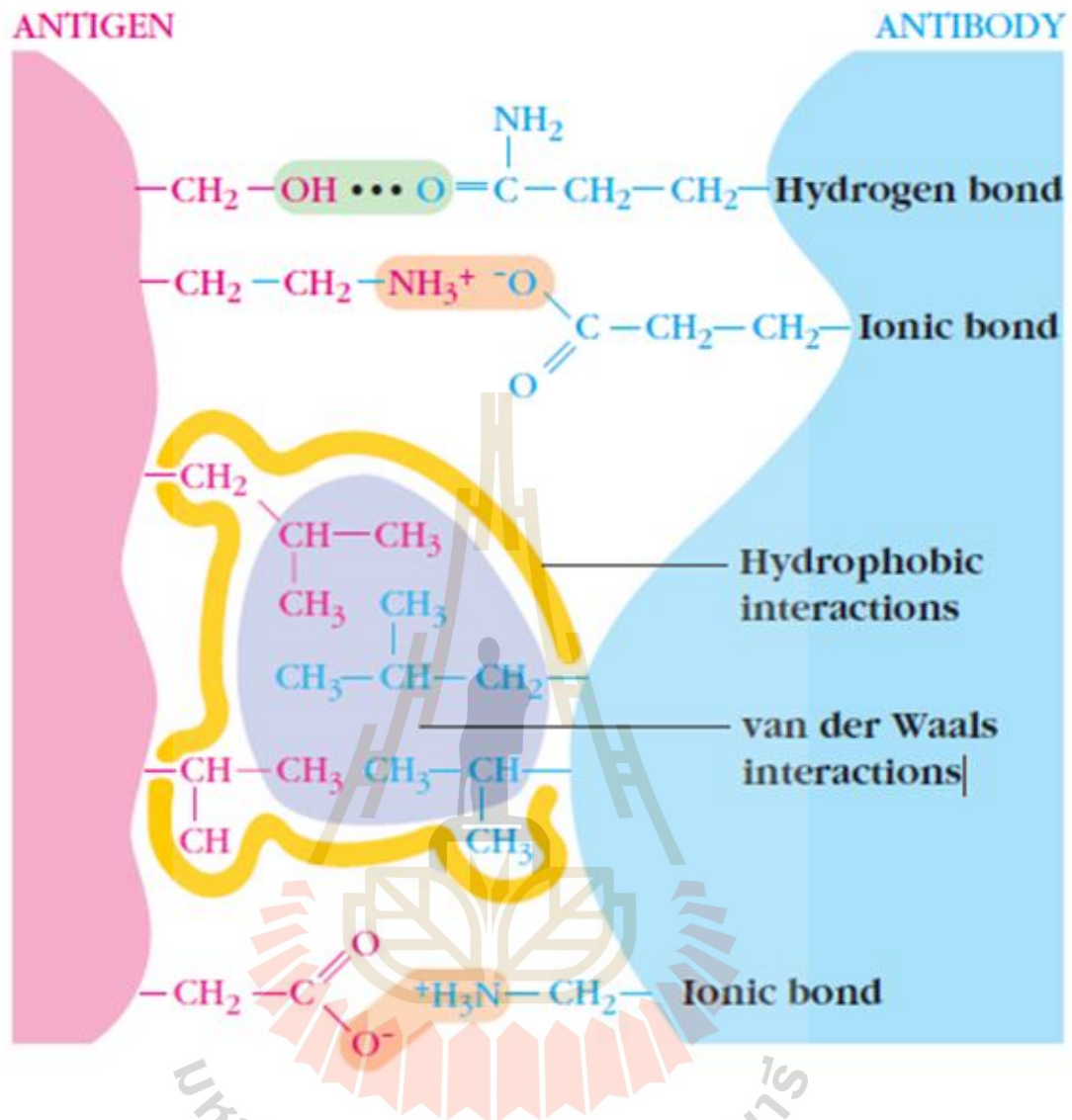
Figure 1.9 Interaction between antibody and antigen.

The forces between antibody-antigen interaction at the binding cleft compose of: (1) hydrogen bonds which hydrogen atom is shared between 2 electronegative atoms; (2) ionic bonds between oppositely charged residues; (3) hydrophobic interactions which water forces hydrophobic groups together; and (4) Van der Waals interactions between the outer electron clouds of 2 or more atoms (Kindt, 2007).

1.3.10 Generation of monoclonal antibody by hybridoma technique

In 1975, Kohler and Milstein first immortalized antibody-secreting lymphocyte by producing hybridoma cells. In this procedure, spleen cells from a mouse that has been immunized with antigens are fused with an enzyme-deficient partner myeloma cell line by using chemicals such as polyethylene glycol (PEG) that can facilitate the fusion of plasma membranes. The formation of hybrid cells retains many chromosomes from both fusion partners. These hybrid cells are placed in a selection medium, hypoxanthine, aminopterin, and thymidine (HAT), which permit the survival of only immortalized hybrids. These hybrid cells are grown as single cell clones and tested for the secretion of the antibody of interest. There are 2 pathways of purine synthesis in most cells, de novo pathway that needs tetrahydrofolate and salvage pathway that uses the enzyme hypoxanthine-guanine phosphoribosyltransferase (HGPRT). Myeloma cells that lack HGPRT are used as fusion partners, and they normally survive using de novo purine synthesis. In the presence of aminopterin, tetrahydrofolate is not made, resulting in a defect in de novo purine synthesis and also a specific defect in pyrimidine biosynthesis, in generating TMP from dUMP. Hybrid cells receive HGPRT from splenocytes and have the capacity for uncontrolled proliferation from the myeloma partner. If they are given hypoxanthine and thymidine, these cells can make DNA in the absence of tetrahydrofolate. As a result, only hybrid cells survive in HAT medium as shown in Figure 1.10. In addition, antibody from hybridomas can be assayed by several methods such as enzyme-linked immunosorbent assay (ELISA), immunoblot, immunofluorescent assay, and flow cytometry. The hybridoma clones that produce a

desired antibody can be expanded or induced as ascetic fluids in a mouse or grown in
serum free medium to produce large amounts of monoclonal (Abbas, 2011).
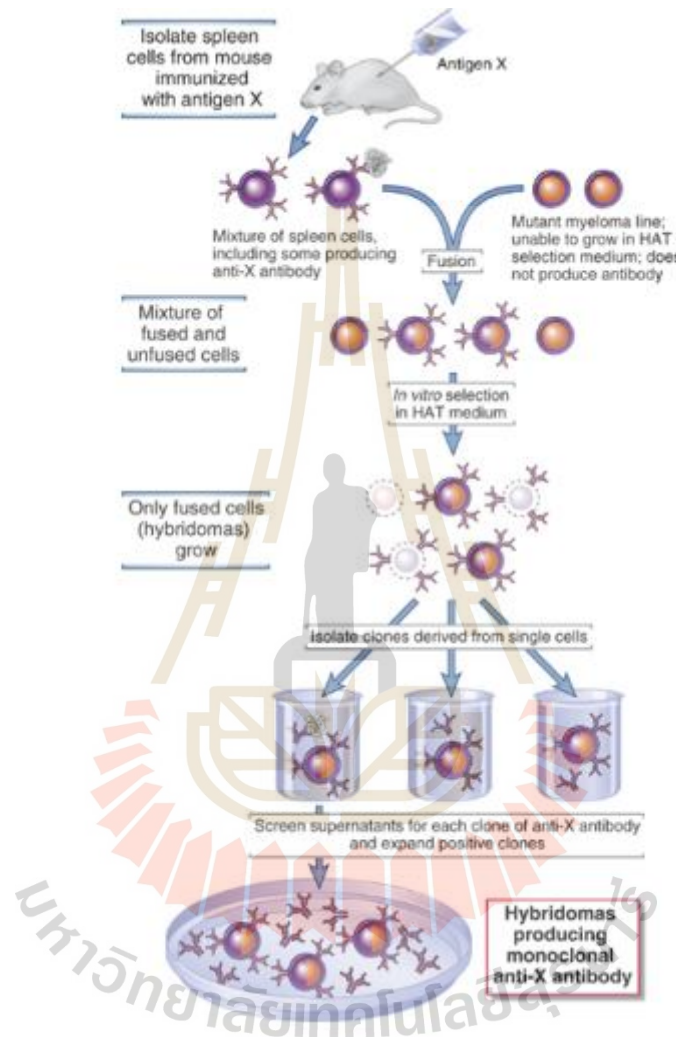
Figure 1.10 Monoclonal antibody production.

> After a mouse was immunized with antigen and the desired antibody was
> produced, the splenocytes were isolated and fused with myeloma cells to
> produce hybrid cells. The single clone that produce specific antibody called
> monoclonal antibody (Abbas, 2011).

1.3.11 Atherosclerosis

Atherosclerosis is the major cause of coronary and cerebrovascular disease, 2 major causes of morbidity worldwide. Elevation of LDL level in circulation that cause the accumulation of lipid-loaded macrophages in the arterial wall are the major risk factors for atherosclerosis development. Atherosclerosis develops when excess cholesterol-rich apoB-containing lipoprotein, LDL, are accumulated which leads to plaque formation in endothelium. When plaque occurs, the wall of blood vessel thicken, the channel in artery was narrowed leading to reduction of blood flow. As a consequence, the amount of oxygen and nutrients to the body will be decreased. Plaque may partially or totally block blood flow to the pivotal organs in the body such as heart, brain, and kidney. A piece of plaque can break off and transport through bloodstream until it gets stuck. Moreover, the possibility of blood clot or thrombus will occur around the plaque and adhere to the inner of the blood vessel. As a result, the artery can be blocked and cutting of blood flow and if the blocked arteries supplies to heart or brain, heart attack or stroke will occur and leading to sudden death. In addition to lipid accumulation, other processes such as inflammatory cell infiltration, cytokine production, and cell death also contribute to their complications. Atherosclerosis was viewed as chronic immune-inflammatory disease, characterized by activation of both innate and adaptive immunity (Anneleen Remmerie, 2018; Viviane Z. Rocha, 2009). Oxidized-LDL triggers inflammatory and immunogenic events that promote endothelial dysfunction and the synthesis and secretion of pro-inflammatory cytokines, leading to immune and autoimmune responses. These can accelerate the intracellular accumulation of lipids within plaques. It has been reported that ox-LDL binds β2-glycoprotein I to form circulating complexes found in both

immune and non-autoimmune atherosclerosis. These complexes associate to early atherogenesis by stimulating pro-inflammatory innate immunity through inflammasome/interleukin-1 pathways (Eiji Matsuura, 2014).

1.3.12 Low density lipoprotein (LDL) cholesterol uptake

LDL can be bound and internalized by LDL receptor on macrophage (Brian W Howell, 2001). Macrophages uptake native LDL in a receptor-independent fashion. Fluid phase endocytosis of native LDL converts macrophages into cholesterol-enriched foam cells. Uptake of native LDL fluid by macrophages in vitro occur both micro and macro-pinocytosis (Howard S. Kruth, 2005).

Oxidized-LDL is considered as a high potential atherogenicity. Modified LDL is ingested by macrophages via receptors-mediated phagocytosis and pinocytosis. Scavenger receptors (SRs), CD36 and SR-A are the most important receptors for the uptake of modified LDL. CD36 is platelet glycoprotein IIIb/IV, an 88 kDa heavily glycosylated transmembrane protein. This molecule is highly expressed in macrophages and acts as a high affinity receptor for ox-LDL. Recent study revealed that increasing of plasma CD36 associated with atherosclerosis, insulin resistance, and fatty liver in non-diabetic healthy population (Handberg, 2012). SR-A is a 77 kDa cell surface glycoprotein, which belongs to a SR family protein. This protein is highly expressed in macrophages and SR-A acts as a mediator for the uptake of ox-LDL into macrophages. Treatment of ox-LDL stimulates the SR-A expression and promotes the uptake of ox-LDL into macrophages (Xiao-Hua Yu, 2013). It has been shown that silencing of SR-A or CD36 alone reduced atherogenesis in LDL receptor deficient apoB-100 mice whereas simultaneous silencing of both receptors has no beneficial effect. This can be indicated that the

compensatory of these 2 receptors is sufficient for the uptake of ox-LDL (Petri I. Makinen, 2010).

Lectin-like oxidized low-density lipoprotein receptor-1 (LOX-1) receptor is the receptor that markedly up-regulated in atherosclerosis. This receptor is not expressed in monocytes, but can be up-regulated in differentiated macrophages. LOX-1 is a main receptor for binding ox-LDL in endothelial cells. This receptor can also sense not fully ox-LDL, indicate that LOX-1 associated with early atherogenic step (Hiroharu Kataoka, 1999).

1.3.13 Role of oxidized LDL in associated with atherosclerosis

Apart from native LDL, modified LDL can be formed both in *vitro* and in *vivo* and considered to be more atherogenic substances. LDL can be oxidized by exposure to oxidizing agent such as copper. It has been proposed that LDL can be oxidized in stepwise manner to become mm-LDL, which is modified solely in the lipid part, and fully oxidized LDL that both lipid and protein parts were oxidized as mentioned in 1.3.5. Mm-LDL can bind to both LDL receptor and scavenger receptors whereas ox-LDL exclusively binds to scavenger receptor as mention in 1.3.12. Native LDL, mm-LDL, and fully oxidized LDL are associated with atherosclerosis. Since LDL can be oxidized in stepwise manner, native LDL and mm-LDL are considered to be associated during the early stage of atherosclerosis progression whereas fully oxidized LDL which is the well-known potential atherogenicity is considered to be associated during the advanced stage. However, more studies need to be elucidated.

1.3.14 Formation of foam cells

At the beginning of atherosclerosis, LDL particles invade the arterial intima and undergo some modifications such as oxidation. Oxidized-LDL can induce endothelial and smooth muscle cells activation. The adhesion molecules were expressed leading to the accumulation of monocytes at sub-endothelial space. Recruitment of monocytes to the arterial wall is a multi-step including capture, rolling, adhesion, and transmigration to endothelium that require the interaction of many chemokines and adhesion molecules such as selectins and integrins (Christian A. Gleissner, 2007; Viviane Z. Rocha, 2009). Once in the intima, monocytes become tissue macrophages which can internalize oxidized-LDL. After modified LDL is phagocytosed by macrophages, lipoproteins are delivered to late endosome and cholesterol ester will be hydrolyzed into free cholesterol by lysosomal lipase. The released free cholesterol is then re-esterified at the surface of endoplasmic reticulum by an integral membrane protein, Acetyl-CoA Acethyl Transferase 1 (ACAT1) to prevent toxicity of the free cholesterol to cells and stored in cytoplasmic lipid droplets. Because of characteristic foamy appearance of these cells, these cells are called foam cells (Hoiroaki Okazaki, 2008). Formation of foam cells in the arterial intima is a hallmark of early stage atherosclerosis (Figure 1.11). Fully oxidized-LDL is well-known to be the potential atherogenicity that can cause foam cell formation. Recently foam cell formation also found to be induced by mm-LDL. Scavenger receptors appear to play a key role in uptake of ox-LDL as mention in 1.3.12, while mm-LDL appears to interact with CD14/TLR4 (Shashkin P., 2005).
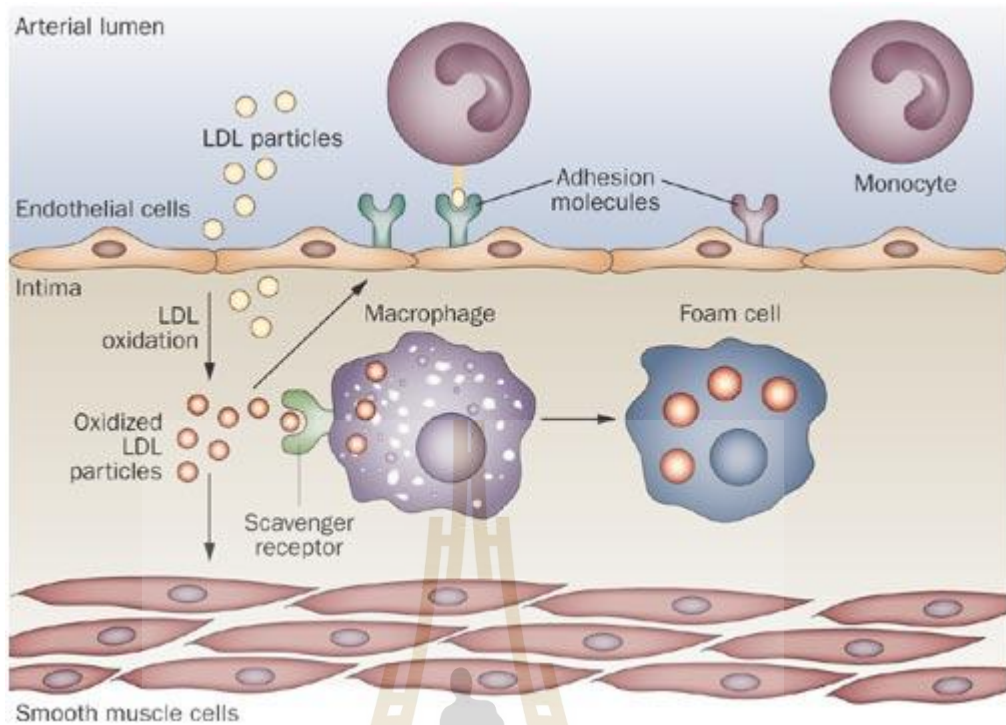
Figure 1.11 Early stage of atherosclerosis.

LDL particles undergo chemical modifications such as oxidation in the arterial intima. Oxidized-LDL induces endothelial and smooth muscle cell activation and expression of adhesion molecules. In the intima, monocytes are differentiated to become tissue macrophages, which are able to engulf oxidized-LDL leading to foam cell formation and atherosclerotic plaque (Viviane Z. Rocha, 2009).

1.3.15 Plaque destabilization and rupture

At the advanced stage of atherosclerosis, plaque was growing and the numbers of foam cells accumulate around plaque and plaque shoulder was increased. Foam cells contribute into the local inflammation through the secretion of pro-inflammatory mediators such as chemokines, cytokines, reactive oxygen species (ROS), and matrix-degrading proteases. It has reported that stability and strength of the fibrous cap covering the plaque is the result of a dynamic process between extracellular matrix such as gelatin, fibrinogen, and collagen and their degradation by matrix metalloproteinases (MMPs) (Figure 1.12) (Hakan Orbay, 2013). After plaque rupture, a small piece of plaque or a clotting blood known as thrombus will flow into the blood circulation leading to cardiovascular disease, cerebrovascular disease, myocardial infarction, stroke, and death.

Several studies report that lipid-loaded macrophages stimulated by ox-LDL associated with the expression of MMPs around the atherosclerotic lesion. Nowadays, MMP-2 and MMP-9 are the most studies among several types of MMPs family (Gabriela M. Sanda, 2017; Yue, 2009). However the effect of native LDL and mm-LDL to MMPs expression is not much understood.

1.3.16 Matrix metalloproteinases

Proteases are involved in the progression of atherosclerosis due to the destruction ability of vascular extracellular matrix. The destruction of extracellular matrix proteins such as collagen, gelatin, elastin, and matrix glycoproteins around fibrous cap and adjacent shoulder regions of atherosclerotic plaque can reduce plaque size, promote plaque instability and rupture. Consequently, thrombus that occurred after plaque rupture can lead to myocardial infarction and stroke.

Matrix metalloproteinases (MMPs), one of protease family are found in atherosclerotic lesions. MMPs family is a large family of proteolytic enzymes consists of 23 human zinc-dependent endopeptidases. These enzymes are excreted by variety of connective tissues and pro-inflammatory cells including fibroblasts, osteoblasts, endothelial cells, macrophages, and lymphocytes (Newby, 2007). There are several types of MMPs based on their substrates. Nowadays, at least 28 human MMPs were found as shown in Table 1.1. Based on their substrate specificity, MMPs are classified into collagenases, gelatinases, stromelysins, and matrilysins. Most of MMPs are secreted form. However, 6 membrane types MMPs (MT-MMPs) that are integral membrane protein which has catalytic domain on the cell surface have been reported (Patricia A.M. Snoek-van Beurden, 2005). Catalytic activity of the MMPs can be inhibited by tissue inhibitors of MMPs (TIMPs) that can inactivate MMPs by blocking their catalytic sites as shown in Figure 1.12.

The general domain structure of metalloproteinases consists of signal peptide (SP), pro-domain (Pro), catalytic domain containing zinc atom at the active site, hinge domain (HG), hemopexin-like domain and some cases contain transmembrane domain (TM) within cytoplasmic tail (CT). A furin cleavage site (F)

between pro-domain and catalytic domain is found in MT-MMPs for MT-MMPs activation as shown in Figure 1.13.

Table 1.1 Member of MMPs family**.** (Patricia A.M. Snoek-van Beurden, 2005)

Subgroup	MMP	Name	Substrate
1. Collagenases	MMP-1	Collagenase-1	Col I, II, III, VII, VIII, X, gelatin
	MMP-8	Collagenase-2	Col I, II, III, VII, VIII, X, aggrecan, gelatin
	MMP-13	Collagenase-3	Col I, II, III, IV, IX, X, XIV, gelatin
2. Gelatinases	MMP-2	Gelatinase A	Gelatin, Col I, II, III, IV, VII, X
	MMP-9	Gelatinase B	Gelatin, Col IV, V
3. Stromelysins	MMP-3	Stromelysin-1	Col II, IV, IX, X, XI, gelatin
	MMP-10	Stromelysin-2	Col IV, laminin, fibronectin, elastin
	MMP-11	Stromelysin-3	Col IV, fibronectin, laminin, aggrecan
4. Matrilysins	MMP-7	Matrilysin-1	Fibronectin, laminin, Col IV, gelatin
	MMP-26	Matrilysin-2	Fibrinogen, fibronectin, gelatin
5. MT-MMP	MMP-14	MT1-MMP	Gelatin, fibronectin, laminin
	MMP-15	MT2-MMP	Gelatin, fibronectin, laminin
	MMP-16	MT3-MMP	Gelatin, fibronectin, laminin
	MMP-17	MT4-MMP	Fibrinogen, fibrin
	MMP-24	MT5-MMP	Gelatin, fibronectin, laminin
	MMP-25	MT6-MMP	Gelatin
6. Others	MMP-12	Macrophage metalloelastase	Elastin, fibronectin, Col IV
	MMP-19		Aggrecan, elastin, fibrillin, Col IV, gelatin
	MMP-20	Enamelysin	Aggrecan
	MMP-21	XMMP	Aggrecan
	MMP-23		Gelatin, casein, fibronectin
	MMP-27	CMMP	Unknown
	MMP-28	Epilysin	Unknown

MMPs are categorized according to the organization of their peptide domains, their substrate specificity, and their sequence similarity (8,12,17,22–24,85–87). MMP, matrix metalloproteinase; MT-MMP, membrane-type matrix metalloproteinase.
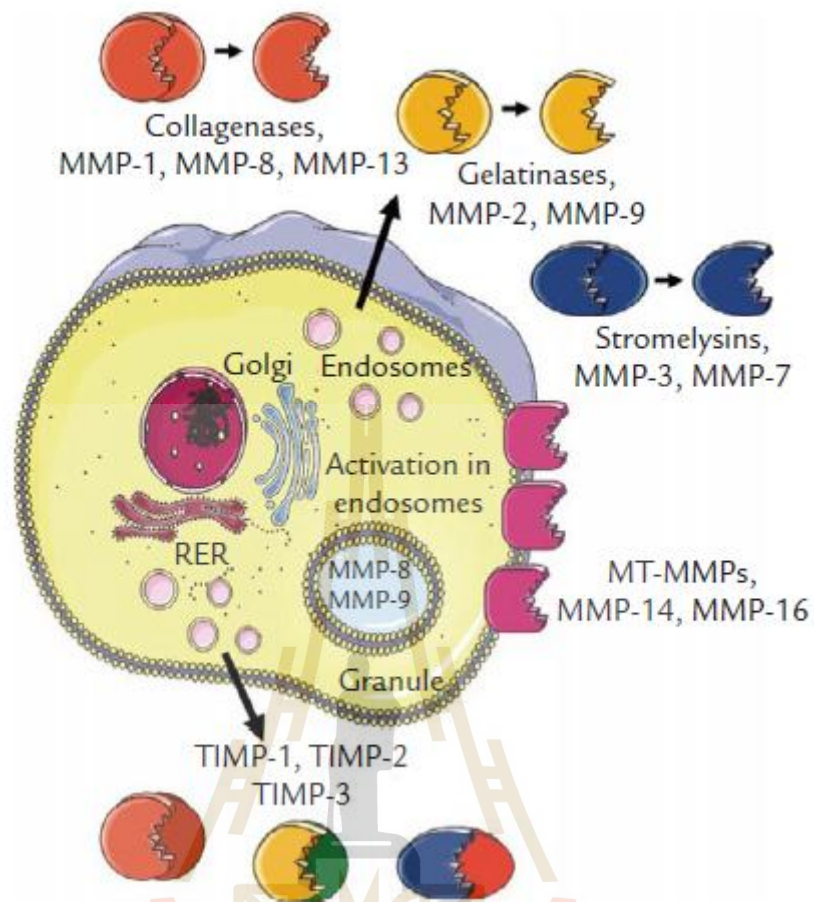
Figure 1.12 MMPs production and activation.

MMPs are synthesized as pro-form in endoplasmic reticulum (ER). Most of MMPs are secreted via endosomal pathway. Secreted MMPs are activated to be an active form by removal of pro-peptide in the extracellular compartment. Some of MMPs are stored in the granule such as MMP-8 and MMP-9. Membrane types of MMPs (MT-MMPs) are expressed on the cell surface and activated in endosomes by furin. Tissue inhibitors of MMPs (TIMPs) are secreted and inactivate MMPs by blocking their catalytic sites (Newby, 2007).
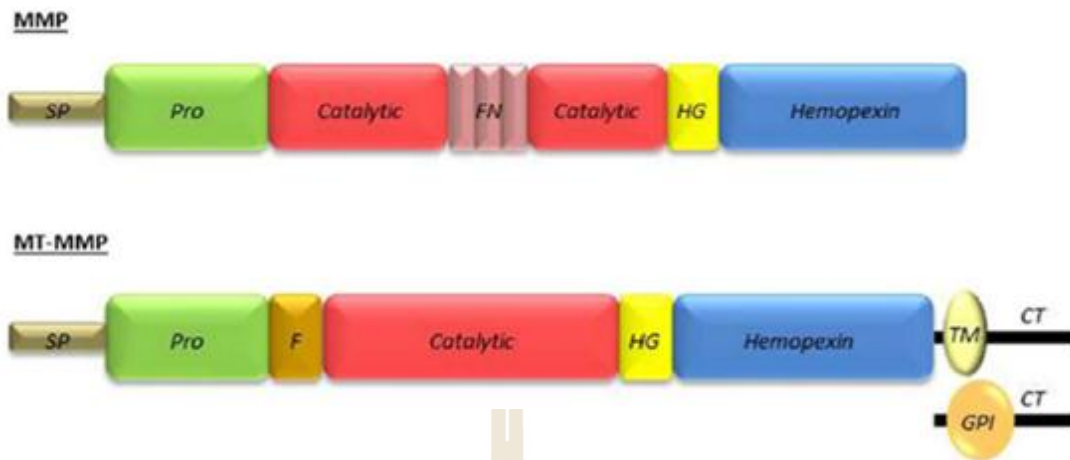
Figure 1.13 MMPs domain structure.

General structural domain of MMPs consists of signal peptide (SP), pro-domain (pro), catalytic domain, hinge region (HG), and hemopexin-like domain. The MMPs in this figure belongs to gelatinases class. It contains fibronectin-like type II repeats (FN) while other classes of MMPs lack this domain. MT-MMPs contain transmembrane domain (TM) or GPI-anchor domain (GPI) with in the cytoplasmic tail. A furin cleavage site (F) between pro-domain and catalytic site is found in general structure of MT-MMPs (Johnson, 2017).

MMPs are expressed as zymogen which has stepwise activation to be an active form. MMPs are synthesized as pro-form. In the pro-domain of MMPs, a cysteine residue as a stabilizer will be cleaved by many proteinases and the non-catalytic zinc will be switch to catalytic form leading to intermediate active MMPs (Johnson, 2017). Moreover, pro-domain of MMPs also can be removed by autolytic cleavage (Eric B. Springman, 1990; Harold E. Van Wart, 1990). Among plaque environment, there are a lot of pathways for MMPs activation including plasmin

system such as tissue plasminogen activator and urokinase plasminogen activator that can generate plasmin from plasminogen in the fibrinolytic system and then indirectly activate multiple MMPs (Lijnen, 2001). Furthermore, MMPs can promote proteolytic through the activation of other MMP members such as activation of MMP-2 by MMP-14 (Alex Y. Strongin, 1994).

Expression of MMPs is associated with many diseases including cancer progression and atherosclerosis. MMPs are involved in atherosclerotic progression including formation of advanced plaques, plaque stability, and the progression of unstable plaque until rupture (Johnson, 2017). Not only removing extracellular matrix protein, but MMPs also promote infiltration of immune-inflammatory cells and enhances angiogenesis of endothelial cells (Pepper, 2001). Both functions of the MMPs are associated with plaque growth and increase vulnerability to rupture (Renu Virmani, 2005).

1.3.16.1 MMP-1

MMP-1 known as collagenase-I is the member of collagenase group which has ability to digest interstitial collagens type I, II, and III. It has reported that cardiotrophin-1, one of pro-inflammatory cytokines belong to IL-6 family induces MMP-1 in human aortic endothelial cells (Akinori Tokito, 2013). It has been proposed that proteolysis of collagens around the fibrous cap of plaque leading to plaque destabilization (Libby, 2013). Up-regulated level of MMP-1 and enhanced collagenolytic activity of MMP-1 is associated with plaque instability (Seppo T. Nikkari 1995; Sukhova GK, 1999). Human MMP-1 was overexpressed in macrophages of apoE knockout mice and shown reduction of plaque size and collagen

content. Thus it has been proposed that MMP-1 may have beneficial for delaying of atherosclerosis progression (Vincent Lemaitre, 2001).

1.3.16.2 MMP-2

MMP-2 known as gelatinase-A is the member of gelatinase group which has ability to digest gelatin and some of collagens. In the catalytic site of native or pro-MMP-2, Zn^{2+} will interact with cysteine residues at the N-terminal of pro-peptide domain leading to inhibiting proteolytic activity. MMP-2 that secreted from the cells can interact with MMP-14 and TIMP-2 which catalyze the proteolytic removal of the pro-peptide domain leading to an active protease. MMP-2 that lack of signal peptide will not be secreted. It can be exposed to reactive oxygen species (ROS) under pathophysiological conditions such as injury and inflammation leading to dissociation of Zn^{2+} at the catalytic site and allowing proteolytic activity (Bryan G. Hughes, 2014). Mechanism of MMP-2 activation is shown in Figure 1.14.
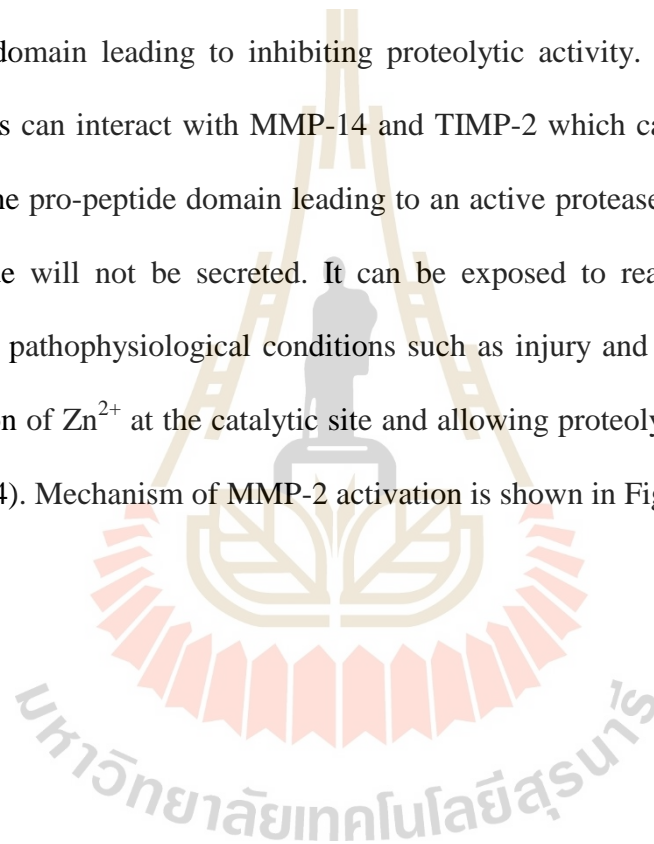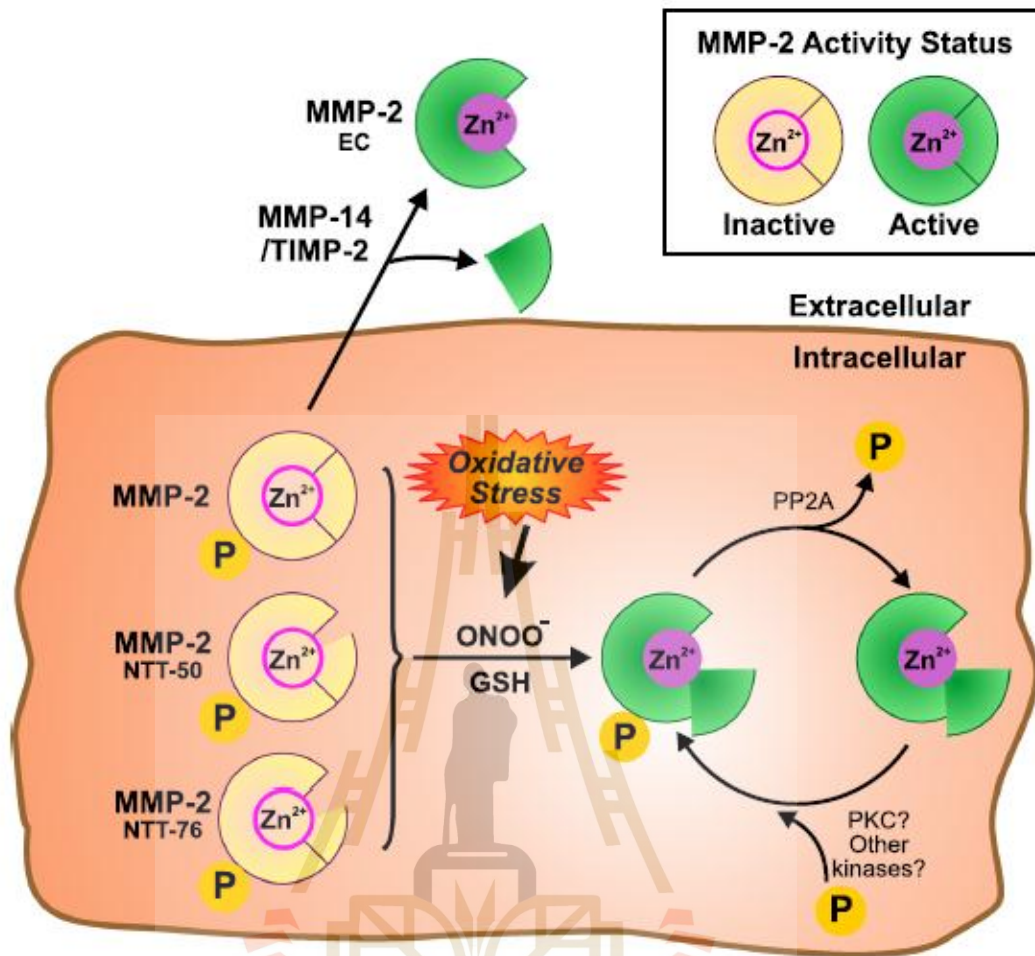
Figure 1.14 Activation of MMP-2.

Reactive oxygen species occurred during oxidative stress such as peroxynitrite (ONOO⁻) and GSH interact with MMP-2 resulting in the S-glutathiolation of the cysteine residue at the pro-peptide domain leading to dissociation of Zn^{2+} at the catalytic site and become active form (Bryan G. Hughes, 2014).

There are evidences support that elevation of plasma MMP-2 was detected in coronary or carotid atherosclerotic plaque complications patients (Beatriz Alvarez, 2004; Hisashi Kai, 1998). They found that MMP-2 expression is associated with less advanced and stable of atherosclerotic plaque. MMP-2 may participate to plaque development through the formation of adaptive intimal thickening since it can attenuate the smooth muscle cells migration from the media into the intima by degrading extracellular matrix proteins that surround the basement membrane barrier, but lacking of MMP-2 did not affect the early phase of inflammation (Masafumi Kuzuya, 2003).

1.3.16.3 MMP-9

MMP-9 known as gelatinase B is the member of gelatinase group which has ability to digest gelatin and type IV collagen. Like all MMPs, MMP-9 is produced in an inactive form called pro-MMP-9 that required activation for enzymatic activity. Chemical or proteolytic mechanisms can trigger the conformational changes that disrupt $Cys-Zn^{2+}$ interaction allowing Zn^{2+} become available for catalytic function (Lakshmi P. Kotra, 2001). The study found that several MMPs can activate pro-MMP-9 such as MMP-2, MMP-3, and MMP-13 (Rafael Fridman, 2003) Figure 1.15.

Pro-MMP-3 is activated by plasmin, which generated from plasminogen by urokinase plasminogen activator (uPA) bound to the uPA receptor on the plasma membrane. This process can lead to pro-MMP-9 activation via plasmin activated MMP-3 (Noemi Ramos-DeSimone, 1999). Pro-MMP-2 is activated by MT1-MMP. Both MT-1 MMP and MMP-2 can activate Pro-MMP-13. Moreover many of serine proteases can also activate MMP-9 (Rafael Fridman, 2003).
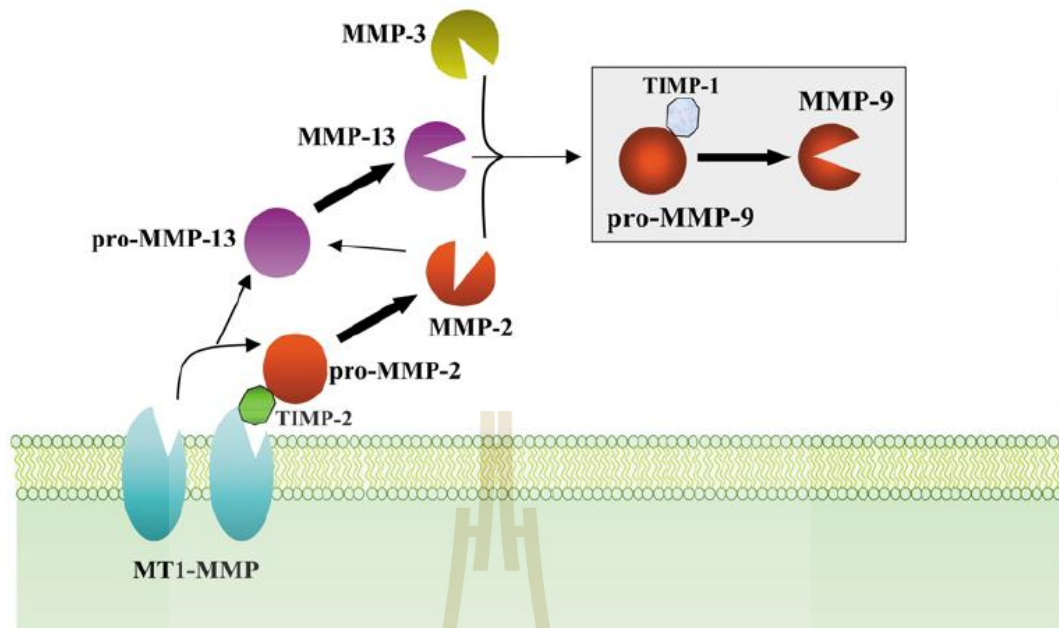
Figure 1.15 Activation of MMP-9.

Pro-MMP-9 can be activated by several MMPs including MMP-2, MMP-3, and MMP-13. This cascade begins with MT1-MMP at the cell membrane and the action of TIMP-2 generates MMP-2. MMP-2 and MMP-13 can further activate pro-MMP-9. MMP-3 is also one of potential pro-MMP-9 activator. Pro-MMP-9 can be found in a complex with TIMP-1 but the role of this complex on activation is unknown (Rafael Fridman, 2003).

While MMP-2 is surface bound, pro-MMP-9 is free in solution. Pro-MMP-9 is not commonly found in the culture cells even contain potential activator, MMP-2. Sometimes, the presence of active MMP-2 does not necessary correlate with pro-MMP-9 activation. Several possibilities may come from TIMPs. Some agents that induce pro-MMP-9 gene expression also induce TIMP-1. TIMPs may inhibit pro-MMP-9 activation by inhibiting the activators. Binding of MMP-9 in

cultured cells will be followed by a rapid dissociation, a process that would not favor activation by a cell surface-associated pro-MMP-9 activator (Rafael Fridman, 2003).

Many studies reported that high MMP-9 level is found in macrophage-rich regions of atherosclerotic lesions. Recent studies found that MMP-9 has a protective role in atherosclerotic plaque since MMP-9 limits plaque growth and promotes stable plaque phenotype. MMP-9 knockout mice increased plaque size in the brachiocephalic artery with less collagen and more macrophages (S. J. G. Jason L. Johnson, Andrew C. Newby, Christopher L. Jackson, 2005). On the other hand, overexpression of pro-MMP-9 has no effect on the size of early or advanced carotid lesions in other studies. It can promote hemorrhage in the advanced plaque lesions but not in the early stage of atherosclerosis (Nooijer, 2006). In addition, macrophage-specific overexpression of active MMP-9 can induce plaque rupture without affecting size or macrophage content (Peter J. Gough, 2006). Moreover, it has been found that increased MMP-9 expression and activity is in response to pro-inflammatory cytokines within atherosclerotic plaque such as IL-1β, TNF-α, and CD40L (Uwe Schonbeck 1997; Zorina S. Galis, 1994).

1.3.16.4 MMP-12

MMP-12, also known as macrophage metalloelastase, was first identified as an elastolytic metalloproteinase secreted by activated macrophages. Function of MMP-12 does not only digests elastin but also other extracellular matrixes such as fibronectin and type IV collagen (Patricia A.M. Snoek-van Beurden, 2005). Recently, MMP-12 was found to be expressed by lipid-loaded macrophages at the lipid core and fibrous area of atherosclerotic plaque whereas no expression was observed in normal artery (Shun-ichiro Matsumoto, 1998). Foam cell macrophages

undergoing apoptosis commonly also express MMP-12 means that MMP-12 may potentiate foam cell macrophages death and contribute to necrotic core expansion (Vincent P. W. Scholtes, 2012).

Many reports found that increasing of MMP-12 is associated with plaque destabilization. They found that MMP-12 can reduce elastin but does not affect the size and cellular composition of early or advanced aortic plaque (Aernout Luttun, 2004). Moreover, overexpression of active MMP-12 will promote inflammation and reduce collagen content of atherosclerotic plaques in rabbits fed extremely cholesterol rich diet (Jingyan Liang, 2006). MMP-12 inhibition in mice was found that the plaque progression was blocked and improved stability since lipid core expansion and macrophages apoptosis was blocked (L. D. Jason L. Johnson, Bertrand Czarny, Sarah J. George, Christopher L. Jackson, Vassilis Rogakos, Fabrice Beau, Athanasios Yiotakis, Andrew C. Newby, Vincent Dive, 2011). Furthermore, patients who have a large number of MMP-12 positive foam cell macrophages were identified as risk of stroke and cardiovascular event (Vincent P. W. Scholtes, 2012).

1.3.16.5 Membrane type MMPs

Six types of MT-MMPs (MT1-MMPs to MT6-MMPs) were found. They have identified as MMP-14, MMP-15, MMP-16, MMP-17, MMP-24, and MMP-25 respectively.

Among 6 of membrane type MMPs, MMP-14 or MT1-MMP has the most studies since they have evidences report that MMP-14 is up-regulated during human atherosclerotic plaque progression (N. P. J. Jason L. Johnson, Wei-Chun Huang, Karina Di Gregoli, Graciela B. Sala-Newby, Vincent P.W. Scholtes, Frans L. Moll, Gerard Pasterkamp, Andrew C. Newby, 2014; Tripathi B.

Rajavashisth, 1999). This type of MMPs is able to secrete as an active form, so it is called membrane-active protease. MMP-14 has broad substrate specificity including gelatin, fibronectin, and laminin (Patricia A.M. Snoek-van Beurden, 2005). High level of MMP-14 was identified in atherosclerotic plaques (Tripathi B. Rajavashisth, 1999). MMP-14 positive foam cell macrophages exhibit increased proliferation and apoptosis which attribute to promote plaque progression and instability. It has been reported that the progression of aortic plaque in rabbits is associated with the increasing of MMP-14 positive foam cell macrophages (G. B. S.-N. Jason L. Johnson, Yasmin Ismail, Concepcion M. Aguilera, Andrew C. Newby, 2008). Numerous evidences suggesting that MMP-14 plays an important role for localized degradation of extracellular matrix associated with plaque rupture because MMP-14 involves in the processing of MMP-2 and MMP-13 activation from inactive to active form (Andrea Lichte, 1996; Vera Knauper, 1996).

For other MT-MMPs family members, they still have not been studied in animal models of atherosclerosis. However, human pathological studies suggest that other MT-MMPs may play a role in atherosclerosis progression. Like MMP-14, MMP-16 is expressed by vascular smooth muscle cells in the media of healthy arteries. It was found that MMP-16 is elevated during coronary plaque progression (Hiroyasu Uzui, 2002).

CHAPTER II

MATERIALS AND METHODS

2.1 Materials

Chemicals, antibodies, cell lines, and instruments used in this study are shown in Appendix A-C.

2.2 Methodology

2.2.1 Preparation of genomic DNA of myeloma cells

P3X63Ag8.653 (ATCC® CRL-1580™) mouse myeloma cells were cultured in 10 cm diameter cell culture dish using Iscove's Modified Dulbecco's Medium (IMDM) (Gibco, Gran Island, NY, USA) supplemented with 10% heat-inactivated FBS (Gibco) at 37°C in 5% CO_2 incubator (Forma Series II water jacket CO_2 incubator, Thermo Scientific, USA). After 80% cell confluences, myeloma cells were harvested and washed twice with 10 ml of incomplete IMDM by centrifugation at 1,500 rpm for each times. The genomic DNA was isolated from the cells using genomic DNA maxi kit for blood and cultured cells (Geneaid®, New Taipei, Taiwan) according to the manufacturer instruction. Polymerase Chain Reaction (PCR) was performed to inspect mycoplasma contamination of myeloma cells before using for hybrid cells preparation.

2.2.2 Detection of mycoplasma contamination by PCR

The mycoplasma DNA was detected using 2 specific primers, forward primer: Ito Myco F1 (5' ACA CCA TGG GAG CTG AT 3') and reverse primer: Ito Myco R1 (5' CCT CWT CGA CTT YCA GAC CCA AGG CAT 3') (BioDesign, Pathumthani, Thailand). Reagents used for amplification reaction were shown in Table 2.1. The PCR cycling condition was 1 cycle at 94°C for 5 min, 35 cycles of denaturation at 94°C for 30 sec, annealing at 55°C for 30 sec, and extension at 72°C for 5 min. The PCR products were analyzed by 1% agarose gel electrophoresis and the DNA bands were visualized under gel documentation system (BIO-RAD, USA) using SYBR green (Thermo Scientific) for a gel staining.
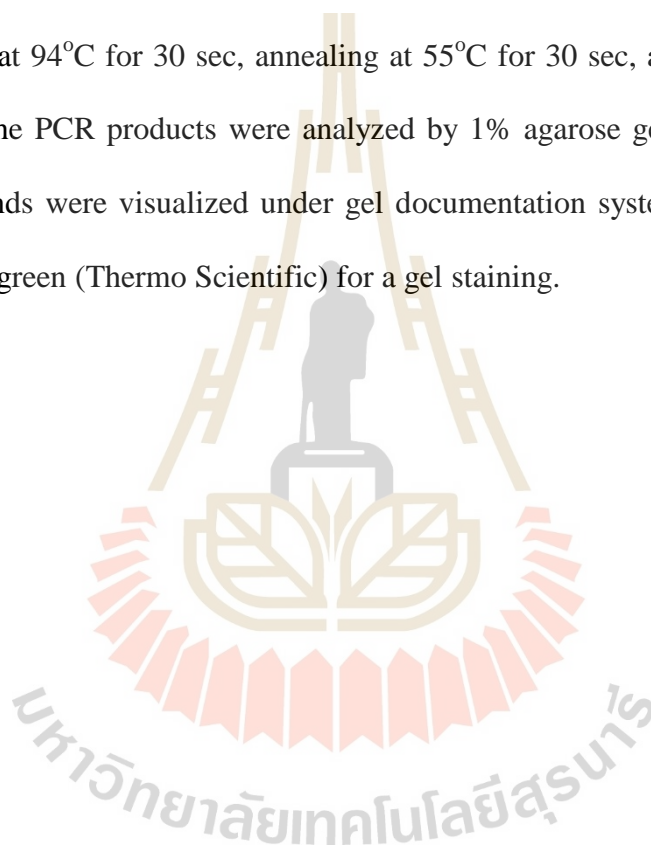
Table 2.1 PCR reaction mixture for mycoplasma detection.

Reaction mixture	Volume (µl)
25 mM MgCl$_2$	2
5X Colorless GoTaq flexi buffer	5
10 mM dNTPs	0.5
10 µM Ito Myco F1	0.5
10 µM Ito Myco R1	0.5
Sterile H$_2$O	11.25
5U/ µl GoTaq DNA polymerase (Promega, Madison, USA)	0.25
50 ng/µl DNA template	5
Total volume	**25**

2.2.3 Production of monoclonal antibodies against human LDL

2.2.3.1 Mouse immunization

Female BALB/c mice (National laboratory animal center, Nakhon Prathom, Thailand) were used in this study. Blood was collected by tail bleeding before immunization. Serum was separated by centrifugation at 4,000 rpm speed for 15 min at RT and used as pre-immunized serum. The mouse was intraperitoneally immunized with 50 µg of commercial human LDL (US Biological, Massachusetts, USA) at 2-weeks interval. Complete Freund's adjuvant (Sigma-Aldrich, St. Louis, MO, USA) was used as an immunopotentiator for the first immunization and incomplete Freund's adjuvant (Sigma-Aldrich) was used in the next immunization. The final volume of each immunization is 300 µl. Two weeks after the third immunization, mouse serum was collected and determined for antibody production by indirect ELISA as described in 2.2.3.2.

2.2.3.2 Indirect enzyme-linked immunosorbent assay (ELISA)

Five hundred nanogram of commercial human LDL was coated onto 96-wells ELISA plate using carbonate/bicarbonate coating buffer pH 9.6 and incubated at RT for 2 h. Then the plate was blocked with 100 µl of 2% skimmed-milk in PBS pH 7.2 at RT. After 1 h of incubation, the blocking solution was discarded and 50 µl of immunized mouse serum, or culture supernatant or purified mAbs was added and incubated at RT for 1 h. The plates were washed using 0.05% Tween®20 in PBS pH 7.2 (0.05% PBST) for 3 times. Fifty microliters of horseradish peroxidase conjugated rabbit anti-mouse immunoglobulins antibody (HRP-Igs) (Dako, Glostrup, Denmark) at dilution 1:5000 was added into each well and incubated at RT for 1 h. To develop color of peroxides reaction, 50 µl of tetramethylbenzidine

(TMB) substrate (Merck, Darmstadt, Germany) was added into each well after 3 times washing with 0.05% PBST. The enzymatic reaction was terminated by adding 100 µl of stop solution (1N HCl) and intensity of the developed color was determined using microtiterplate spectrophotometer (BIO-RAD) at a wavelength of 450 nm.

2.2.3.3 Hybridoma cell generation by standard hybridoma technique

The immunized mouse that produced our desired antibody was sacrificed after 5 days of intraperitoneally boosting with 50 µg of commercial human LDL in 300 µl of incomplete Freund's adjuvant. The spleen was aseptically removed and placed in a 10 cm tissue culture dish containing 7 ml of IMDM medium. Splenocytes were gently isolated by homogenization and the suspension cells were transferred to 50 ml centrifuge tube and let the cell debris to settle down for 10 min. Then, cells suspension was collected by centrifugation at 1,500 rpm for 5 min while contaminated red blood cells were lysed by 0.83% NH_4Cl hypotonic solution. The obtained splenocytes were washed twice with IMDM medium using centrifugation at 1,500 rpm for each time. Number and viability of spleen cells were counted in a Neubauer-improved bright line hemacytometer (Marien Feld, Germany) using Turk's solution and 0.4% trypan blue.

To produce the hybrid cells, splenocytes of the immunized mouse were mixed with P3X63Ag8.653 mouse myeloma cells at the ratio 2:1 and centrifuged at 1,500 rpm for 10 min at room temperature (RT). Briefly, the mixed cell pellet was incubated at $37^{o}C$ for 5 min before fusing together using 50% polyethylene glycol (PEG) (Sigma) following the standard hybridoma technique (Araya Ranok, 2013; Panida Khunkaewla, 2007). The fusion procedure started by

dropping 1.5 ml of 50% PEG into the cell mixture within 1 min and gentle stirred for another 1 min. The cell mixture was suddenly diluted with incomplete IMDM medium by adding the medium and mixing thoroughly with the following rate, 1 ml within 1 min, 3 ml within 1 min, and 16 ml within 2 min. The fused cells were collected by centrifugation at 1,500 rpm for 5 min at RT and warmed at 37°C for 5 min. After removing of the supernatant, the fused cells were re-suspended in 100 ml of Hypoxanthine-Aminopterin-Thymidine (HAT) selection medium (Sigma) supplemented with 10% BM condimed H1 condition medium (Roche Diagnostics, Mannheim, Germany). One hundred microliter of the fused cells was seeded into each well of 96-wells cell cultured plate with flat bottom and cultivated at 37°C in 5% CO_2 incubator to expand the cells. After 5 days of cultivation, 150 µl of Hypoxanthine-Thymidine (HT) medium (Sigma) supplemented with 10% BM condimed H1 condition medium was added into each well. The cells were continually cultured at 37°C in 5% CO_2 incubator to allow the growth of hybridoma clones (Apiratmateekul, 2007).

2.2.3.4 Hybridoma cells screening

The hybridoma cells growth and expansion were observed under CKX 41 inverted light microscope (Olympus, Japan). The clone size was scored into 4 levels as following (Apiratmateekul, 2007):

Very small	clone size was less than 1 in 8 of well
Small	clone size was approximately 1 in 8 of well
Medium	clone size was approximately 1 in 4 of well
Large	clone size was bigger than 1 in 4 of well

Culture supernatants from the large hybridomas containing wells were collected and screened for antibody reactivity against human LDL using indirect ELISA as described in 2.2.3.2.

2.2.3.5 Single cell cloning

To obtain the monoclone antibody producing cells, the hybridoma clones those are positive with human LDL were chosen for single cell cloning by limiting dilution technique. The hybridomas were counted and adjusted the cell concentration to 4, 2, and 1 cell per 150 µl of 10% FBS-IMDM supplemented with 10% BM condimed H1 condition medium. The cells were seeded into 96-wells tissue cultured plate with flat bottom and cultured at 37^oC in 5% CO_2 incubator to allow cell growth for a week. The hybridoma clones size was monitored under an inverted light microscope (CKX41, Olympus). Culture supernatants from the single clone containing wells were collected and screened for antibody reactivity with human LDL using indirect ELISA as describe in 2.2.3.2. The limiting dilution was repeated until the specific antibodies from monoclone were obtained (Apiratmateekul, 2007).

2.2.4 Biochemical characterization of the newly generated mAbs against human LDL

2.2.4.1 Determination of activity and cross-reactivity of the generated mAbs against human LDL

To detect the activity and cross-reactivity of newly generated mAbs against human LDL, indirect ELISA and Western blot analysis were performed as described in 2.2.3.2 and 2.2.4.2 respectively.

2.2.4.2. Western blot analysis

Five microgram of either human LDL (US Biological) or VLDL (Abcam, England) was resolved on 10% SDS-PAGE under non-reducing or reducing condition using SDS-PAGE apparatus (BIO-RAD), then electrophoretically transferred onto PVDF blotting membrane (Millipore, Billerica MA, USA) by semi-dry transferring technique using trans-blot semi-dry transfer cell (BIO-RAD). After protein transferring, non-specific binding was blocked by 5% (w/v) skimmed-milk in 1x PBS pH 7.2 and incubated at RT for 1 h on the rocking shaker (Rocker II Model 260530, Boekel Scientific, Feasterville, P.A.). The blocked membrane was rinsed once with 1x PBS pH 7.2, cut into 1 cm strip and then incubated each membrane for additional 1 h in culture supernatant containing the generated mAb against human LDL at RT. The membrane was washed using 0.1% PBST for 5 times at RT, 5 min for each wash. Signals representing antibody-protein interactions were detected with HRP-conjugated rabbit anti-mouse Igs (Dako) at dilution of 1:5000 using enhance chemiluminescence method. Briefly, the chemiluminescent substrate reagent was applied to cover all surface of the membrane at RT for 3 min. The protein band was visualized by developing with x-ray film (Carestream, Rochester, NY, USA) at various time points.

2.2.4.3 Isotypic determination

To determine the isotype of our generated mAbs, the mouse monoclonal antibody isotyping reagents (Sigma Aldrich) was used according to the manufacturer procedure. Briefly, known antibodies against different isotypes of immunoglobulin (IgA, IgG_1, IgG_{2a}, IgG_{2b}, and IgM) were diluted in carbonate/bicarbonate coating buffer pH 9.6 at dilution of 1:1000 and coated onto 96-

wells, ELISA plate for 50 µl per well and incubated at $4^{o}C$ for overnight. The plate was blocked with 100 µl of 2% skimmed-milk in 1x PBS pH 7.2 for an hour at RT. After removing of blocking solution, 50 µl of culture supernatant of each clone was added into each well and incubated at RT for an hour. Then the plate was washed with 0.05% PBST for 3 times. Then 50 µl of HRP-Igs at a dilution of 1:5000 was added into each well and incubated at RT for 1 h. Then the plate was washed with 0.05% PBST for 3 times. Finally, 50 µl of TMB substrate was added into each well and incubated at RT. the reaction was terminated by adding 100 µl of 1N HCl and the absorbance value was measured using microplate spectrophotometer (BIO-RAD) at a wavelength of 450 nm.

2.2.5 Monoclonal antibody purification

High amount of newly generated mAbs against human LDL was prepared by culturing the mAbs against human LDL producing hybridomas in ISF-1: serum-free medium (Biochrom AG, Berlin, Germany) at $37^{o}C$ in CO_2 incubator. Culture supernatant containing mAb to human LDL was collected for further purification.

2.2.5.1 Monoclonal antibody purification by affinity chromatography

Culture supernatant containing each clone of specific mAb against human LDL in serum free medium was collected and centrifuged at 1,500 rpm for 5 min at $4^{o}C$ to removed cell contamination. Purification of the mAbs were performed using either HiTrap Protein G HP column (GE Healthcare, Uppsala, Sweden) or HiTrap IgM purification HP column (GE Healthcare) for IgG and IgM isotype purification respectively that linked to AKTA start protein purification system

(GE Healthcare). The purification procedure was followed manufacturer instruction. After purification, the purified mAb was dialyzed against PBS pH 7.2 at 4°C for overnight using Spectrum™ Spectra/Por™ dialysis membrane which molecular weight cut off 12,000 to 14,000 dalton (Thermo Scientific) and the concentration of purified mAb was measured by Pierce™ BCA protein assay kit (Thermo Scientific).

2.2.5.2 Purity of purified mAbs

Purity of the purified mAbs was examined by SDS-PAGE. Five microgram of purified mAbs was resolved in 10% SDS-PAGE under non-reducing and reducing condition at constant voltage 120 volt. Protein bands were visualized by staining the gels with Coomassie Brilliant Blue R250.

2.2.5.3 Activity and cross-reactivity examination of the purified mAbs

The activity and cross-reactivity of the purified mAbs were examined by Western blot as described in 2.2.4.2 and indirect ELISA as described in 2.2.3.2.

2.2.6 Conjugation of the generated mAbs against human LDL with Sulfo-NHS-LC-Biotin

Conjugation of the generated mAbs with EZ-Link NHS-LC-Biotin (Thermo Scientific) was performed according to the manufacturer instruction. Briefly, the molar ratio of biotin to antibody was adjusted to 20-fold or 50 –fold molar excess of biotin reagent for 1-10 mg or 50-200 µg of mAbs in 500 µl of PBS pH 7.2, respectively. One milligram of biotin was dissolved in 180 µl of sterile water to prepare 10 mM of biotin working reagent. Then the calculated volume from the desired ratio of biotin was added to the antibody solution. The reaction was performed

by rotation the mixing solution at 4°C for 2 h. The excess biotin was removed by dialysis against 1x PBS pH 7.2 at 4°C for overnight. The concentration of the conjugated mAbs was determined using BCA protein assay kit (Thermo Scientific). The appropriate concentration of the conjugated mAbs against human LDL was titrated for the optimum concentration used in the experiment by indirect ELISA as described in 2.2.3.2. HRP-conjugated streptavidin (Invitrogen, USA) at dilution 1:2500 was used as a detector instead of HRP-Igs.

2.2.7 Epitope binding determination of the generated mAbs against human LDL

To assess the binding epitope among the generated mAbs against human LDL, inhibition ELISA was performed. Briefly, 500 ng of human LDL was coated onto ELISA plate using carbonate/bicarbonate coating buffer pH 9.6 and incubated at RT for 2 h. The plate was then blocked by adding of 100 μl of 2% skimmed-milk in 1xPBS pH 7.2. After 1 h of incubation at RT, the blocking solution was discarded before adding of 500 ng of unconjugated-mAb against human LDL and incubated at RT for 1 h. The plate was washed with 200 μl of 0.05% PBST for 3 times. After that, 50 μl of the appropriated concentration of biotinylated-mAbs against human LDL was added and incubated at RT for an hour. The plate was washed with 200 μl of 0.05% PBST for 3 times. Fifty microliters of HRP-conjugated streptavidin at dilution 1:2500 was added and incubated at RT for 1 h. The color of peroxide reaction was developed by adding 100 μl of TMB substrate into each well after 3 times washing with 0.05% PBST. The enzyme reaction was terminated by adding 100 μl of 1N HCl. The intensity of the developed color was determined

spectrophotometrically using microtiterplate spectrophotometer (BIO-RAD) at a wavelength of 450 nm.

2.2.8 Direct LDL measurement

2.2.8.1 Titration for an optimal concentration of the mAbs against human LDL used for development of LDL level assessment

The suitable concentration of the generated mAbs against human LDL used for determination of LDL level in human plasma was titrated using indirect ELISA as described in 2.2.3.2. Various concentrations of the generated mAbs against human LDL were prepared in 2-fold serial dilution range from 0.078 to 10 μg/ml.

2.2.8.2 LDL precipitation using heparin/citrate pH 5.04

Human plasma was isolated from heparinized whole blood by centrifugation at 1,500 x g speed for 30 min at RT. For 100 μl of plasma was mixed with 1 ml of heparin citrate pH 5.04 solution, 0.064 M trisodium citrate pH 5.04 containing 5,000 IU/ml of heparin (Troikaa Pharmaceuticals, India), the final pH of the mixture was adjusted to 5.11 and let the mixture was stood at RT for 10 min. The LDL pellet was collected by centrifugation at 1,000 x g speed for 10 min at RT. The pellet was dissolved in 100 μl of 1x PBS pH 7.2 (Heinrich Wieland, 1983).

2.2.8.3 Direct LDL assessment by sandwich ELISA using the generated mAbs against human LDL

Human LDL was precipitated using heparin/citrate pH 5.04 as described in 2.2.8.2. The amount of precipitated LDL was then directly measured by the developing technique based on sandwich ELISA. Two generated mAbs that recognize different epitope of human LDL were applied for this method; hLDL-E8

(IgG$_1$) and biotinylated-hLDL-2D8 (IgG$_{2b}$) were used as captured and detected antibody, respectively. Briefly, 500 ng of mAb against human LDL clone hLDL-E8 was coated onto 96-wells ELISA plate as a captured antibody and incubated at RT for 2 h. The plate was then blocked for 1 h with 2% skimmed-milk in 1x PBS pH 7.2 at RT. Fifty microliters of commercial standard LDL (United States Biological, Massachusetts, U.S.A.) or specimen was then added and incubated at RT. Concentration of the standard LDL were prepared in 1x PBS pH 7.2 by performing 2-fold serial dilution, range from 0.3125-10 μg/ml. For the specimen, the precipitated LDL was diluted in 1x PBS pH 7.2 to 1:500. After incubation, the plate was washed with 200 μl of 0.01% PBST for 3 times. Fifty microliters of 0.04 μg/ml of the biotinylated-mAb against human LDL clone hLDL-2D8 was added as a detected antibody and incubated for an hour at RT. After incubation, the plate was washed by 200 μl of 0.01% PBST for 3 times and 50 μl of the HRP-conjugated streptavidin at a dilution 1:1250 was added as a reporter and incubated at RT for another 1 h. Excess HRP-conjugated streptavidin was removed by washing with 200 μl of 0.01% PBST for 3 times. Fifty microliters of TMB substrate was added to develop the color of peroxidase reaction. The reaction was terminated by adding of 100 μl of stop 1N HCl and intensity of the developed color was measured using microtiterplate spectrophotometer (BIO-RAD) at a wavelength of 450 nm.

2.2.8.4 Statistical analysis

Statistical analysis and data management were carried out using GraphPad Prism 5.0 (GraphPad Software, Inc., San Diego, CA). Data analysis was performed using one-way, two-way ANOVA, and linear regression analysis. Results were considered significant if $p < 0.05$ (***, $p < 0.001$; **, $p < 0.01$; *, $p < 0.05$).

2.2.9 Study of the role of mm-LDL cholesterol in matrix metalloproteinases (MMPs) expression

2.2.9.1 Preparation of oxidized-LDL

Oxidized-LDL was generated using 10 μM of $CuSO_4$ as an oxidizing agent. First, heparinized blood was collected from randomized donors and plasma was separated by centrifugation at 1,500 x g speed for 30 min at RT. LDL was then precipitated from plasma sample using heparin/citrate pH 5.04 as described in 2.2.8.2. Precipitated LDL at a final concentration 1 mg/ml was incubated with 10 μM of $CuSO_4$ in a final concentration at $37^{o}C$ at 9 and 48 h. for mm-LDL and fully ox-LDL respectively.

2.2.9.2 Determination of LDL oxidation degree by Thiobarbituric Acid Reactive Substances (TBARS) assay

One hundred microliter of different types of LDL; native LDL, precipitated LDL, mm-LDL, and ox-LDL at the same concentration were mixed with 500 μl of 25% CH_3COOH and 500 μl of 1% thiobarbituric acid (TBA) and incubated at $95^{o}C$ for 45 min to allow the development of pink color of MDA-TBA complex. The mixtures were centrifuged at 1,000 x g for 30 min at RT. Then supernatant was collected and measured the intensity of the pink color of MDA-TBA complex at wavelength 532 nm using Genesys 20 spectronic spectrophotometer (Thermo Scientific). To quantify the amount of lipid oxidation, standard malondialdehyde (MDA) (Acros Organics, New Jersey, USA) was used for preparation of standard curve.

2.2.9.3 Determination of protein modification of LDL

To determine the modification of protein part in the human LDL particle, the generated mAbs against human LDL were used as a tool to track the modified protein by indirect ELISA. Same concentration of different types of LDL; native LDL, precipitated LDL, mm-LDL, and ox-LDL was coated onto 96-wells ELISA plate using carbonate/bicarbonate coating buffer pH 9.6 and incubated at RT for 2 h. The following steps of indirect ELISA were performed as described in 2.2.3.2.

2.2.9.4 Differentiation of human monocytic cell lines into macrophages cells

Human monocytic cell lines; U937 and THP1 were cultured in RPMI-1640 medium (Gibco) containing 10% heat-inactivated fetal bovine serum (FBS). Five hundred thousand cells were seeded into 12-wells tissue culture plate and phorbol 12-myristate 13-acetate (PMA) (Sigma Aldrich), as an activator to promote their differentiation into adherent macrophages was added into the cells to get a final concentration 100 ng/ml. The final volume of each well is 1 ml. The cells were allowed to differentiate to become macropahges by incubation at $37^{o}C$ in 5% CO_2 incubator. After 48 h of incubation, non-adherent cells were removed by aspiration and the adherent cells, which were supposed to be macrophages were washed 2 times by incomplete RPMI-1640 and re-cultured in Optimem® reduced serum medium (Gibco) for further study.

2.2.9.5 Investigation of foam cell formation induced by different degree of LDL oxidation

PMA-derived macrophages from 2.2.9.4 were continuously cultured in Optimem® reduced serum medium. Different types of LDL; native LDL, precipitated LDL, mm-LDL, and ox-LDL were added into each well to get a final concentration of 50, or 100, or 200 µg/ml. The cells were re-cultured at 37°C in, 5% CO_2 incubator at various time points range from 6 to 48 h. The morphological of the macrophages-derived foam cells was observed by staining the lipid droplets in foam cells with Oil Red O and visualized under CKX41 inverted light microscope. The treated cells were gently rinsed with 1 ml of 1x PBS pH 7.2, fixed by 1 ml of 0.1% filtrate paraformaldehyde for 1 min and aspirated out. The treated cells were gently rinsed with 1 ml of 1x PBS pH 7.2 and then 1 ml of 60% isopropanol was used to permeate the cells for 15 seconds. Oil Red O working solution was prepared by dilution of 0.5% Oil Red O in deionized H_2O at the ratio of 6:4 and filtrated before use. The treated cells were stained by 1 ml of Oil Red O working solution for 1 min at RT. Then the stained cells were immediately de-stained by 1 ml of 60% isopropanol for 15 seconds. Finally, the stained cells were gently rinsed by 1 ml of 1 x PBS pH 7.2 for 3 times. The red oil droplets of lipid in the macrophages were observed under inverted light microscope (IX51, Olympus). The amount of red oil droplets in each condition was counted by using 10 fields randomized, 40X magnification of objective lens as representative.

2.2.9.6 Investigation of MMPs expression from macrophage-derived foam cells induced by different degree of LDL oxidation

To study the effect of different degrees of LDL oxidation on the expression of MMPs, PMA-activated macrophages were treated with different types of LDL; native LDL, precipitated LDL, mm-LDL, and ox-LDL at various concentrations (50, 100, and 200 µg/ml) as described in 2.2.9.5. The treated cells were used for determination of the MMPs expression at the mRNA level as described in 2.2.9.9 and the culture supernatants were used for determination of the MMPs at the proteins level as described in 2.2.9.10.

2.2.9.7 RNA extraction

The total RNA of treated cells was firstly extracted using Trizol® reagent (Invitrogen). According to the manufacturer instruction, treated cells from 2.2.9.6 were lysed by adding of 500 µl of Trizol reagent and the cells suspension was mixed well by pipetting up and down for several times. The mixture was transferred into a new microcentrifuge tube and stood at RT for 5 min to allow a complete dissociation of nucleoprotein complexes. One hundred microliters of chloroform (Carlo Erba, Milan, Italy) was added and the mixture was vigorously shaken for 15 seconds and stood at RT for 15 min before centrifugation at 12,000 x g for 15 min at 4°C. The colorless top layer was transferred to new microcentrifuge tube and 250 µl of isopropanol was added. The tube was inverted and incubated at RT for 10 min. The RNA pellet was collected by centrifugation at 12,000 x g for 10 min at 4°C. Supernatant was discarded and the pellet was washed with 500 µl of 75% ethanol and centrifuged at 7,500 x g for 5 min. Ethanol was removed and the RNA pellet was dried by air for 3-5 min. Then the RNA pellet was dissolved in 30 µl of sterile water.

Concentration and purity of the extracted RNA was measured using ND-1000 nanodrop spectrophotometer (Thermo Scientific).

2.2.9.8 First strand cDNA synthesis

First strand cDNA was synthesized from the extracted RNA according to an instruction of the Viva cDNA synthesis kit (Vivantis, Selangor Darul Ehsan, Malaysia). Briefly, RNA and specific primers were firstly mixed according to the recipe shown in Table 2.2 and incubated at $65^{o}C$ for 5 min before chilling on ice for 2 min. The cDNA synthesis mix was prepared separately according to Table 2.3 and then added into the RNA mixture. The reaction was performed by incubation at $42^{o}C$ for 60 min and terminated by incubation at $85^{o}C$ for 5 min. The first strand cDNA synthesized was kept at $-80^{o}C$ until used. Concentration of the cDNA was measured using ND-1000 nanodrop spectrophotometer (Thermo Scientific).

Table 2.2 RNA and primer mixture.

Mixture	For 1 reaction
Total RNA	1 µg
Oilgo d(T)	1 µl
10 mM dNTP mix	1 µl
Nuclease free water	Top up to 10 µl

Table 2.3 cDNA synthesis reagents.

Component	For 1 reaction
10X Buffer M-MuLV	2 µl
M-MuLV reverse transcriptase	100 unit
Nuclease free water	Top up to 10 µl

2.2.9.9 Determination of MMPs expression at mRNA level

RT-PCR was performed for detection of mRNA expression of MMPs using LightCycler® 480 SYBR Green I Master and LightCycler® 480 Real-Time PCR system (Roche Diagnostics, Mannheim, Germany). The specific primers used for each MMP (BioDesign) are shown in Table 2.4 and the recipes for amplification reaction are shown in Table 2.5. The PCR cycling condition is shown in Table 2.6. The expression of MMPs at mRNA level was quantified by CT value compared with gene expression of actin, a house keeping gene. The specificity of the primers used was analyzed by melting curve analysis. The amplified products were analyzed by 1% agarose gel electrophoresis and the DNA bands were visualized and observed using SYBR green (Thermo Scientific) as a gel staining under gel documentation system (BIO-RAD).

Table 2.4 The specific primers used for MMPs detections.

Sequence name	Direction (5' → 3')	
MMP-1	Forward	CCA-TAT-ATG-GAC-GTT-CCC-AAA
	Reverse	CGC-ATG-TAG-AAT-CTG-TCT-TTA-AAG
MMP-2	Forward	TGA-CCA-AGG-GTA-CAG-CCT-GT
	Reverse	AGA-CGC-CCC-ATA-GAG-CTC-CT
MMP-9	Forward	CTC-TGG-AGG-TTC-GAC-GTG-AA
	Reverse	GGC-TTT-CTC-TCG-GTA-CTG-GA
MMP-12	Forward	CCC-TGT-ATG-GAG-ACC-CAA-AAG
	Reverse	CCA-GAA-GAA-CCT-GTC-TTT-GAA-G
MMP-14	Forward	CTT-CAA-AGG-AGA-CAA-GCA-TTG-G
	Reverse	CGG-TAG-TAC-TTG-TTT-CCA-CGG
MMP-16	Forward	CAA-TGT-GGA-GGT-TTG-GTT-ACA-A
	Reverse	CAT-CCA-GTC-AAT-TGT-GTT-TCT-GTC

Table 2.5 The reaction mixture for RT-PCR.

Reaction mixture	Volume (µl)
2X SYBR green I master mix (Roche)	10
Nuclease free water	4
10 ng/µl cDNA	5
10 µM forward primer	0.5
10 µM reverse primer	0.5
Total volume	**20**
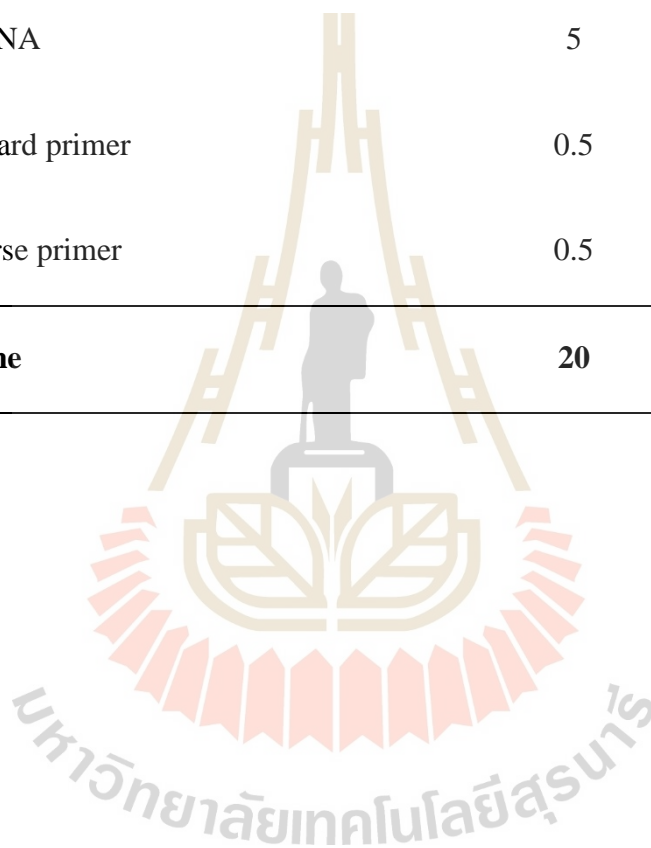
Table 2.6 RT-PCR cycling conditions.

Pre-incubation

$95^{o}C$	5 minutes	

Amplification

$95^{o}C$ for denaturation	10 seconds	
$59^{o}C$ for annealing (depends on Tm of primer)	15 seconds	40 cycles
$72^{o}C$ for extension	20 seconds	

Melting curve analysis

$95^{o}C$	5 seconds	
$65^{o}C$	1 minutes	1 cycle

Cooling

$4^{o}C$	10 seconds	

2.2.9.10 Examination of MMPs expression at protein level

Gelatin zymography was performed to detect MMP-2 and MMP-9 expression at protein level. Culture supernatants from cultivation of the macrophages with different types of LDLs from 2.2.9.5 were collected and protein concentration was measured by Pierce™ BCA protein assay kit (Thermo Scientific). An equal amount of protein from the cultured supernatants of each treatment was resolved under non-reducing condition on 7.5% resolving gel contained 0.2% gelatin (Sigma Aldrich) based on SDS-PAGE. After protein separation, the gel was washed with re-nature buffer (2.5% V/V Triton x-100® in H_2O) for 40 min at RT and was subsequently incubated in activation buffer (50 mM Tris-HCL, 0.15 M NaCl, and 10 mM $Cacl_2$) at 37^oC for 24 h. Lastly, the gel was stained with Coomassie Brilliant Blue R250. The obtaining clear zone on the gel was representing protein expression of the MMP-2 and MMP-9.
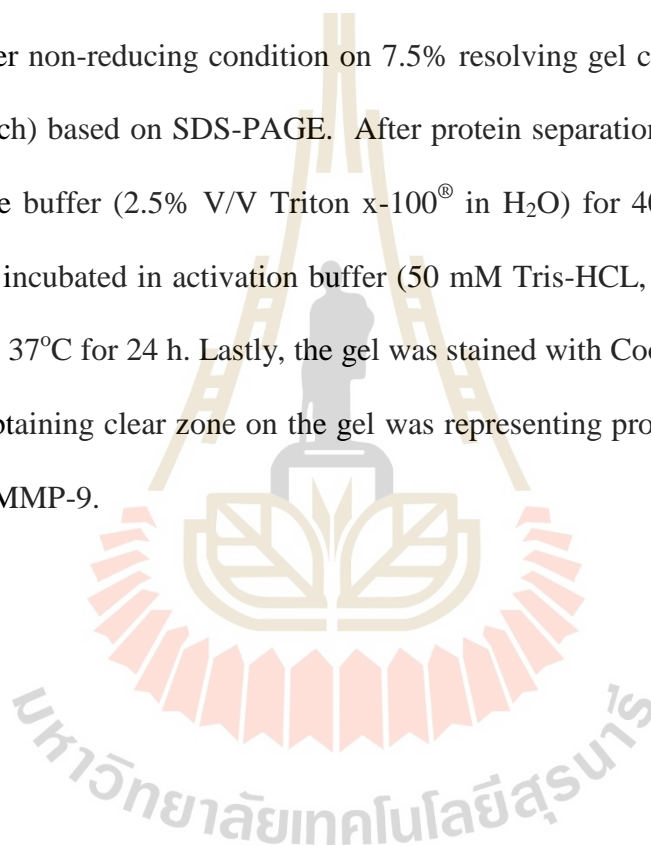
CHAPTER III

RESULTS

3.1 Monoclonal antibodies against human LDL were generated and used for development of direct plasma LDL measurement method

3.1.1 Seven mAbs against human LDL were successfully generated by hybridoma technology

To produce mAb against human LDL, the induction of antibody producing cells was firstly performed by intraperitoneal immunization of a BALB/c mouse with commercial human LDL for 3 times. Pre-immunized serum and the third bleed serum were collected for checking of the antibody response by indirect ELISA.

As shown in Figure 3.1, the titer of the antibody response to human LDL more than 3,200 fold was found in the 3rd bleeded serum compared to the pre-immunized serum, suggesting that the immunized mouse produced antibody against human LDL. To ensure that the mouse myeloma cells used for this study are mycoplasma free, PCR screening for mycoplasma infection using specific primer for 4 strains of mycoplasma was performed before cell fusion. The result showed that no PCR products found from DNA samples of 2 different dishes of mouse myeloma cells. This result indicated that the mouse myeloma cells used for this study are mycoplasma free.

After cell fusion and drug section, 530 wells containing hybrid cells out of 1,788 were grown (29.6%). Only culture supernatant from 150 wells containing large or very large size of hybridoma clones were collected and screen for specificity of the mAbs by indirect ELISA. The result showed that hybridoma clones from 60 wells (3.36%) have positive reactivity with the human LDL. To get the monoclone of anti-human LDL producing hybridomas, 14 of positive clones (0.8%) that show a high antibody response were selected to perform single cell cloning. By performing these experiments, 7 specific mAbs against human LDL (0.4%): designated as hLDL-1E2, hLDL-G10, hLDL-G11, hLDL-E8, hLDL-2D8, hLDL-B6, and hLDL-D4 were obtained. The summary of mAbs against human LDL production yield was shown in Table 3.1.

.
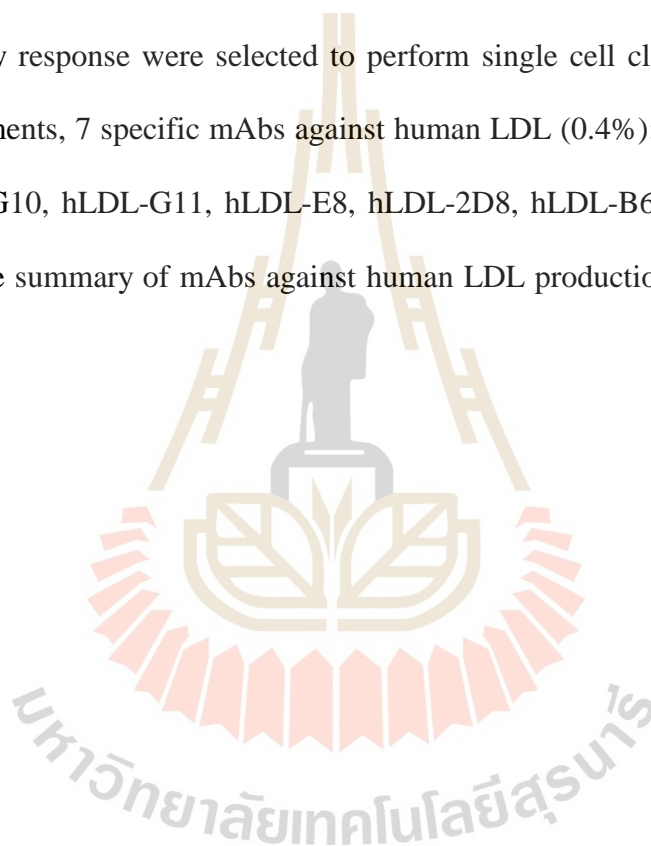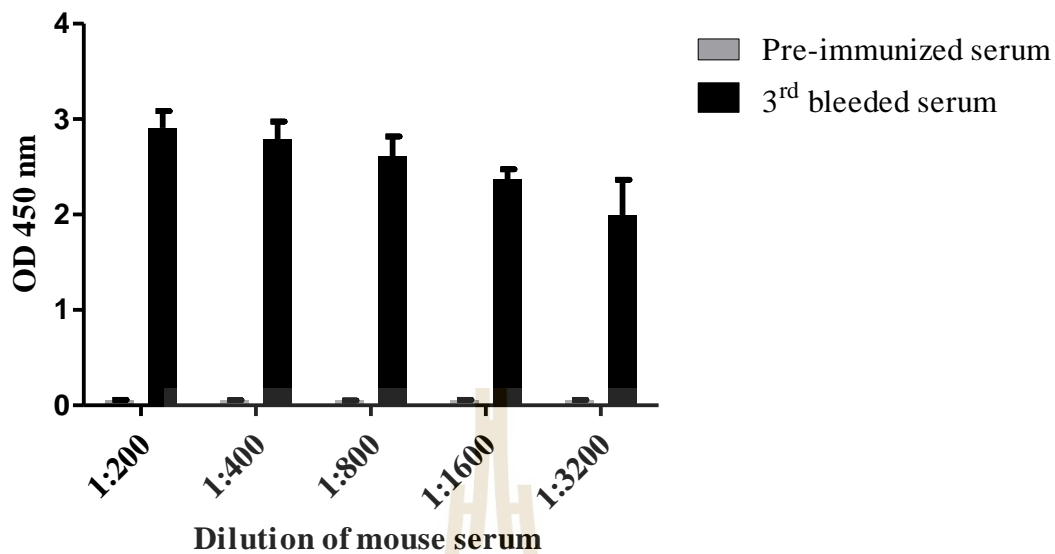
Figure 3.1 Antibody responses in the immunized mouse.

Immune responses against human LDL in serum of the immunized mouse were determined after the third immunization and compared to the pre-immunized serum by indirect ELISA. The data represent the mean ± SD of three independent experiments.

Table 3.1 Percent yield of anti-human LDL mAb producing clone obtained by standard hybridoma technique.

	Number	**%**
Beginning	1788 wells	100
Hybridomas survived	530 wells	29.6
Positive clones with antibody response to human LDL	60 wells	3.36
Selected positive clones for limiting dilution	14 clones	0.8
Final number of specific mAbs against human LDL	7 clones	0.4

3.1.2 Biochemical characterization of newly generated mAbs against human LDL

3.1.2.1 Isotypes of newly generated mAbs against human LDL

Isotypes of mAbs were examined by captured ELISA. As shown in Figure 3.2, the mAbs against human LDL clone hLDL-1E2, hLDL-G10, hLDL-G11, and hLDL-E8 are IgG_1 isotype. Clone hLDL-2D8 is IgG_{2b} isotype. Clone hLDL-B6 and hLDL-D4 are IgM isotype.
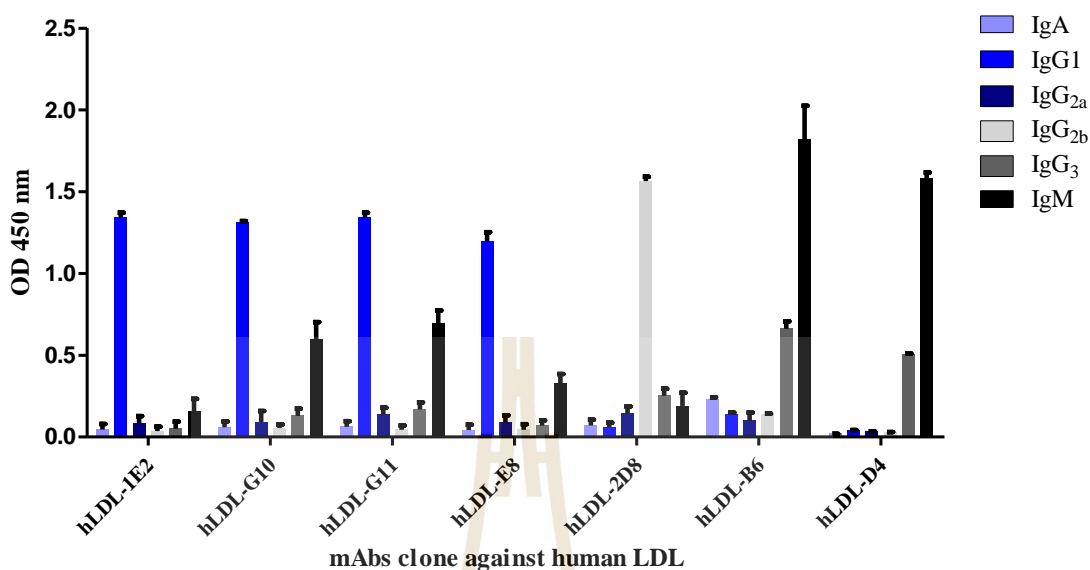
Figure 3.2 Isotypes of the generated mAbs against human LDL.

Culture supernatants containing mAb were determined for their isotyping using captured ELISA kit from Sigma®. The data represent the mean ± SD of two independent experiments.

3.1.2.2 Purity of the generated mAbs against human LDL

To use the generated mAbs against human LDL for further study, high yield of the pure mAbs against human LDL were needed. To obtain the enough pure mAbs, the anti-LDL producing hybridomas were grown in ISF-1 serum free medium (Biochrom). Culture supernatants containing the specific mAbs against human LDL were collected and further purified by affinity chromatography using either HiTrap® protein G sepharose for the IgG isotype mAbs or IgM purification column for the IgM isotype mAbs that linked to AKTA START protein purification system (GE Healthcare).

Purity of the purified mAbs was examined by performing 10% SDS-PAGE under non-reducing and reducing condition. Under reducing condition, 2 protein bands of heavy chain and light chain were found at a molecular weight of 55 and 25 kDa, respectively. While under non-reducing condition, only a band of whole molecule of antibody at a molecular weight about 150 kDa was observed as shown in Figure 3.3.
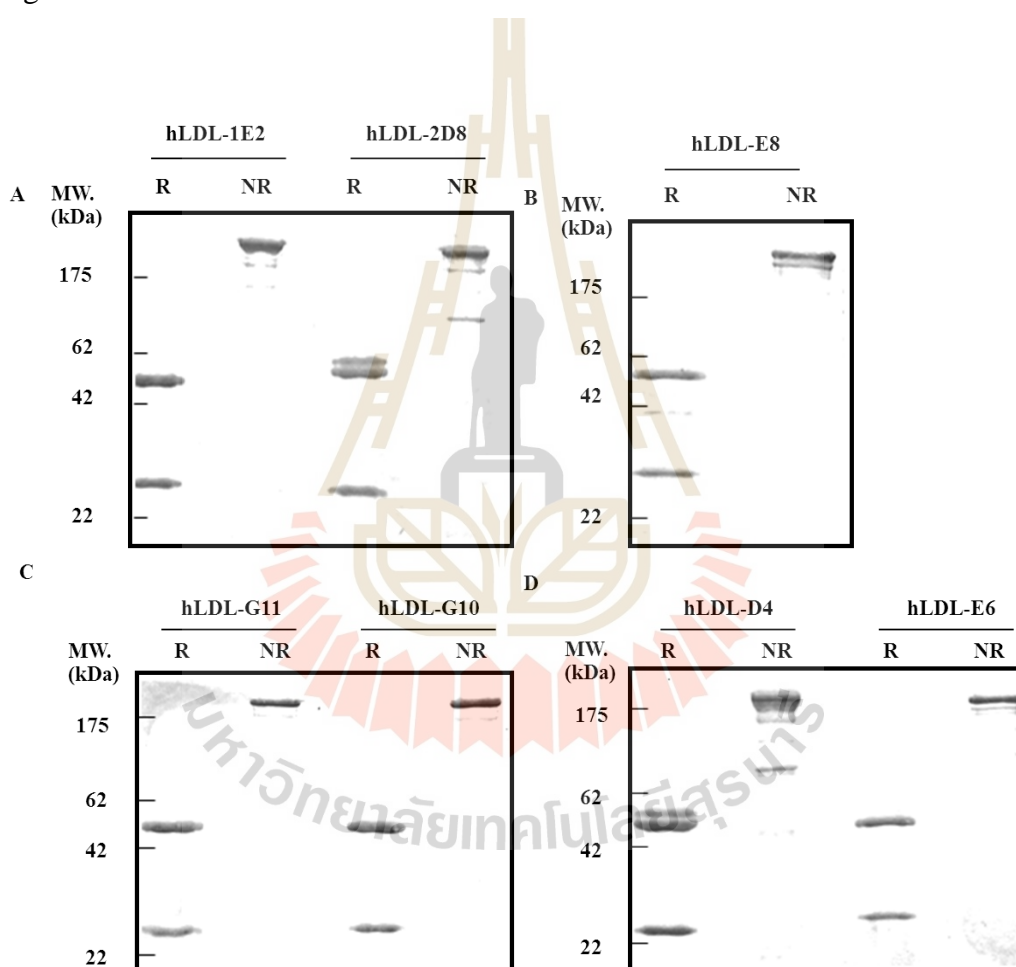
Figure 3.3 Purity of purified mAbs against human LDL.

Purity of the purified mAbs was analyzed by performing 10% SDS-PAGE under reducing condition (R) and non-reducing condition (NR). A representative result from one of three independent experiments is shown.

3.1.2.3 Newly generated mAbs against human LDL specifically bind to apoB-100

Determination of the specificity of newly generated mAbs was performed using Western blot analysis. Different sources of human LDL and VLDL including commercial human LDL from US Biological®, commercial human VLDL from Abcam, supernatant and precipitated apolipoproteins from proteins precipitation using heparin/MnCl$_2$ were used for this study. The proteins were resolved by 10% SDS-PAGE under reducing condition and transferred onto PVDF membrane. Immunoblot was performed using the purified mAbs against human LDL. As shown in Figure 3.4, mAbs clone hLDL-1E2, hLDL-2D8, hLDL-B6, hLDL-D4, and hLDL-E8 were strongly bound to the band of apoB-100 (514 kDa). While lower band of proteins were supposed to be the degrade form of apoB-100. Clones hLDL-G10 and hLDL-G11 were weakly bound to apoB-100. As the apoB-100 is also found in VLDL, we performed LDL precipitation using heparin/MnCl$_2$ and determined the binding activity of the generated mAbs to apolipoproteins found either in the supernatant or precipitant. The results showed that the generated mAbs clone hLDL-1E2, hLDL-2D8, hLDL-B6, hLDL-D4, and hLDL-E8 strongly bound to apoB-100 presented in the precipitant but not reacted with apoE (34 kDa) and apoA1 (29.1 kDa) presented in the supernatant (Figure 3.5). These results suggested that the generated mAbs specifically bind to apoB-100 that found in LDL particle but not apoE and apoA1 which found as the component of other human lipoproteins.
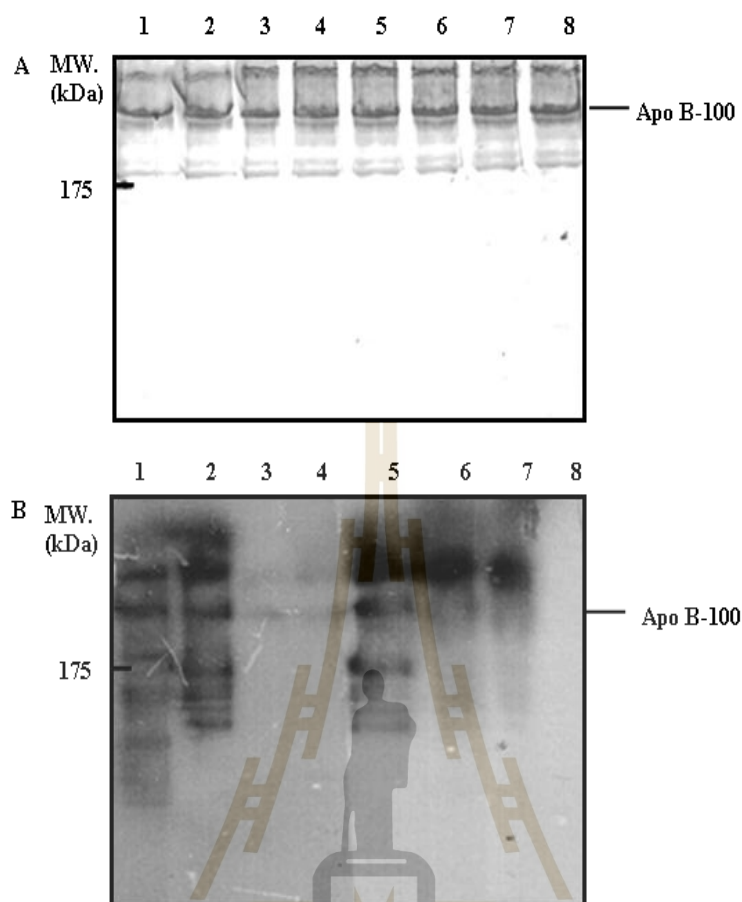
Figure 3.4 SDS-PAGE and Western blot analysis of mAbs against human LDL. Commercial human LDL from US Biological® was resolved by 10% SDS-PAGE under reducing condition and the protein bands were visualized by Coommassie brilliant blue staining (A). Western blot analysis of the commercial human LDL from US Biological® using the purified mAbs against human LDL (B) (lane1: hLDL-1E2; lane 2: hLDL-2D8; lane 3: hLDL-G10; lane 4: hLDL-G11; lane 5: hLDL-B6; lane 6: hLDL-D4; lane 7: hLDL-E8; and lane 8: conjugate control). A representative result from one of three independent experiments is shown.
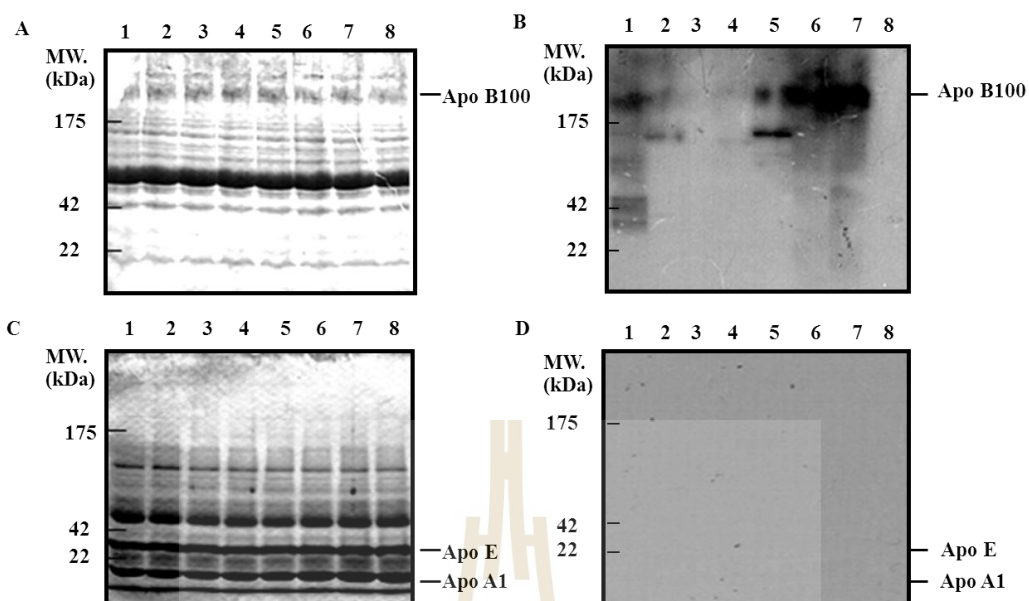
Figure 3.5 Activity and cross-reactivity of newly generated mAbs against human LDL.

Precipitant (A, B) and supernatant (C, D) from proteins precipitation using heparin/MnCl$_2$ were separated by 10% SDS-PAGE under reducing condition. The proteins were transferred onto PVDF membrane and performed immunoblot using the purified mAbs against human LDL. (lane1: hLDL-1E2; lane 2: hLDL-2D8; lane 3: hLDL-G10; lane 4: hLDL-G11; lane 5: hLDL-B6; lane 6: hLDL-D4; lane 7: hLDL-E8; lane 8: conjugate control). A representative result from one of three independent experiments is shown.

3.1.2.4 MAbs against human LDL were conjugated with Sulfo-NHS-LC-Biotin and titrated for an optimal concentration used for the study

In order to determine the binding epitope among the generated mAbs against human LDL using inhibition ELISA, direct conjugation of the mAbs using Sulfo-NHS-LC-Biotin was firstly prepared according to the manufacturer instruction (Thermo Scientific). Before performing the assay, both unconjugated and biotinylated mAbs against human LDL were titrated to find the optimum concentration using indirect ELISA. For unconjugated mAbs assay shown in Figure 3.6, all mAbs showed the best reactivity with the antigen at the final concentration at 10 μg/ml. Thus, this concentration was selected for further experiments.

For the titration of the optimal concentration of the biotinylated mAbs, each clone of the generated mAb was titrated using indirect ELISA. The commercial LDL was used as the antigen of this assay. The results showed that the optimal concentration of the biotinylated-hLDL-2D8 was 0.04 μg/ml at a dilution of 1:5000 for HRP-conjugated streptavidin as a reporter (Figure 3.7) and the optimal concentration of the biotinylated-hLDL-B6 was 0.625 or 0.3125 μg/ml at a dilution of 1:20000 for HRP-conjugated streptavidin as a reporter (Figure 3.8).
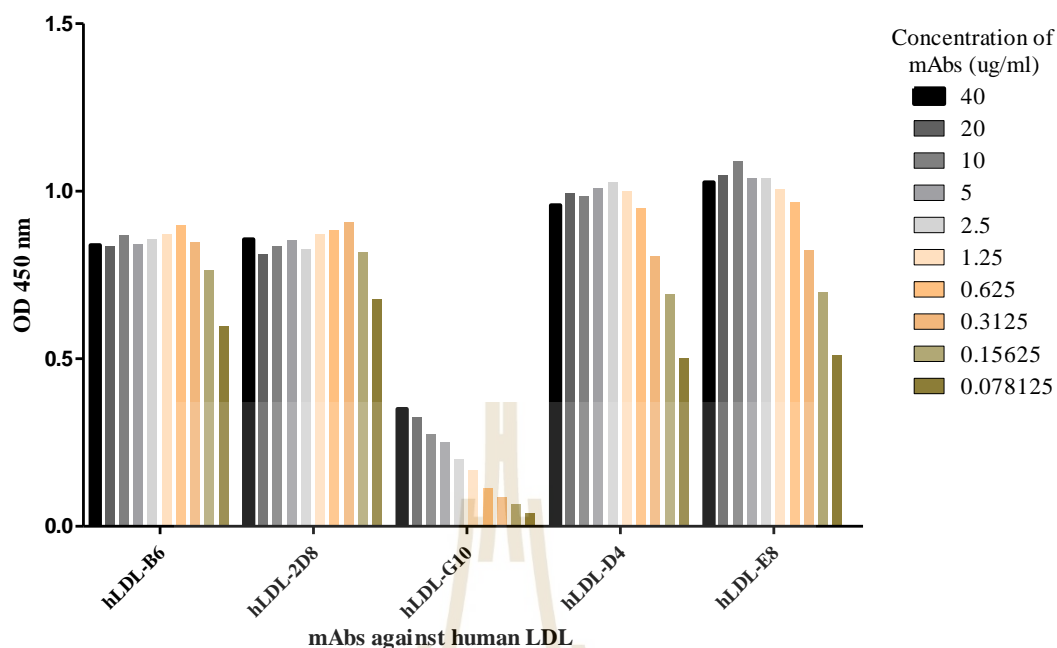
Figure 3.6 Titration of unconjugated mAbs against human LDL

Five hundred nanogram of commercial human LDL was immobilized on ELISA plate. Various concentrations of the newly generated mAbs against human LDL were added and the binding affinity of each concentration was detected using HRP-Igs at dilution 1:5000 and TMB substrate for developing of the color. Optical density of the developed color was measured using microplate spectrophotometer at a wavelength 450 nm. A representative result from one of three independent experiments is shown.
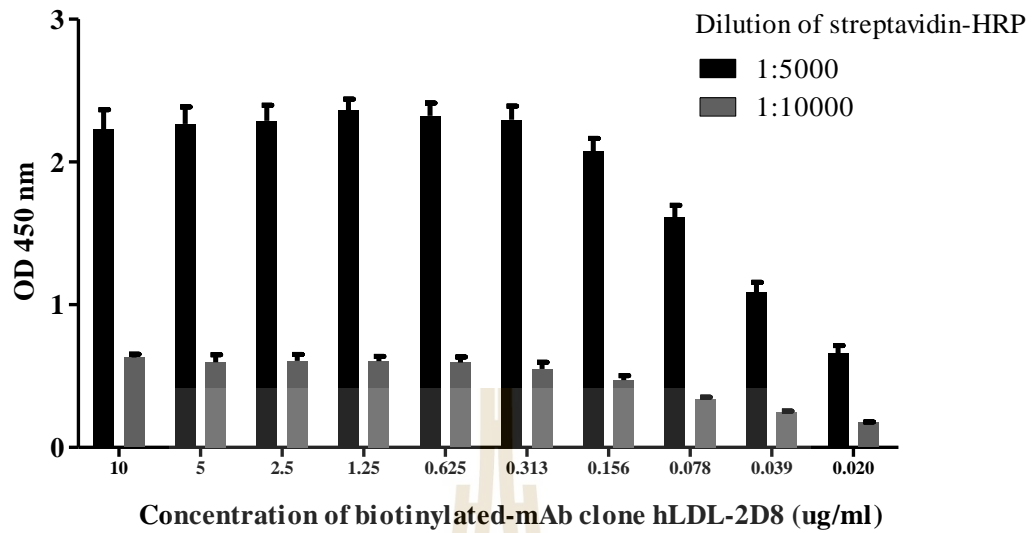
Figure 3.7 Titration of biotinylated mAb against human LDL clone hLDL-2D8.

Various concentrations of the biotinylated mAb clone hLDL-2D8 range from

0.02 - 10 μg/ml were used for determination of the human LDL. The data

represent the mean ± SD of three independent experiments.
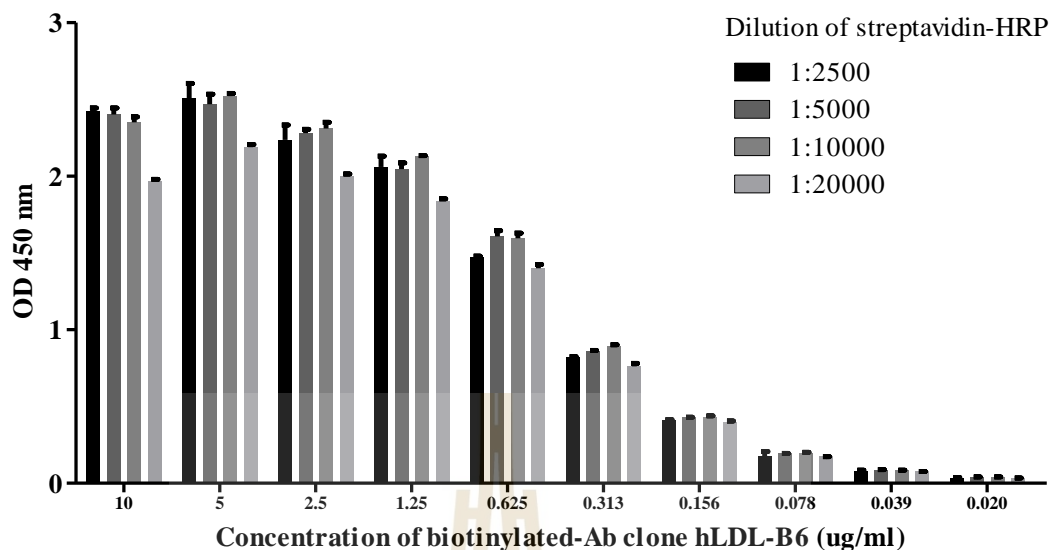
Figure 3.8 Titration of biotinylated mAb against human LDL clone hLDL-B6.

The optimal concentration of the biotinylated mAb to human LDL clone hLDL-B6 was examined by performing indirect ELISA. Five hundred nanogram of commercial human LDL was coated onto each well of ELISA plate. Various concentrations of biotinylated mAb clone hLDL-B6 range from 0.02 – 10 μg/ml were used as a primary antibody and HRP-conjugated streptavidin at dilutions of 1:2500 to 1:20000, were used as the detecting antibody. The data represent the mean ± SD of two independent experiments.
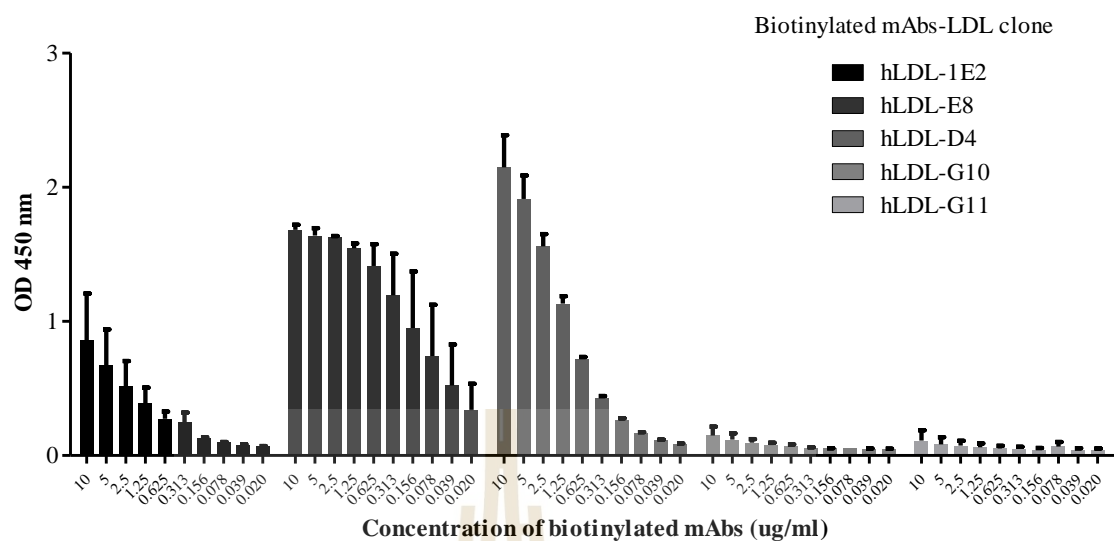
Figure 3.9 Titration of biotinylated mAbs against human LDL clone hLDL-1E2, hLDL-E8, hLDL-D4, hLDL-G10, and hLDL-G11.

Five hundred nanogram of commercial human LDL was coated onto each well of the ELISA plate. Various concentrations of biotinylated mAb range from 0.02-10 μg/ml was added and the antigen-antibody interaction was examined using HRP-conjugated streptavidin at a dilution 1:5000. The color representative of positive result was visualized by adding of TMB substrate into each well. The absorbance value was measured at a wavelength of 450 nm using ELISA plate reader. The data represent the mean ± SD of two independent experiments.

3.1.2.5 Epitope binding site among the generated mAbs against human LDL

To determine the epitope binding site among the generated mAbs against human LDL, inhibition ELISA was performed. To do this, biotinylated of each mAb was used as the detected mAb and was added after the primary unconjugated mAbs. If the biotinylated mAbs can bind to the LDL, positive reactivity will be obtained, which means the different binding epitope with the primary unconjugated mAbs whereas negative reactivity means the primary unconjugated mAb prevented binding of the biotinylated mAb indicating the same or nearly epitope binding site. As shown in Figure 3.10, mAb clone hLDL-D4 and hLDL-E8 bind at different epitope of clone hLDL-2D8 whereas clone hLDL-B6 and hLDL-1E2 bind nearby or same epitope of clone hLDL-2D8. On the other hand, using the biotinylated mAb hLDL-E8 as the secondary antibody, the same result was observed that mAb clone hLDL-B6, hLDL-1E2, and hLDL-2D8 bind at different epitope of the mAb clone hLDL-E8 whereas mAb clone hLDL-D4 binds nearby or same epitope of mAb clone hLDL-E8 as shown in Figure 3.11. Moreover, the experiments were performed using the biotinylated-hLDL-B6 or biotinylated-hLDL-1E2 as the detection antibodies as shown in Figure 3.12 and Figure 3.13. From all vice versa of epitope binding assay, we can conclude that mAb clone hLDL-D4 and hLDL-E8 bind at different epitope of mAb clone hLDL-2D8 whereas mAb clone hLDL-B6 and hLDL-1E2 bind nearly or same epitope of mAb clone hLDL-2D8. The summary of epitope binding site among the generated mAbs against human LDL is shown in Table 3.2. MAbs clone hLDL-E8 and hLDL-2D8 that recognized different epitope of human LDL were selected as a tool for development of direct plasma LDL measurement.
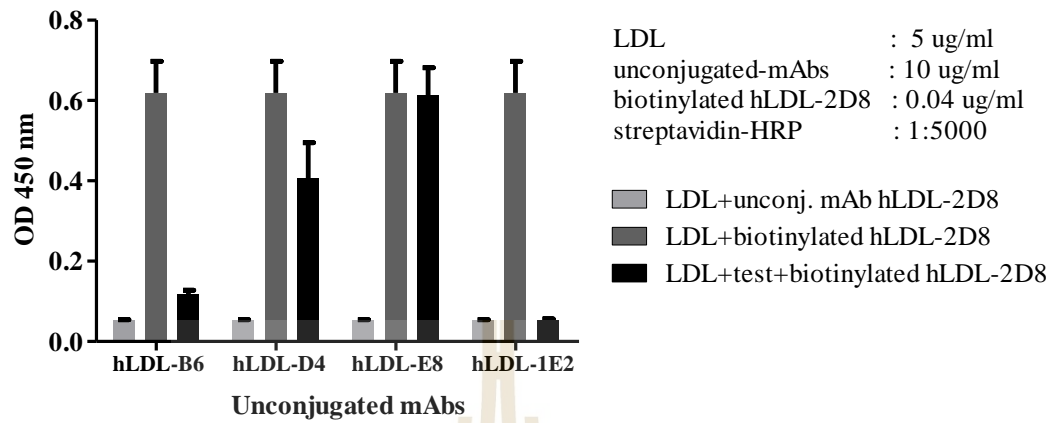
Figure 3.10 Epitope binding assay using biotinylated mAb against human LDL clone

hLDL-2D8.

Epitope binding assay was performed using inhibition ELISA. The binding of

biotinylated-mAb was tracked by HRP-conjugated streptavidin (dilution

1:5000). Unconjugated mAb was used as negative control and biotinylated

mAb was used as positive control. The data represent the mean ± SD of three

independent experiments.
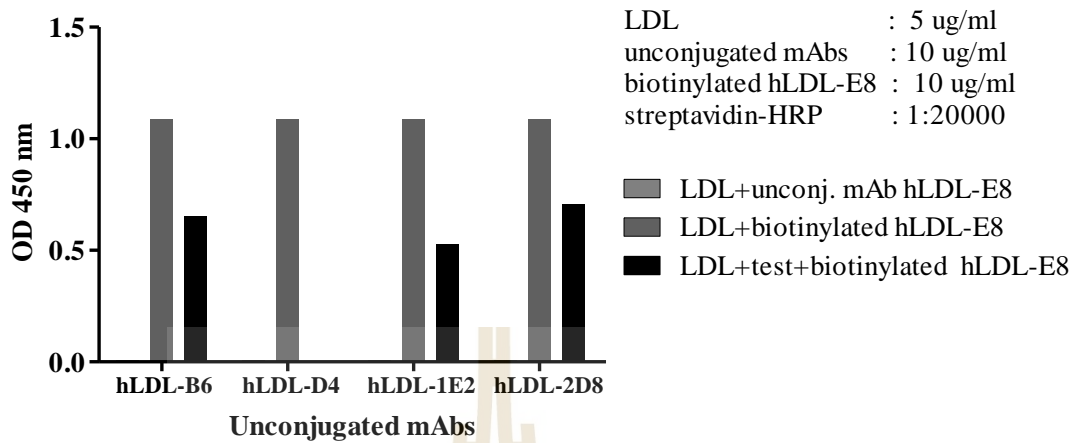
Figure 3.11 Epitope binding assay using biotinylated mAb against human LDL clone hLDL-E8.

Epitope binding assay was performed using inhibition ELISA. The binding of biotinylated-mAb was tracked by HRP-conjugated streptavidin (dilution: 1:5000). Unconjugated mAb was used as negative control and biotinylated mAb was used as positive control. A representative result from one of three independent experiments is shown.
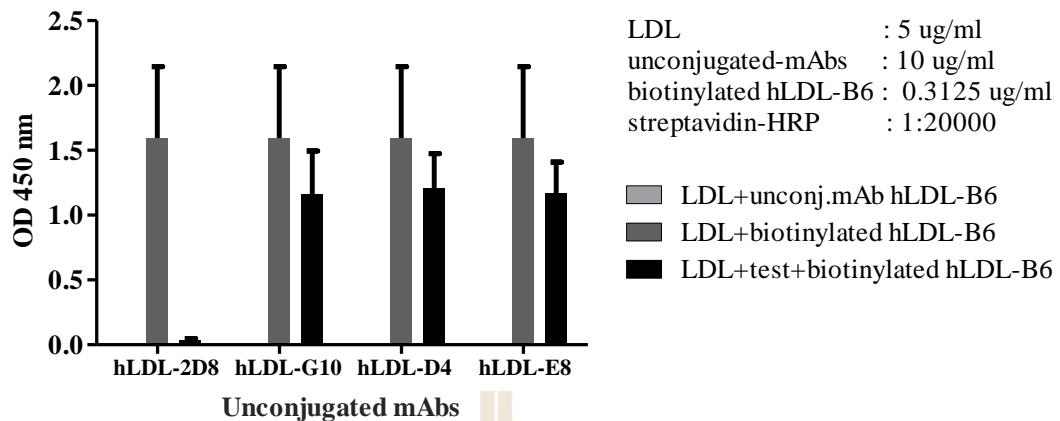
Figure 3.12 Epitope binding assay using biotinylated mAb against human LDL clone

hLDL-B6.

Epitope binding assay was performed using inhibition ELISA. The binding of

biotinylated-mAb was tracked by HRP-conjugated streptavidin (dilution:

1:5000). Unconjugated mAb was used as negative control and biotinylated

mAb was used as positive control. The data represent the mean ± SD of two

independent experiments.
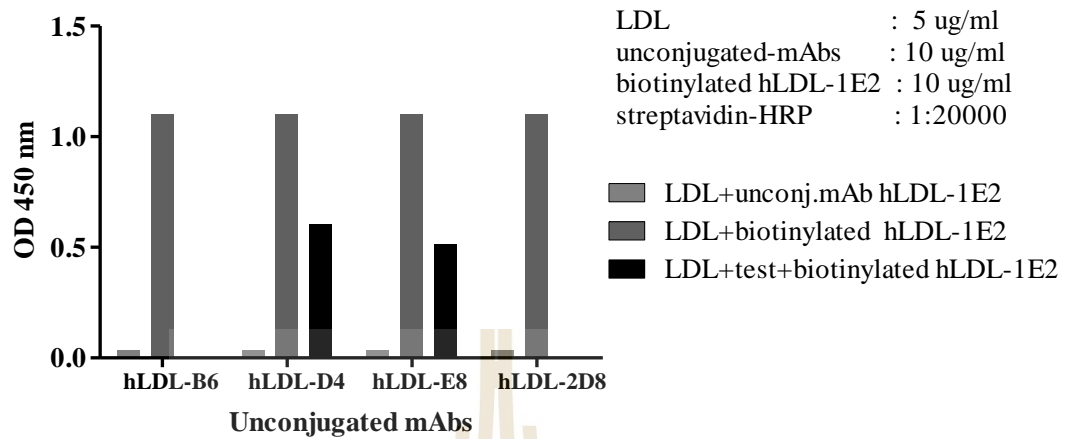
Figure 3.13 Epitope binding assay using biotinylated mAb against human LDL clone hLDL-1E2.

Epitope binding assay was performed using inhibition ELISA. The binding of biotinylated-mAb was tracked by HRP-conjugated streptavidin (dilution: 1:5000). Unconjugated mAb was used as negative control and biotinylated mAb was used as positive control. A representative result from one of three independent experiments is shown.

Table 3.2 Summary of epitope binding site among generated mAbs against LDL.

	biotinylated hLDL-2D8	biotinylated hLDL-E8	biotinylated hLDL-1E2	biotinylated hLDL-B6
hLDL-B6		X		
hLDL-D4	X		X	X
hLDL-E8	X		X	X
hLDL-1E2				
hLDL-2D8		X		

X means recognize different epitope of human LDL

3.1.3 Newly generated mAbs against human LDL were used as a tool for development of direct plasma LDL measurement method

To apply the generated mAbs against human LDL for developing the direct plasma LDL measurement as an alternative method, sandwich ELISA was used as a model and the generated mAb clone hLDL-E8 and hLDL-2D8 which recognize at different epitope of human LDL were used as a developing tool. Unconjugated mAb clone hLDL-E8 was used as a captured antibody and mAb clone hLDL-2D8 was biotinylated and used as a detected antibody respectively. In order to find the optimum concentration of captured and detected antibody for developing the measurement method, concentration of unconjugated mAb clone hLDL-E8 and biotinylated mAb clone hLDL-2D8 were titrated by indirect ELISA. The result

showed that at the final concentration of 10 μg/ml is an optimum concentration for the captured mAb (hLDL-E8), while the optimal concentration for the detected mAb is 0.04 μg/ml. HRP-conjugated streptavidin also was titrated and found that at a dilution 1:2,500 – 5,000 is suitable for used. (Figure 3.14 and 3.15)

To confirm whether mAbs clone hLDL-E8 and hLDL-2D8 are suitable for being captured and detected antibody. Exchanging between the captured antibody and detected antibody was performed. As shown in Figure 3.16. and 3.17, the signal generated by using mAb clone hLDL-E8 as a captured antibody and biotinylated mAb clone hLDL-2D8 as detected antibody gave a better signal than using mAb clone hLDL-2D8 as a captured antibody and biotinylated mAb clone hLDL-E8 as detected antibody. Thus this condition was used for the direct LDL measurement based on sandwich ELISA using our generated mAbs clone hLDL-E8 and hLDL-2D8.
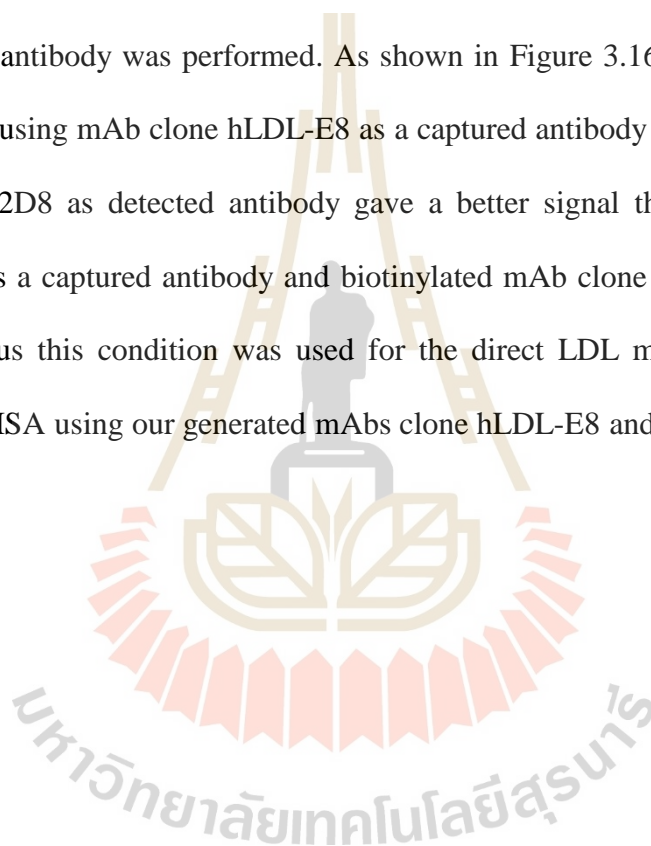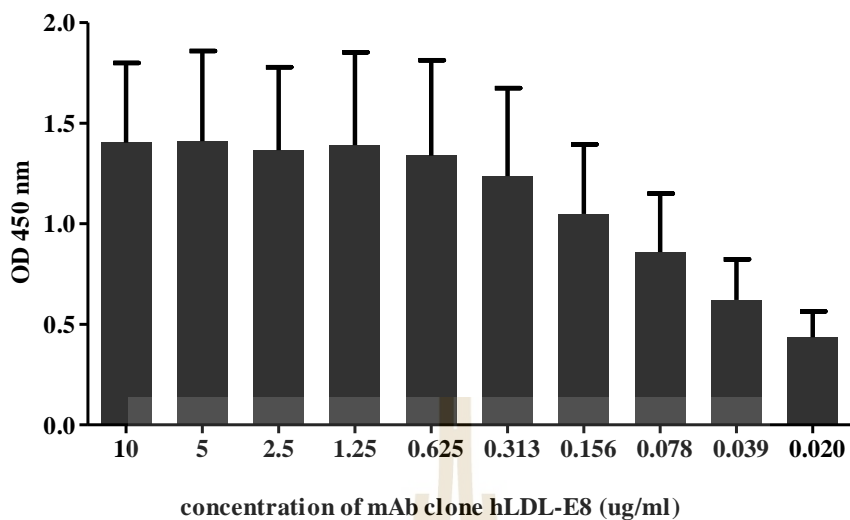
Figure 3.14 Titration for the optimal concentration of the captured antibody.

Five hundred nanogram of commercial human LDL was coated onto each well of the ELISA plates. Various concentrations of mAb against human LDL clone hLDL-E8 that used as a captured antibody was titrated using indirect ELISA. Since we need the excess concentration of captured antibody to capture antigen before detection, from this graph, mAb against human LDL clone hLDL-E8 at a concentration 10 ug/ml was selected for LDL measurement using sandwich ELISA. The data represent the mean ± SD of two independent experiments.
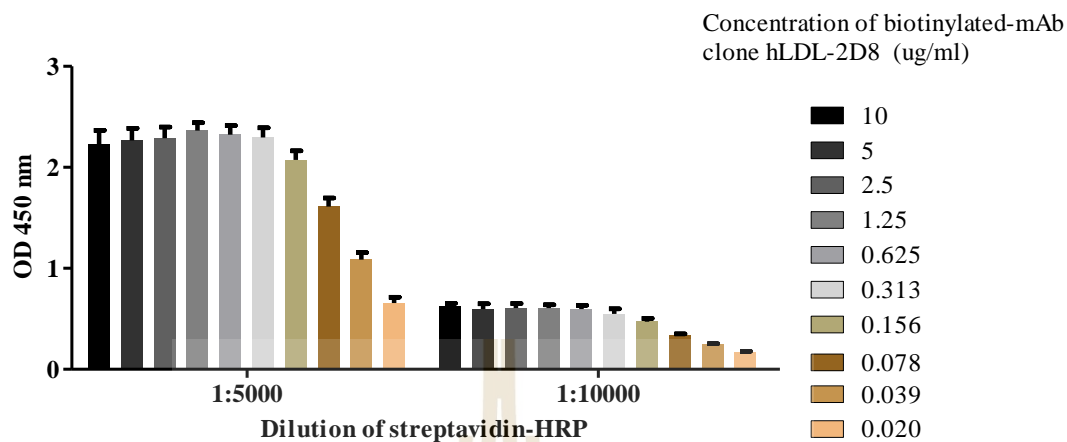
Figure 3.15 Titration for the optimal concentration of detected antibody.

MAb against human LDL clone hLDL-2D8 was conjugated with Sulfo-NHS-LC-biotin and used for detected antibody. The optimum concentration of biotinylated mAb and HRP-conjugated streptavidin were titrated by indirect ELISA. From this graph, biotinylated-mAb clone hLDL-2D8 at a concentration 0.04 ug/ml and HRP-conjugated streptavidin at a dilution 1:5000 were selected for further LDL measurement using sandwich ELISA. The data represent the mean ± SD of three independent experiments.
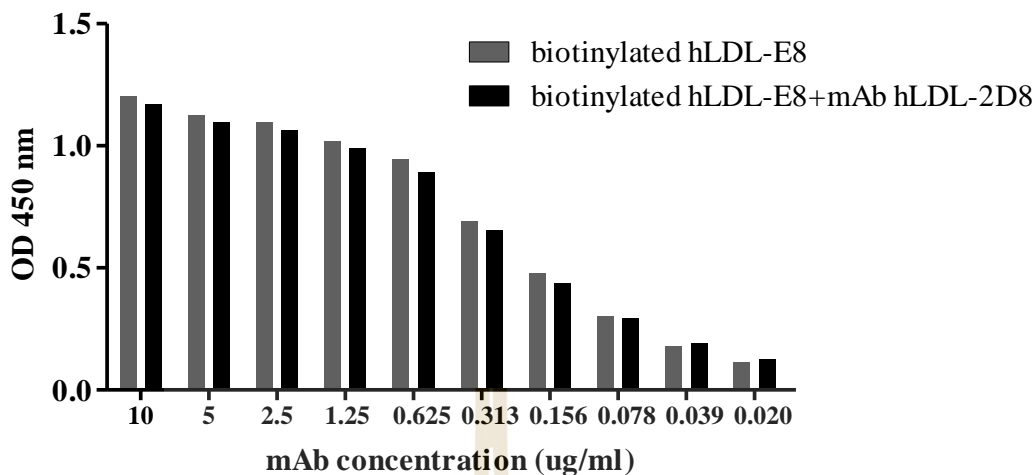
Figure 3.16 Sensitivity test using unconjugated mAb clone hLDL-2D8 and biotinylated-mAb clone hLDL-E8.

To find the better signal of the system, role of mAb clone hLDL-E8 and hLDL-2D8 was switched and the signal was compared. In this figure, mAb clone hLDL-2D8 was used as captured antibody and biotinylated-mAb clone hLDL-E8 was used as detected antibody. A representative result from one of three independent experiments is shown.
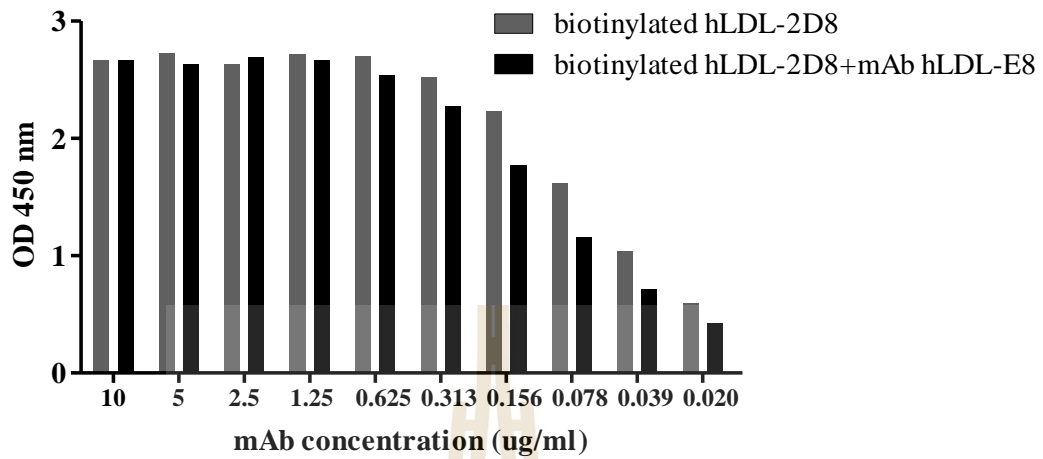
Figure 3.17 Sensitivity test using unconjugated mAb clone hLDL-E8 and biotinylated

mAb clone hLDL-2D8.

MAb clone hLDL-E8 and hLDL-2D8 were switched and the signal was

compared. In this figure, mAb clone hLDL-E8 was used as captured antibody

and biotinylated-mAb clone hLDL-2D8 was used as detected antibody. A

representative result from one of three independent experiments is shown.

3.1.3.1 Sample preparation prior LDL quantification

Since the generated mAbs against human LDL react with apoB that also can be found in VLDL, selectively preparation of apoB containing LDL from the specimen was needed before quantitative measurement. Thus, the developing procedure for direct plasma LDL measurement using the generated mAbs, LDL precipitation was included. To avoid the contamination of the apoB containing VLDL or chylomicron, there are 2 well known precipitating reagents for LDL precipitation, heparin/MnCl$_2$ or heparin/citrate pH 5.04**.** By using heparin/MnCl$_2$ as a precipitating agent, apoB-100 (550 kDa) and apoB-48 (250 kDa) were precipitated in the pellet fraction whereas apoE (34 kDa) and apoA1 (28.1 kDa) were remained in the supernatant as shown in Figure 3.18.

Since precipitation using heparin/MnCl$_2$ is the method that used for precipitation of apoB-containing lipoprotein (Joyce Corey Gibson, 1984). Thus this type of precipitation reagent might create the contamination of VLDL in the precipitant fraction. Therefore, the other precipitating reagent was used to avoid this.

Heparin/citrate pH 5.04 was used for LDL precipitation. Heparin-treated plasma was separated from heparinized blood and LDL was precipitated according to the materials and methods 2.2.8.2. The precipitant was dissolved using 100 μl of PBS pH 7.2, the human apolipoproteins in the precipitant and supernatant fraction were resolved by 10% SDS-PAGE under reducing condition. The results showed that apoB-100 (550 kDa) was precipitated in the precipitant fraction and shown in Figure 3.19. However, not only apoB100 (550 kDa) were precipitated but also other proteins in human plasma still present in precipitant when using heparin/citrate pH 5.04 as a precipitating agent. Thus, 2 steps precipitation was

used to solve this problem. For 2 steps precipitation, LDL was firstly precipitated from human plasma by heparin/MnCl$_2$ and the precipitant was solubilized and performed the second precipitation using heparin/citrate pH 5.04. However, this technique needed several steps and was not suitable for developing the direct plasma LDL measurement. Therefore, quantification of LDL after heparin/citrate pH 5.04 and two steps precipitation was compared. By performing sandwich ELISA using the generated mAbs against human LDL, the result showed that no significantly different between the samples obtained from precipitation using heparin/citrate pH 5.04 and from 2 steps precipitation shown in Figure 3.20 means that other plasma proteins remained in the precipitant from heparin/citrate pH 5.04 precipitation are not interfere our measurement. According to these results, heparin/citrate pH 5.04 was used for LDL precipitation from plasma samples before LDL quantification.
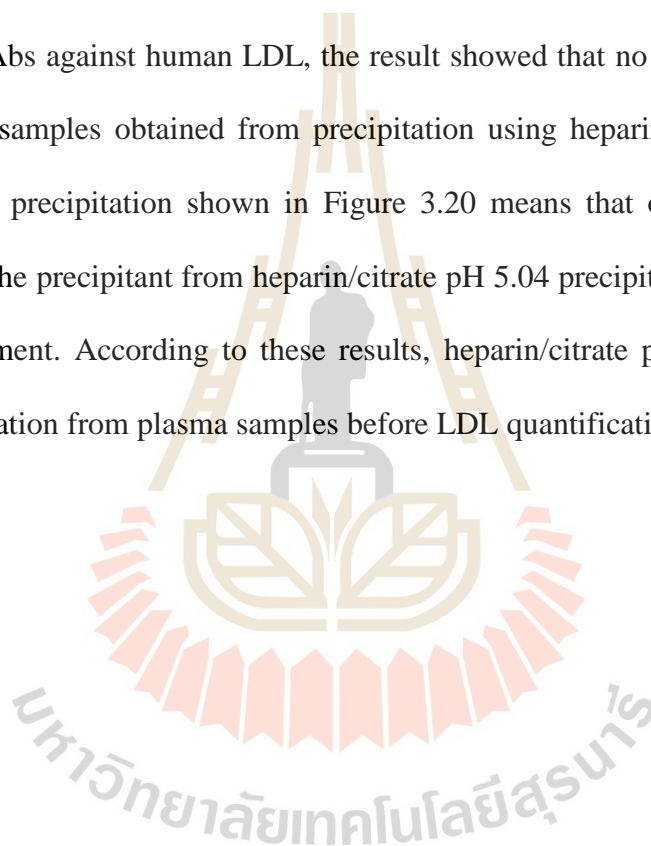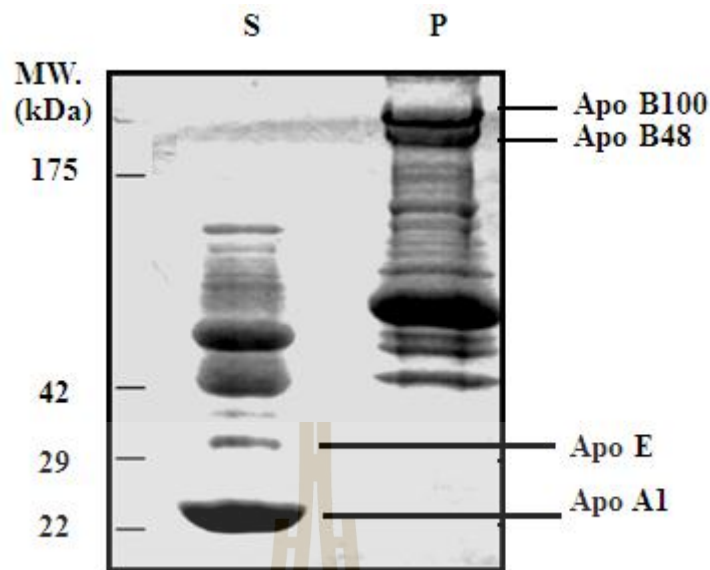
Figure 3.18 LDL precipitation using heparin/MnCl$_2$.

Human plasma LDL was precipitated by heparin/MnCl$_2$ precipitation technique. The human apolipoproteins in the precipitant fraction and supernatant fraction were separated by 10% SDS-PAGE under reducing condition. The results showed that apoB-100 (550 kDa) and apoB-48 (250 kDa) were precipitated in the pellet fraction (P) whereas apoE (34 kDa) and apoA1 (28.1 kDa) were remained in the supernatant (S). A representative result from one of three independent experiments is shown.
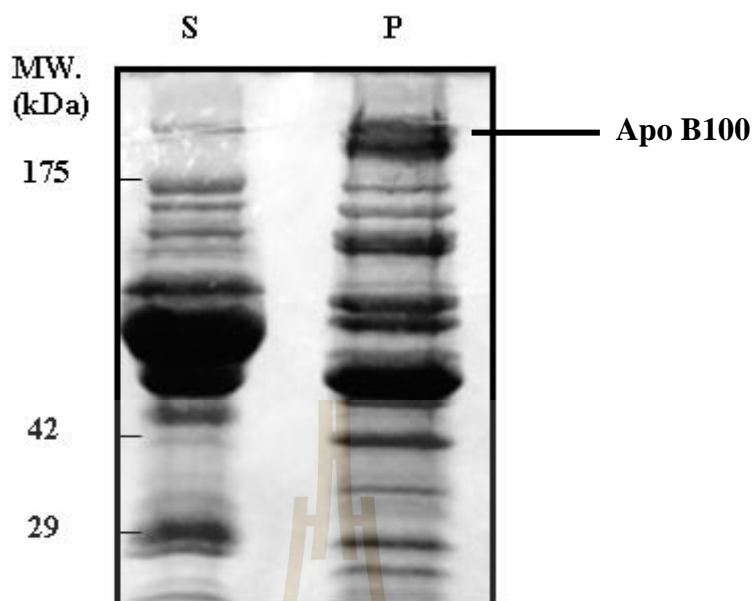
Figure 3.19 LDL precipitation using heparin/citrate pH 5.04.

Human plasma LDL was precipitated by heparin/citrate pH 5.04. The human apolipoproteins in precipitant and supernatant fraction were separated by 10% SDS-PAGE under reducing condition. ApoB-100 (550 kDa) and apo-B48 (250 kDa) were precipitated in the precipitant fraction (P). (S) is representative of supernatant. A representative result from one of three independent experiments is shown.
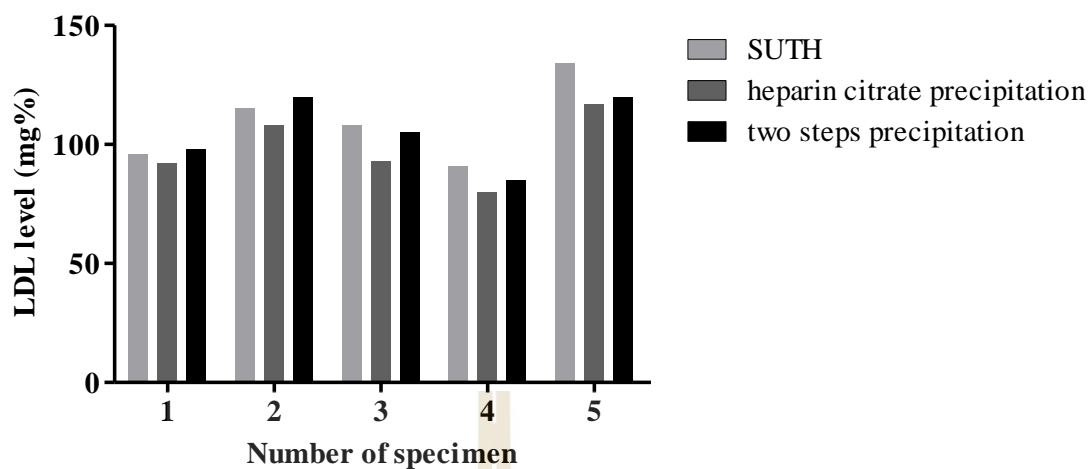
Figure 3.20 LDL level of the samples obtained from heparin/citrate pH 5.04 precipitation and 2 steps precipitation.

LDL was precipitated from 5 different plasma samples from SUT hospital using either heparin/citrate pH 5.04 or 2 steps precipitation. The precipitated samples were determined for LDL level by direct measurement by sandwich ELISA using the generated mAbs against human LDL. The obtained results were also compared to the results obtained from the SUT hospital.

3.1.3.2 LDL level obtained from direct LDL measurement procedure using the generated mAbs to human LDL was high correlated with the results obtained from the hospital.

To apply the generated mAbs to clinical diagnosis field, direct LDL measurement based on sandwich ELISA using the generated mAbs against human LDL was developed. Based on sandwich ELISA technique, 2 mAbs that recognize at different epitope of the antigen were needed. In this study, 2 clones of the generated mAbs, hLDL-E8 and hLDL-2D8 that bind to the distinct epitope of human LDL were applied for this technique. The mAb hLDL-E8 was used as the captured antibody while the biotinylated mAb hLDL-2D8 was used as a detected antibody. Known concentration of commercial LDL (US Biological) was used for setting up the standard curve used for quantification of the samples.

Two hundred and eight specimens from SUT hospital were randomized. The samples were firstly precipitated using heparin/citrate pH 5.04 and follow by the direct measurement, using the developed methods. The samples were diluted at 1:250 before quantification with this technique. The obtained results were compared with SUT hospital report (calculated measurement). From 208 specimens, mean of LDL level from the developed method and SUT hospital method were 126.6±43.1 mg/dl (range 90.0 to 258.0 mg/dl) and 123.2±42.3 mg/dl (range 34.0 to 236.0 mg/dl), respectively. The results from our developed method and SUT hospital were highly correlated according to simple linear regression analysis (Pearson's correlation coefficient r = 0.8491, p-value < 0.0001) as shown in Figure 3.21. Although, the mean value of LDL level from our developed method was a bit higher than the value reported by SUT hospital, the differences were not significant.
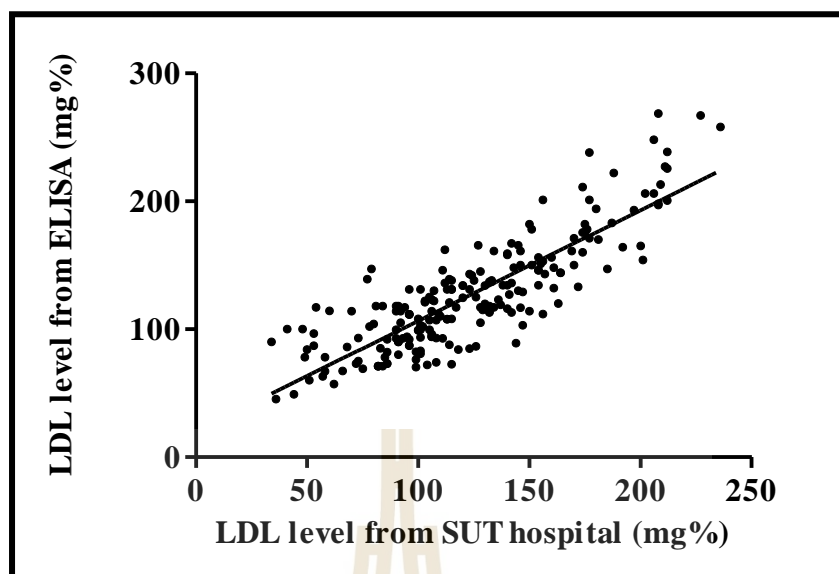
Figure 3.21 Correlation of direct LDL measurement by our developed method using our generated mAbs against human LDL compared with calculated LDL measurement reported by SUT hospital.

Plasma LDL level of 208 samples obtained from the developed technique (direct measurement) were compared to the plasma LDL level obtained from the SUT hospital (calculated measurement). The direct measurement from our in-house ELISA was not significantly difference from SUT hospital report and highly correlated according to simple linear regression analysis. $Y = 0.8639X+20.22$, Pearson's correlation coefficient $r = 0.8491$, $r^2 = 0.7210$, $P < 0.0001$ (solid line).

.

Although the mean value of LDL level obtained from the developed method showed a bit higher than the value obtained from SUT hospital, those values were not significantly different. The absolute differences between LDL level obtained by the developed method and from the SUT hospital were compared. As shown in Figure 3.22, simple linear regression analysis suggested that difference in LDL measurements was negatively correlated with SUT hospital method and positively correlated with direct measurement from our in-house ELISA.
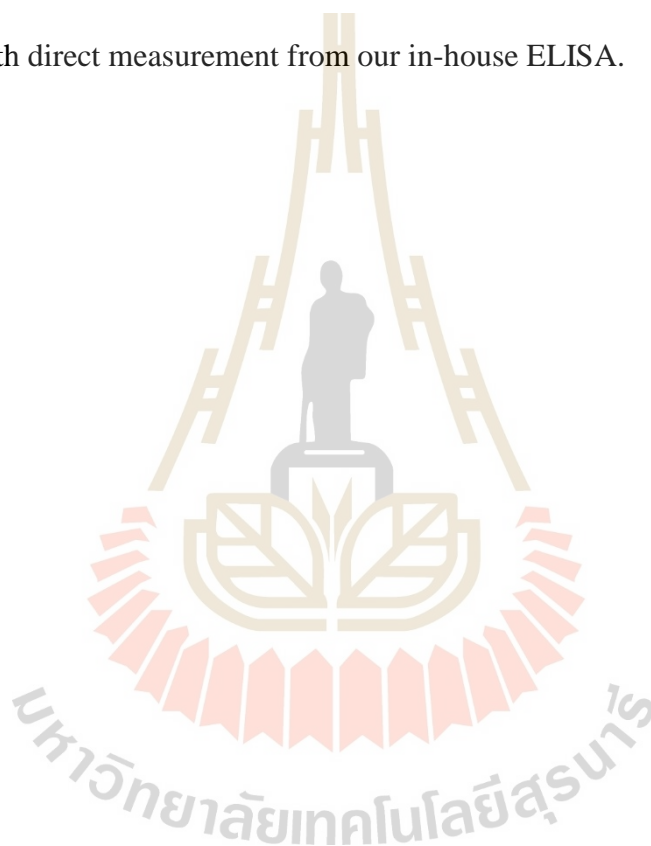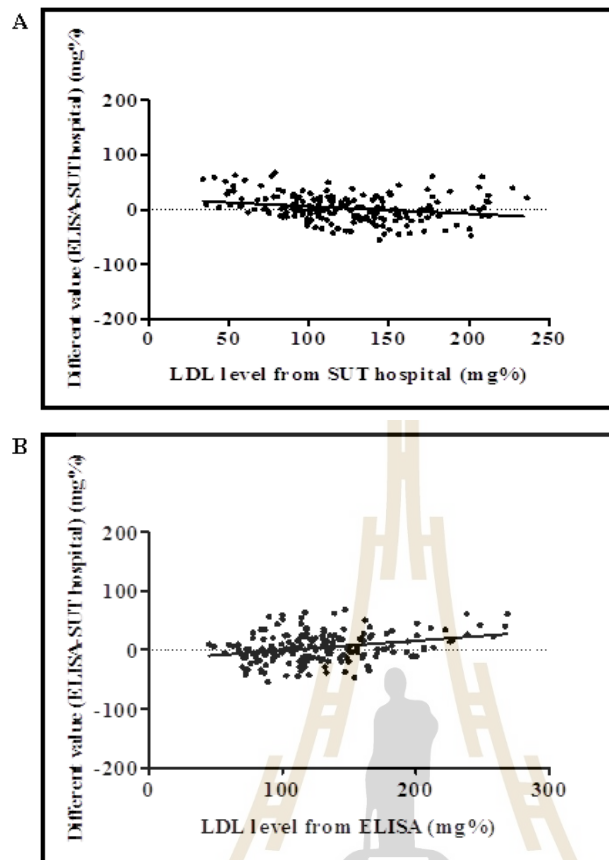
Figure 3.22 Linear graph of the correlation between the LDL differences of calculated LDL values from SUT hospital and direct LDL measured using the developed method.

Correlation between LDL differences and calculated LDL measured from SUT hospital were plotted (A) $Y = -0.1361X+20.22$, $r = -0.2455$, $r^2 = 0.06027$, $P = 0.0004$. Correlation between LDL differences and the LDL level obtained by direct LDL measured using the developed method (B) Y 0.1654X-17.52, $r = 0.3035$, $r^2 = 0.09213$, $P < 0.0001$ for simple linear regression (solid line).
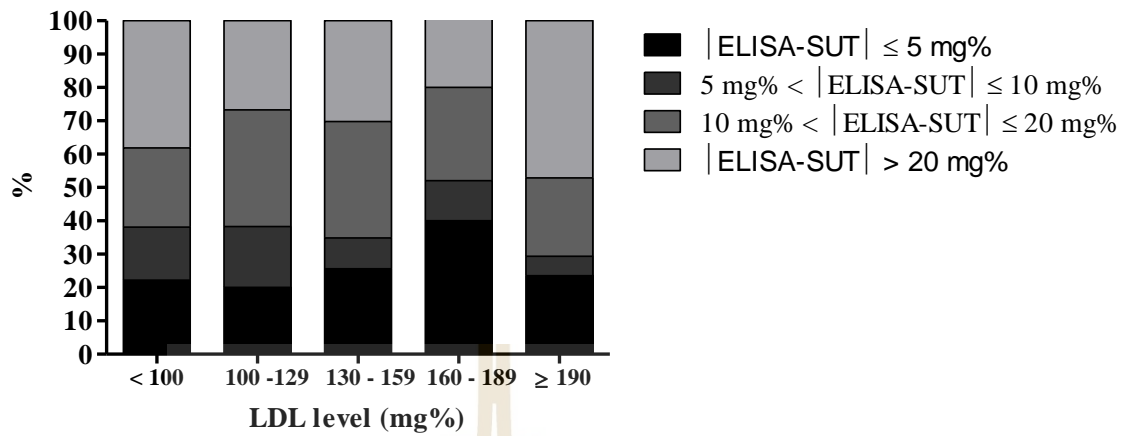
Figure 3.23 Percent distribution (%) of the absolute differences in LDL measurement according to LDL level from SUT hospital.

Two hundred and eight randomized specimens found that 63% of total specimens, the absolute difference of LDL measurement was more than 10 mg/dl and among this group, 53.4%, direct LDL measurement from our in-house ELISA were higher than SUT hospital report. Moreover, 33.2% of total specimens, the absolute difference of LDL measurements was more than 20 mg/dl mostly in LDL level less than 100 and more than 190 mg% and among this group, 60.9% of these specimens, the direct LDL measurements from our in-house ELISA also were higher than SUT hospital report.
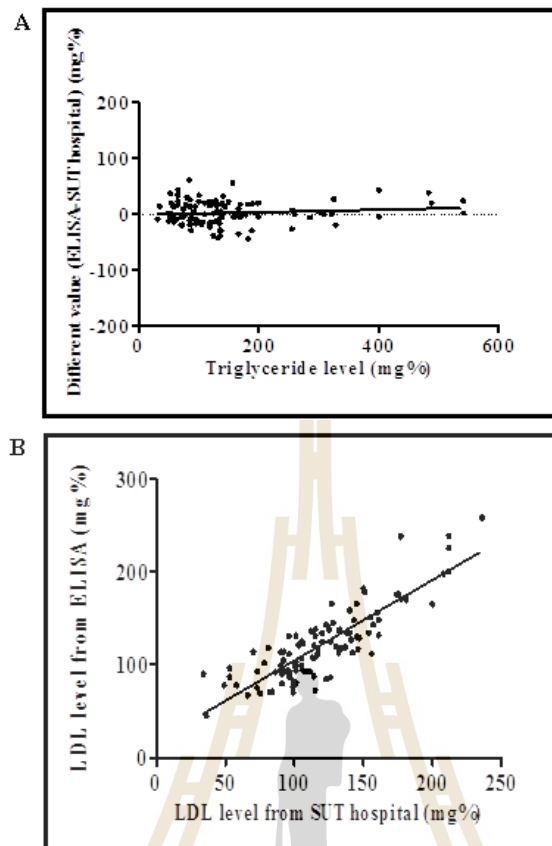
Figure 3.24 Correlation between difference of LDL measurement and triglyceride level.

Simple linear regression analysis was plot between the LDL difference, the different value between LDL level obtained from the SUT hospital and the developed method, and triglyceride level. The difference of LDL measurements was positively correlated with triglyceride (TG) level (analyzed from 117 specimens). The results from our in-house ELISA and SUT hospital were highly correlated according to simple linear regression analysis. (A) Correlation of LDL difference and triglyceride level. $Y = 0.02313X-1.082$, Pearson's correlation coefficient $r = 0.1152$, $r^2 = 0.01328$, $P = 0.2161$ for simple linear regression (solid line). (B) Correlation of direct LDL measured

using in house ELISA and calculated LDL measured from SUT hospital. Y = 0.8650X+18.29, Pearson's correlation coefficient r = 0.8534, r^2= 0.7283, P < 0.0001 for simple linear regression (solid line).

To investigate whether triglyceride level has an influence on the LDL quantification using our developed technique, standard triglyceride (Sigma Aldrich) was added into specimens to a final concentration of either 300 or more than 500 mg/dl respectively. The results showed that LDL level was not significantly difference between normal samples and triglyceride added samples. The results are highly correlated according to simple linear regression analysis (figure 3.25). These results suggested that triglyceride level does not have influence on direct LDL quantification using our developed method.
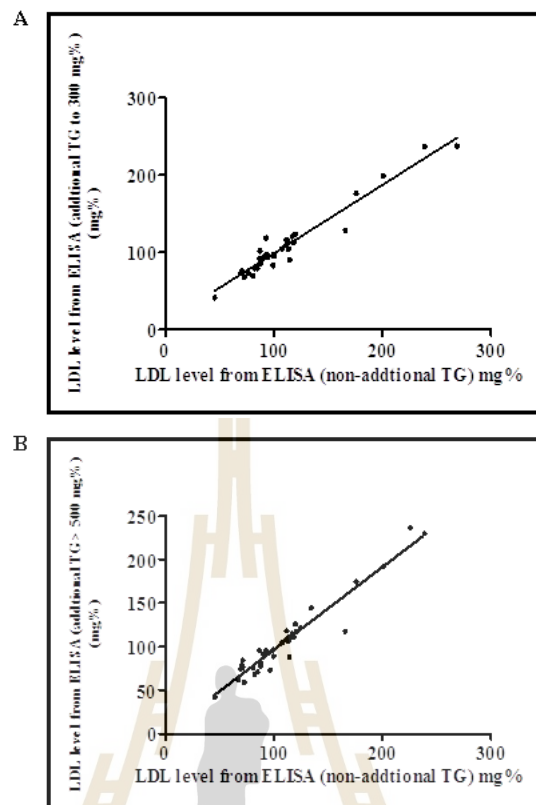
Figure 3.25 Correlation between LDL level from normal samples and triglyceride added samples.

48 and 57 specimens, standard triglyceride was added until 300 and more than 500 mg/dl respectively. The result shown that there were not significantly difference between the LDL level that non-additional triglyceride and additional triglyceride samples. Simple linear regression analysis showed that LDL level gained from non-additional triglyceride with either additional triglyceride to 300 mg/dl (A) or more than 500 mg/dl (B) were highly correlated. Correlation of the normal and additional of TG are shown in (A) Y = 0.8868X+10.17, r = 0.9512, r^2= 0.9048, P < 0.0001. (B) Y = 0.9485X+1.771, r = 0.9503, r^2= 0.9031, P < 0.0001 (solid line).
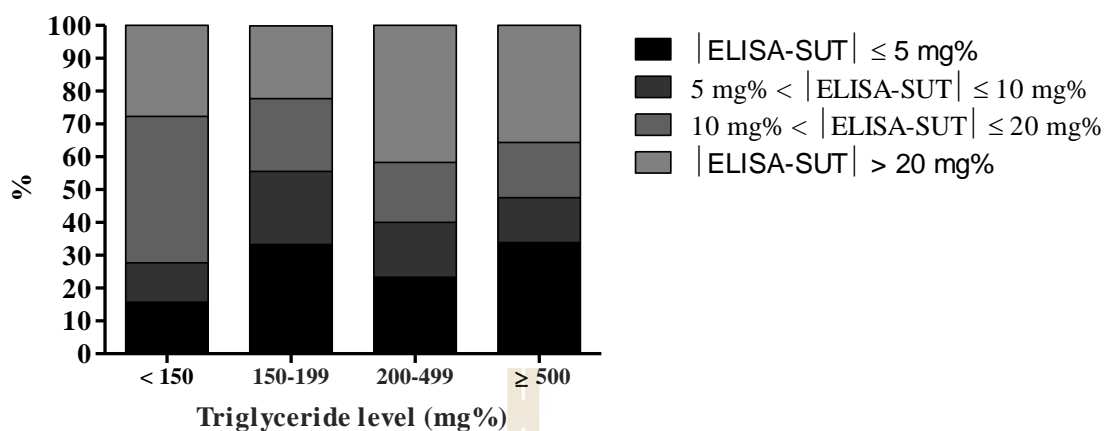
Figure 3.26 Distribution (%) of the absolute differences in LDL measurement according to triglyceride level.

From total specimens, the difference of LDL results from our in-house ELISA and SUT report were higher than 20 mg/dl in high triglyceride population more than low triglyceride population.

For other markers in lipid profile, our study found that total cholesterol and HDL cholesterol were not affected to direct LDL measurement using our developed method (Figure 3.27).
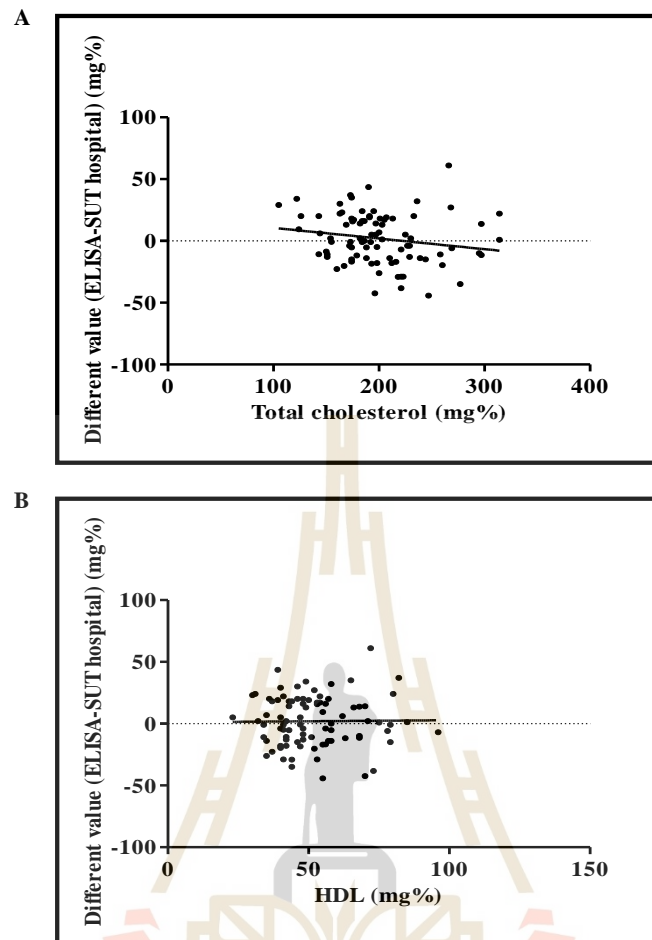
Figure 3.27 Correlation between difference in LDL measurement with total cholesterol and HDL cholesterol.

Simple linear regression analysis showed that the difference in LDL measurements was negatively correlated with total cholesterol and HDL cholesterol (analyzed from 87 specimens). Correlation between differences in LDL measurement with total cholesterol (A) $Y = -0.08604X+19.16$, $r = -0.1818$, $r^2 = 0.03306$, $P = 0.0919$ and HDL cholesterol (B). $Y = 0.01748X+1.050$, $r = 0.01234$, $r^2 = 0.0001524$, $P = 0.9097$.

3.2 Role of different degree of LDL oxidation in atherosclerosis progression

3.2.1 MM-LDL and ox-LDL were generated using CuSO$_4$ as an oxidizing agent.

To study the role of different degree of LDL oxidation in atherosclerosis progression, mm-LDL and ox-LDL were generated using CuSO$_4$ as an oxidizing agent. Termination of the oxidation reaction was performed by addition of Cu^{2+}, chelating agent EDTA. Degree of lipid oxidation was measured by TBARS assay and protein modification of oxidized-LDL was determined by indirect ELISA using the generated mAbs against human LDL that specifically react with apolipoproteinB.

Dialyzation was performed to exchange the buffer to PBS pH 7.2. The lipid peroxidation of LDL was examined by TBARS assay. As shown in Figure 3.28, high level of lipid peroxidation product was observed for both incubation time at 24 h and 48 h. Unfortunately, the results showed that dialyzation decreased the level of lipid peroxidation. On the other hand, dialyzation has no affect on protein modification during oxidation reaction as shown in Figure 3.29. From these results, dialyzation was not performed after oxidation reaction.
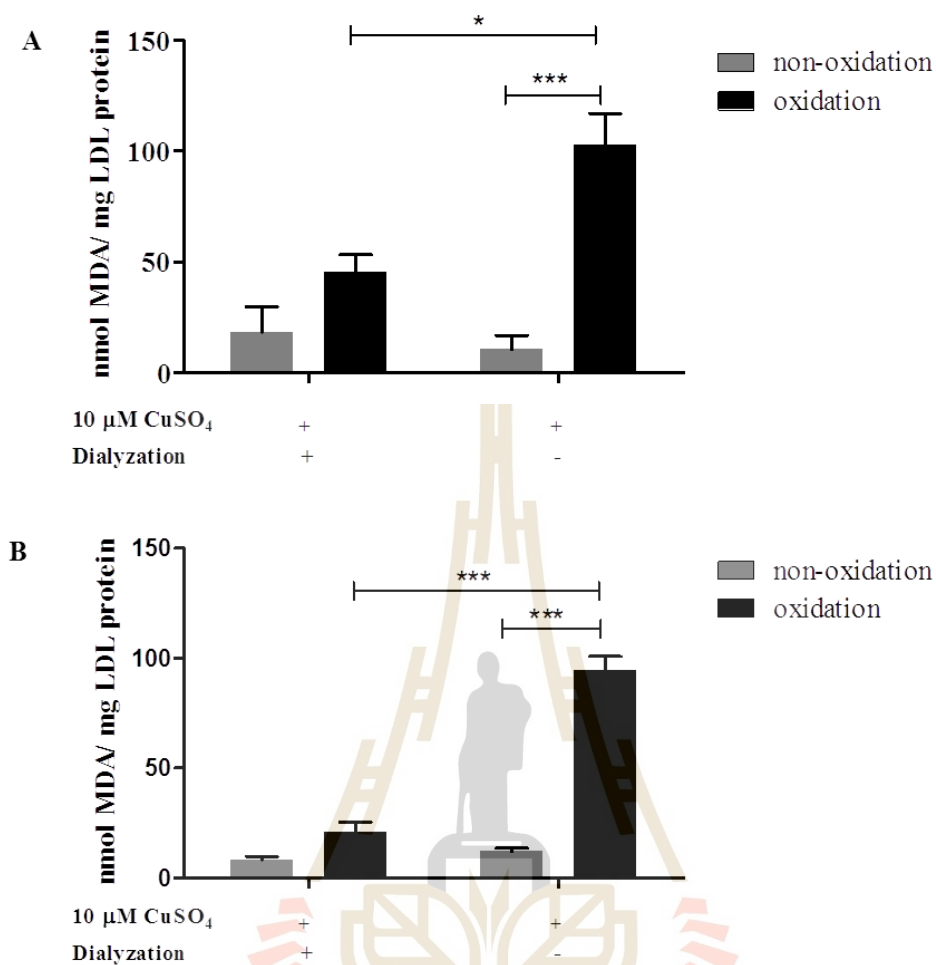
Figure 3.28 Effect of dialyzation onto lipid peroxidation product during oxidation reaction.

One milligram per milliliter of precipitated-LDL was incubated with $CuSO_4$ at a final concentration of 10 μM for 24 h (A) and 48 h (B) and the reaction was terminated by 0.1 mM EDTA. Degree of LDL oxidation was measured by TBARS assasy. The data represent the mean ± SD of three independent experiments. * indicates $p < 0.05$ and *** indicates $p < 0.001$.
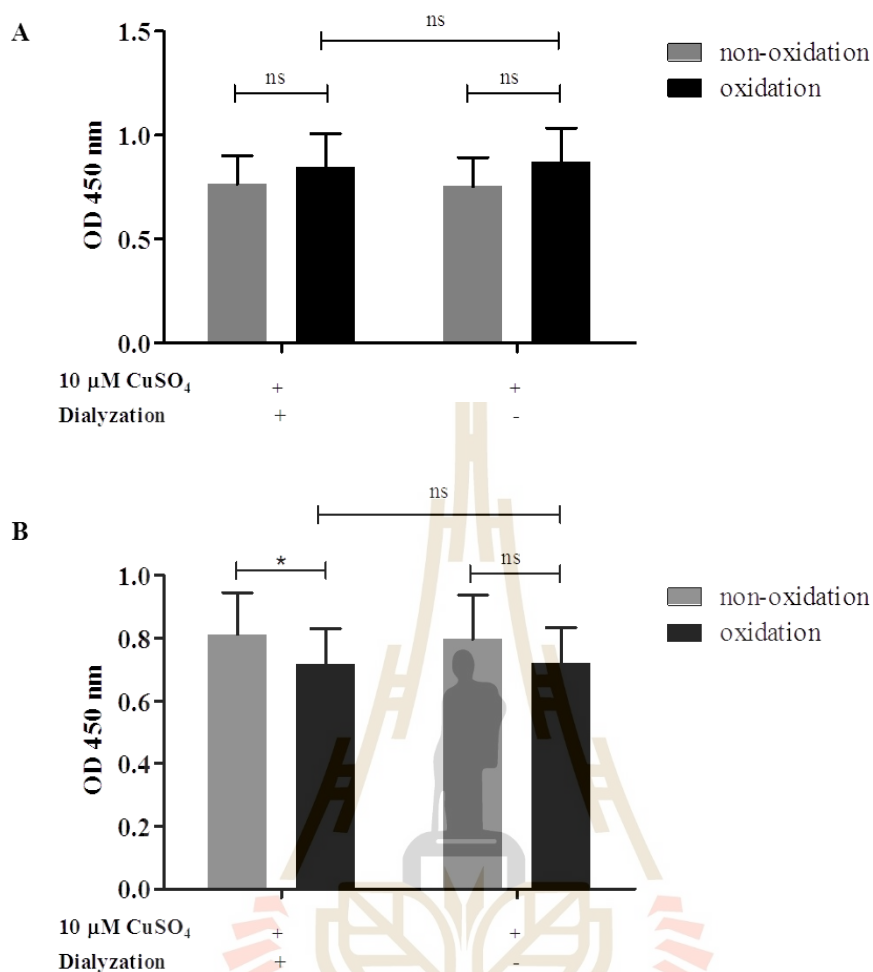
Figure 3.29 Effect of dialyzation onto protein modification of oxidized-LDL during

oxidation reaction.

One milligram per milliliter of precipitated-LDL was incubated with $CuSO_4$ at

a final concentration of 10 μM for 24 (A) and 48 (B) h and the reaction was

terminated by 0.1 mM EDTA. Modification of the protein compartment of

human LDL was examined by indirect ELISA using the generated mAb-LDL

clone hLDL-E8. The data represent the mean ± SD of three independent

experiments. * indicates $p < 0.05$.

Since LDL was oxidized in stepwise manner, to generate the mm-LDL that only lipid part was oxidized and fully ox-LDL that both lipid and protein parts were oxidized, various incubation times during oxidation reaction was performed and found that the degree of LDL oxidation was maximized at 9-12 h when using TBARS assay Figure 3.30. The protein modification of ox-LDL was modified at 48 h determined by indirect ELISA using the generated mAbs. Once the protein was modified, binding epitope of apoB-100 might be changed their conformation, which lead to decreasing of the binding affinity of the generated mAb to its specific protein as shown in Figure 3.31. To compare effect of LDL oxidation on various epitopes of the apoB, different clones of our generated mAbs against human LDL were determined by indirect ELISA. As shown in Figure 3.32, apoB of the oxidized LDL was not significantly changed at 9 h of incubation whereas the protein part was clearly modified at 48 h of incubation time. These results suggested that the lipid part of LDL was completely modified at 9-12 h whereas the protein part was modified at 48 h. Therefore the incubation time for generation of mm-LDL and ox-LDL were 9 h and 48 h, respectively.
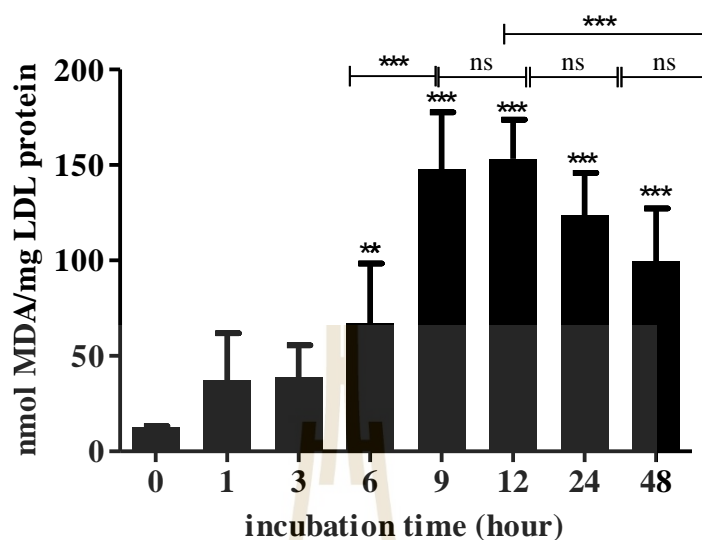
Figure 3.30 Degree of LDL oxidation at different incubation times of oxidation reaction.

One milligram per milliliter of precipitated-LDL was incubated with $CuSO_4$ at a final concentration of 10 μM at different incubation times and kept at 4^oC to stop reaction before used. Degree of lipid oxidation was measured by TBARS assay. The result showed that degree of LDL oxidation seems to be maximized at 9 h. The data represent the mean ± SD of 4 independent experiments. ** indicates $p<0.01$ and *** indicates $p<0.001$ when compared with non-oxidized LDL.
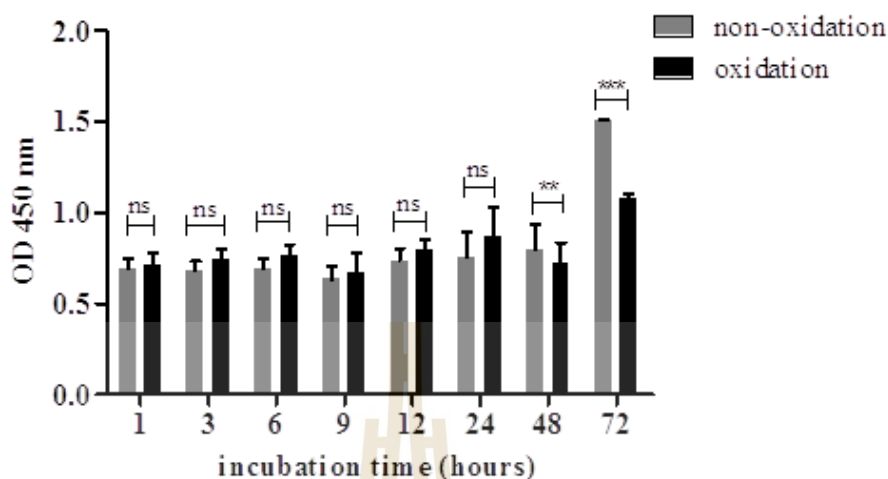
Figure 3.31 Protein modification of oxidized-LDL at different incubation times of oxidation reaction.

One milligram per milliliter of precipitated-LDL was incubated with $CuSO_4$ at a final concentration of 10 μM at different incubation times. The oxidation reaction was terminated by adding of EDTA to 0.1 mM. The protein modification of oxidized-LDL was determined by indirect ELISA using the generated mAb against human LDL clone hLDL-E8. The data represent the mean ± SD of three independent experiments. ** indicates $p<0.01$ and *** indicates $p<0.001$ when compared with non-oxidized LDL.
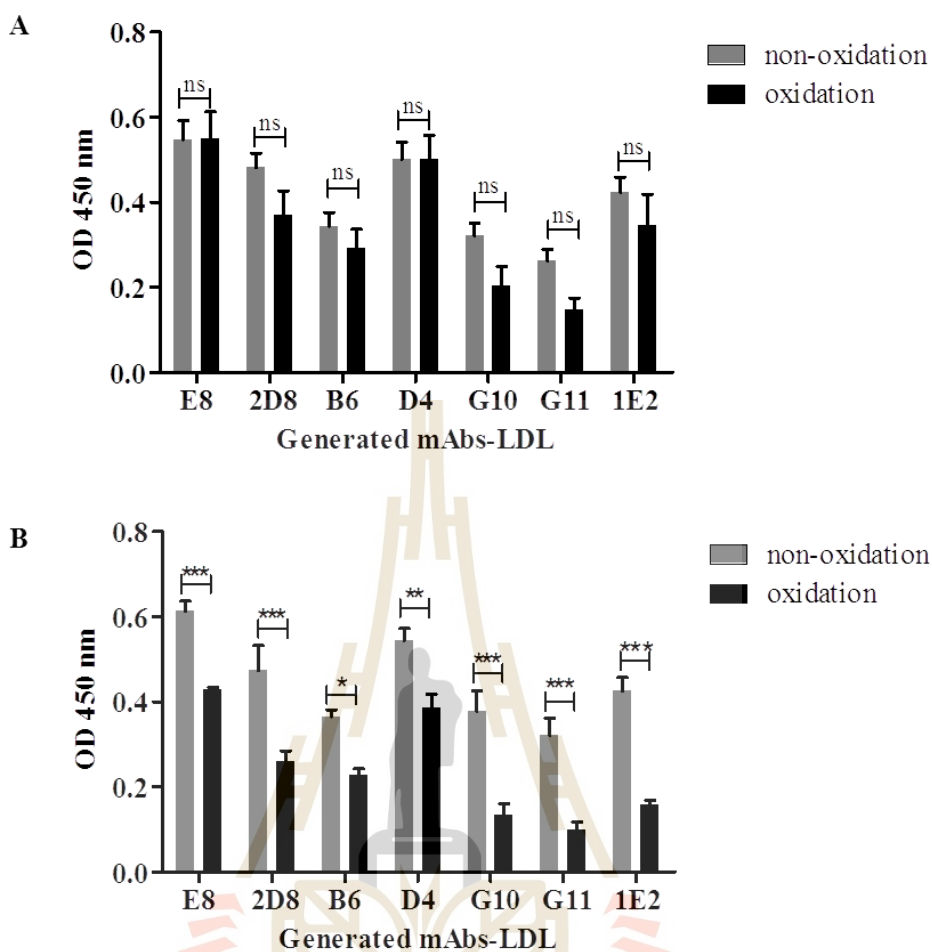
Figure 3.32 Protein modification of oxidized-LDL determined by indirect ELISA using different clones of the generated mAb against human LDL.

Precipitated-LDL at a final concentration of 1 mg/ml was incubated with $CuSO_4$ at a final concentration of 10 μM for 9 h (A) and 48 h (B). The oxidation reaction was terminated by adding of EDTA to a final concentration of 0.1 mM. The oxidized-LDL was subjected for indirect ELISA using different clones of the generated mAbs to human LDL. The data represent the mean ± SD of four independent experiments. * indicates $p < 0.05$, ** indicates $p < 0.01$ and *** indicates $p < 0.001$ when compared with non-oxidized LDL.

According to previous results, dialyzation was not performed after oxidation reaction. Thus, the EDTA used to stop the oxidation reaction was remained in the solution. Once the prepared mm-LDL and ox-LDL were added to the PMA-derived macrophages, we found that EDTA has some affects to the cells and the results were hardly interpreted. Therefore, EDTA was not suitable for our study. To solve this problem, the oxidized-LDL was kept at 4°C to stop the oxidation reaction instead of using EDTA. The result from TBARS assay (Figure 3.33) and indirect ELISA (Figure 3.34) showed that there were not significantly different between termination of the oxidation reaction by either EDTA or storing at 4°C for both incubation time at 9 h and 48 h.

As a consequence, the oxidized-LDL was kept at 4°C before used to stop the oxidation reaction. However, this technique has limitation because mm-LDL will be easily further modified if it is kept for a long time. To avoid this problem, both mm-LDL and fully ox-LDL will be freshly prepared before using in further experiments.
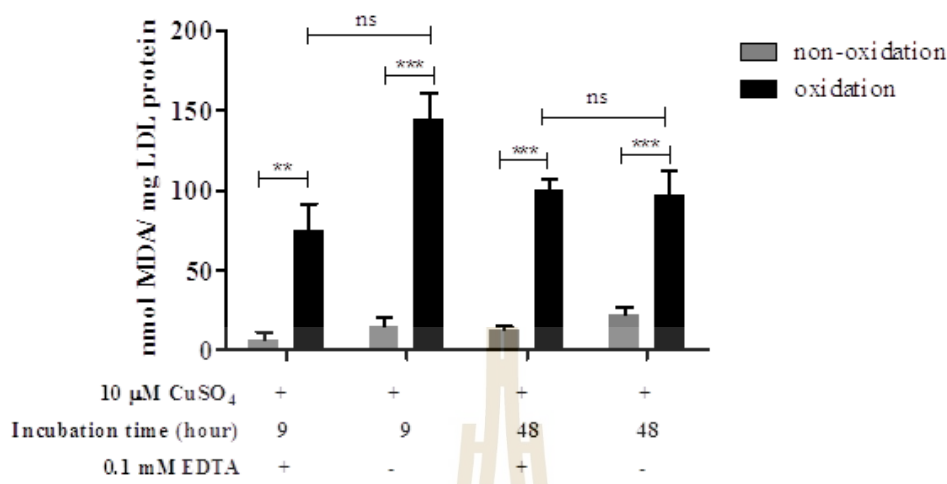
Figure 3.33 Effect of non-using EDTA onto lipid peroxidation product during oxidation reaction.

One milligram per milliliter of precipitated-LDL was incubated with $CuSO_4$ at a final concentration of 10 µM for 9 h or 48 h. Degree of LDL oxidation that measured the lipid peroxidation product was measured by TBARS assay. The results showed that non-using EDTA to stop reaction and the oxidation products were kept at 4^oC instead were not significantly different from using EDTA to stop the reaction for both 9 h and 48 h of oxidation time. The data represent the mean ± SD of three independent experiments. * indicates p<0.05, ** indicates p<0.01, and *** indicates p < 0.001.
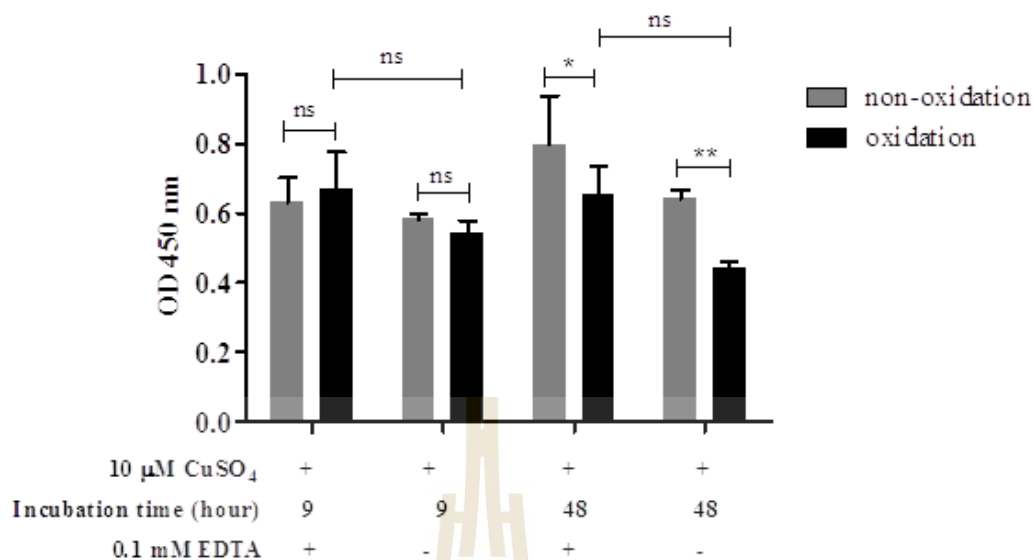
Figure 3.34 Effect of EDTA onto protein modification of oxidized-LDL during oxidation reaction.

One milligram per milliliter of precipitated-LDL was incubated with $CuSO_4$ at a final concentration of 10 μM for 9 h or 48 h. The protein modification of oxidized-LDL was examined by indirect ELISA using mAb clone hLDL-E8. The results showed that stop reaction by using, non-using EDTA, or keeping the oxidation product at $4^{o}C$ were not significantly for both 9 h and 48 h of oxidation time. The data represent the mean ± SD of three independent experiments. * indicates $p<0.05$ and ** indicates $p<0.01$.

3.2.2 Different degree of LDL oxidation can induce foam cell formation

In order to study whether different degree of LDL oxidation can induce foam cell formation, different types of LDL; native LDL, mm-LDL, and ox-LDL at different concentrations were added into PMA-derived macrophages. Foam cell formation was examined by detection of the lipid droplet in the macrophages, which were visualized by staining with 0.5% Oil Red O and the red oil droplets were observed under inverted light microscope (Figure 3.35).

The red oil droplets positive cells were counted at randomized 10 fields using 40X magnification of inverted light microscope. The result showed that all different types of LDL with different degree of oxidation can induce macrophage-foam cells formation in a dose dependent manner. Although macrophages that engulf native-LDL showed oil droplets positive cells more than macrophages engulf mm-LDL and ox-LDL (Figure 3.36), the number and characteristic of lipid droplets in lipid-loaded macrophages induced by high degree of LDL oxidation are higher and larger than native LDL as shown in figure 3.37.

A

B

Positive oil droplets
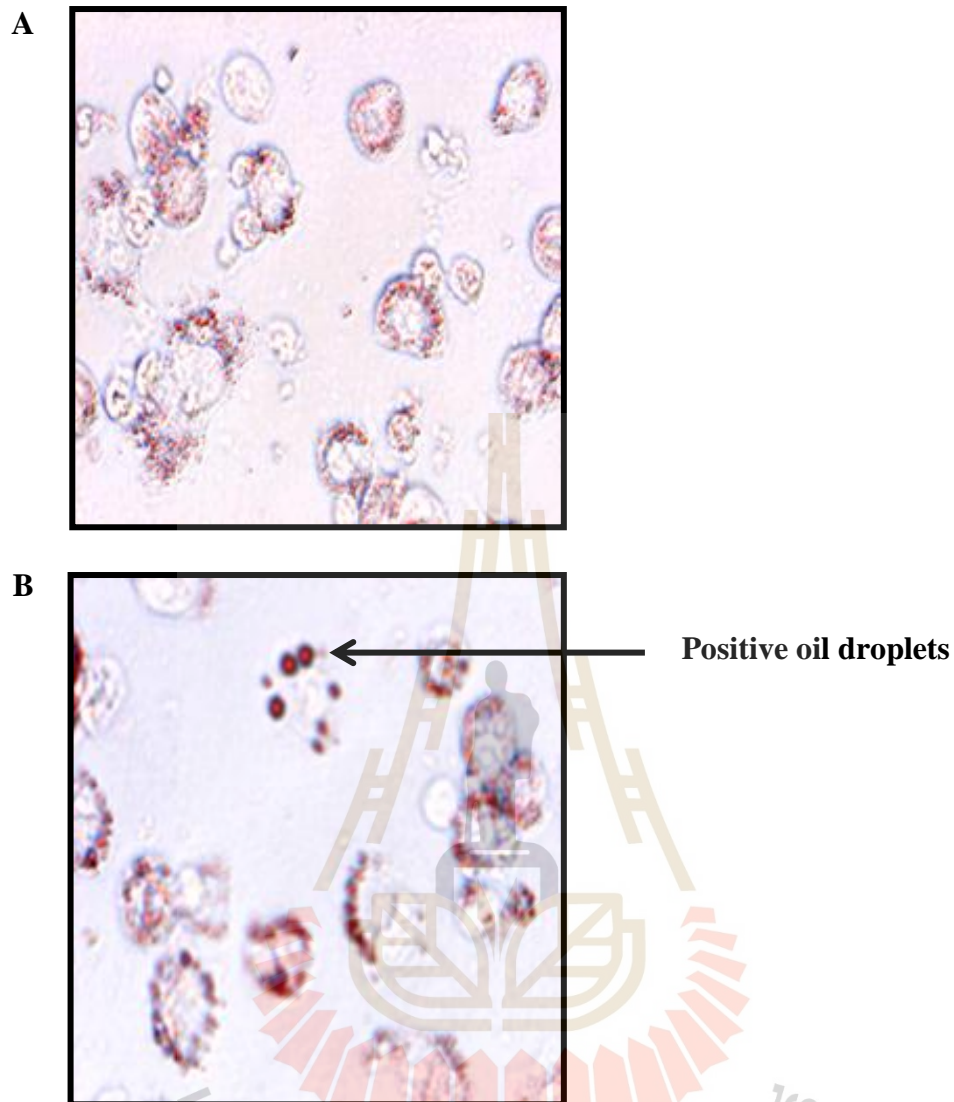
Figure 3.35 Foam cell formation.

PMA-derived macrophages were cultured in the absence (A) or presence (B) of the ox-LDL at a final concentration of 200 μg/ml for 48 h. Lipid-loaded foam cells were stained by Oil Red O and observed under inverted light microscope. A representative result from one of three independent experiments is shown.
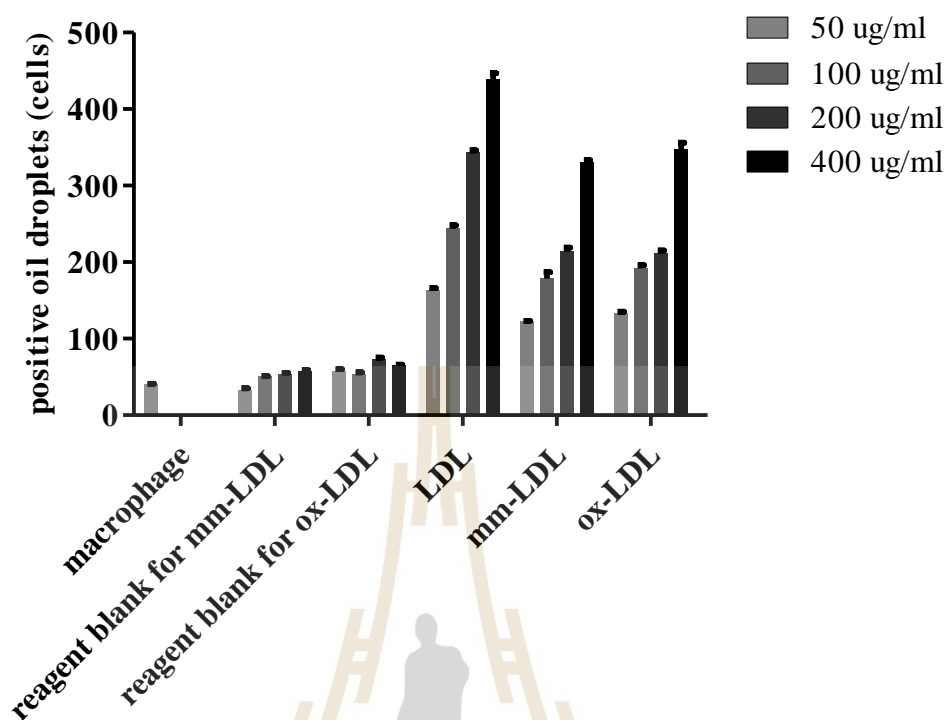
Figure 3.36 Number of oil droplet positive cells induced by different types of LDL. PMA-derived macrophages were cultured in the absence or presence of the different LDL oxidation at various concentrations for 48 h. The cells were stained by Oil Red O and observed under inverted light microscope. Ten randomized fields were selected as a representative for oil droplet positive cells count using 40X magnification of inverted light microscope. The data represent the mean ± SD from one of three independent experiments.
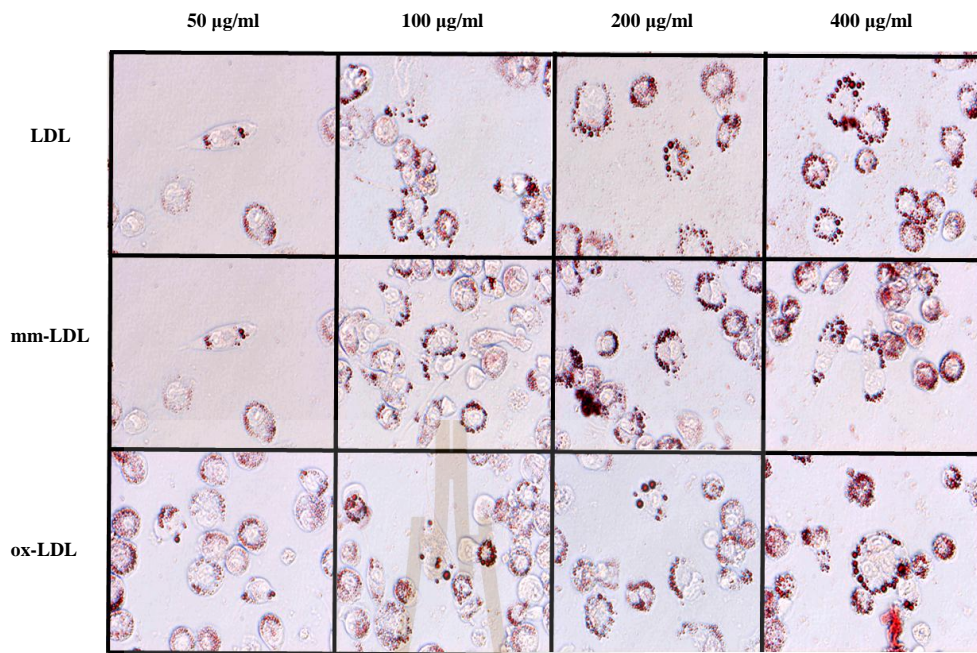
Figure 3.37 Characteristic of lipid oil droplets in macrophage-derived foam cells.

The lipid oil droplets in foam cells induced by different types of LDL oxidation were stained by Oil Red O and observed under inverted light microscope. The result showed that the number and size of lipid oil droplets in each cell that engulf high oxidation degree of LDL are higher and larger than the cells that engulf lower oxidation degree of LDL. A representative result from one of three independent experiments is shown.

3.2.3 Effect of different degree of LDL oxidation onto MMP-2 and MMP-9 expression at protein level

It has been reported that MMPs play an important role in plaque formation and rupture during atherosclerosis progression. Thus we would like to compare the effect of different types of LDL oxidation in production of different MMPs. As known that macrophages are the cell that responsible for engulfment of the excess LDL leading to foam cell formation and finally forming of the atherosclerotic plaque. Therefore, PMA-derived macrophages generated by stimulation of THP-1 or U937 cell line with PMA were used as a study model. The PMA-derived macrophages were cultured in the presence or absence of different types of LDL at various concentrations and incubation time points. Culture supernatant from different conditions of cultivation were collected and protein concentration was measured prior the assay.

Expression of MMP-2 and MMP-9 at protein level were examined by gelatin zymography. The result showed that at 6 h of cultivation, the expression of MMP-2 induced by different types of LDL was not significantly difference compared with un-stimulated macrophages or macrophages that were incubated with the reagent blank as shown in figure 3.38. However, expression of MMP-9 was decrease in a dose dependent manner while the cells were cultivated with mm-LDL. The ox-LDL can increase the MMP-9 expression when the concentration was increased while native-LDL has no significant difference. Moreover, the expression of active form of MMP-2 was found by stimulation of the cells with LDL at 12 h and oxidized-LDL at 24 h respectively. Nevertheless, active form of MMP-2 induced by both mm-LDL and ox-LDL was increased until the concentration 100 µg/ml and then decreased (Figure 3.39

and Figure 3.40). The expression of MMP-9 induced by mm-LDL and ox-LDL was decreased when increase the incubation time in a dose dependent manner. (Figure 3.39, 3.40)
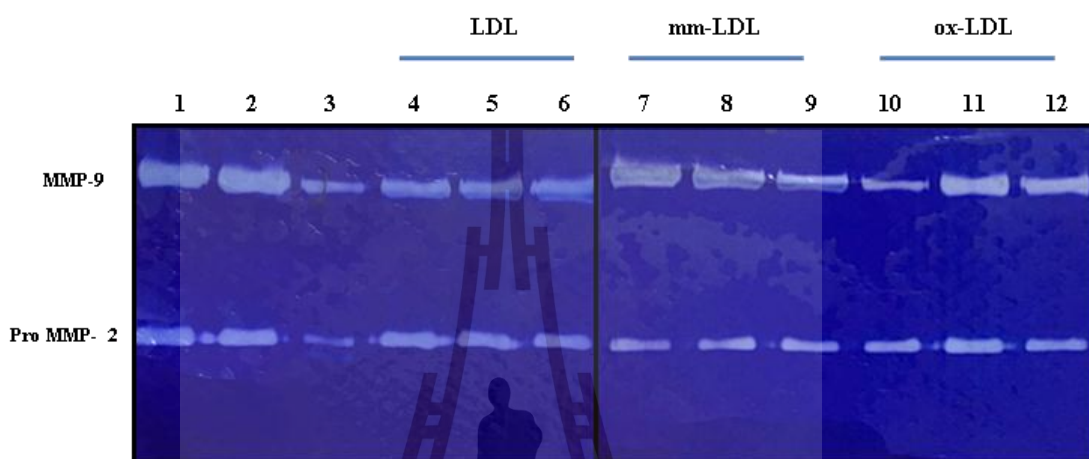
Figure 3.38 Gelatin zymography at 6 h.

Culture supernatant from cultivation of the PMA-derived macrophages with different types of LDLs at 6 h of incubation time was performed gelatin zymography. The result showed that expression of MMP-2 induced by different types of LDL was not significantly difference compared with macrophage (1) and macrophage with reagent blank (2). However, expression of MMP-9 was decrease in a dose dependent manner while the cells were cultivated with mm-LDL. The ox-LDL can increase the MMP-9 expression when the concentration was increased while native-LDL has no significant difference. Tunicamycin was used as positive control of active MMP-2 (3). Concentration of different types of LDL is 50 (4), (7), (10), 100 (5), (8), (11), and 200 (6), (9), (12) μg/ml. A representative result from one of three independent experiments is shown.
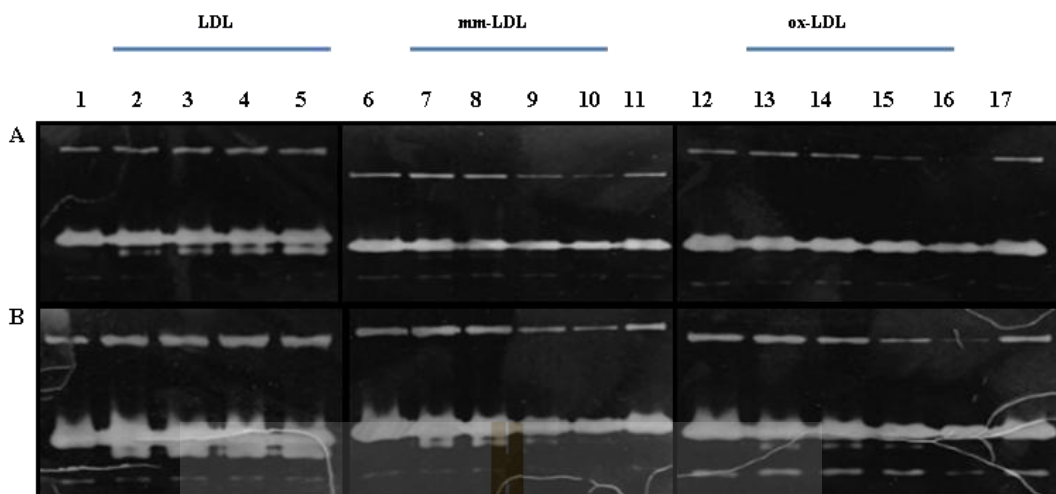
Figure 3.39 Gelatin zymography at 12 and 24 h.

Culture supernatants from cultivation of PMA-derived macrophages with different types of LDLs at incubation time 12 h (A) and 24 h (B) were performed gelatin zymography. The result showed that the expression of active form of MMP-2 induced by different types of LDL was increased whereas MMP-9 expression was weak compared with macrophage (1), (6), (12) and macrophage with reagent blank (11), (17). Concentration of different types of LDL is 50 (2), (7), (13), 100 (3), (8), (14), 200 (4), (9), (15) and 400 (5), (10), (16) μg/ml. A representative result from one of three independent experiments is shown.
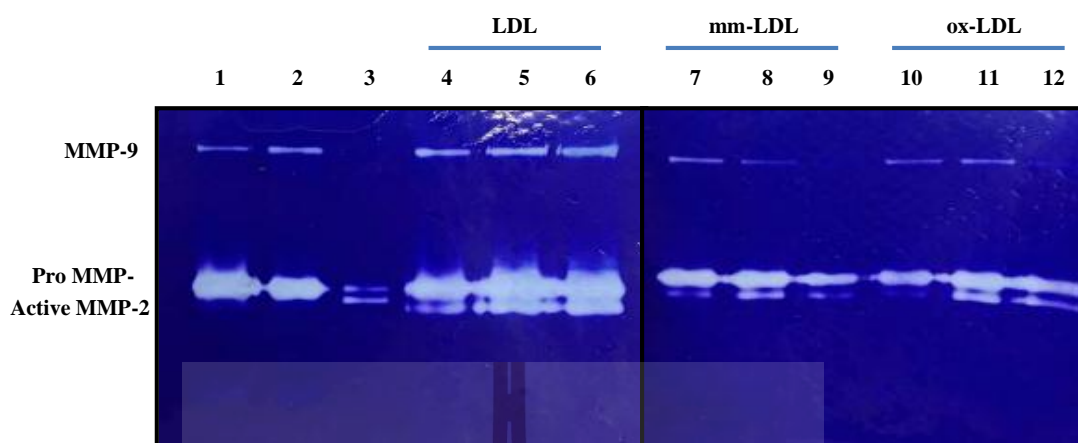
Figure 3.40 Gelatin zymography at 48 h.

Active MMP-2 was expressed after macrophages were incubated by different types of LDL whereas the expression of MMP-9 was reduced after macrophages were incubated with oxidized-LDL in a dose dependent manner. Macrophage (1) and macrophage with reagent blank (2) were used as reference. Tunicamycin was used as positive control of active MMP-2 (3). Concentration of different types of LDL is 50 (4), (7), (10), 100 (5), (8), (11), and 200 (6), (9), (12) μg/ml. A representative result from one of three independent experiments is shown.

3.2.4 Up-regulation of MMPs expression at mRNA level was observed when the degree of LDL oxidation was increased.

It has been reported that ox-LDL can up-regulate the expression of MMP-2 and MMP-9 using U937 cell line as the model. Since there are several MMPs produced from macrophage both in soluble and membrane type. We therefore interested whether the different degree of LDL oxidation have effects on those MMPs expression on macrophage. The expression of different MMPs, included MMP-1, MMP-2, MMP-9, MMP-12, MMP-14, and MMP-16, at the mRNA level upon induction by different types of LDL at different concentrations were studied using RT-PCR. The result showed that after stimulation of the PMA-derived macrophages with the different types of LDL for 48 h, the mRNA expressions of all studied MMPs was increased when the degree of LDL oxidation increased. Strong induction of mRNA expression was found in MMP-1, MMP-2, and MMP-9 and weak expression was found in MMP-12, MMP-14, and MMP-16. In addition, mRNA expression of MMP-1, MMP-2, and MMP-9 induced by mm-LDL was increased when the concentration of mm-LDL increased whereas mRNA expression of MMP-1 and MMP-2 induced by ox-LDL were decreased when the concentration of ox-LDL increased (Figure 3.41).
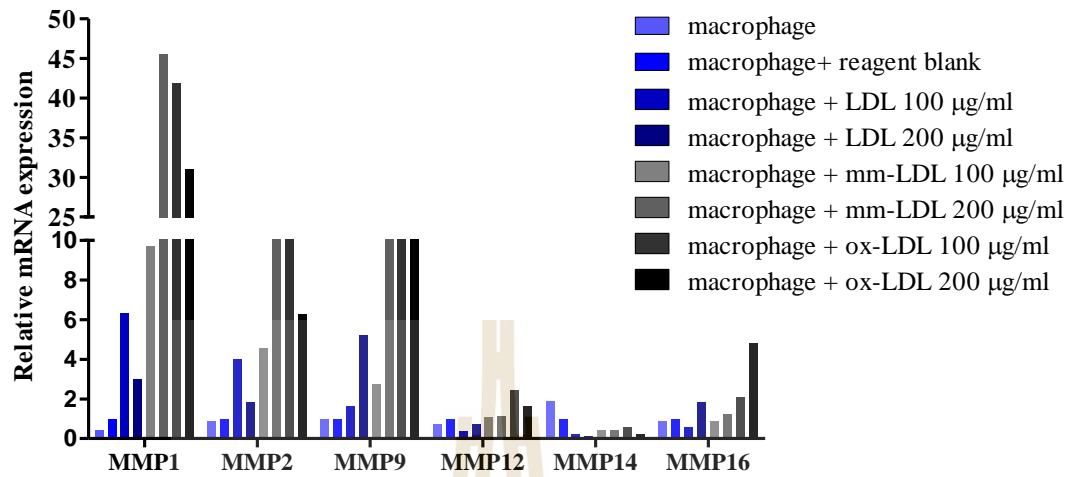
Figure 3.41 MMPs expression at mRNA level.

PMA-derived macrophages were cultured in the absence or presence of different degree of LDL oxidation at various concentrations for 48h. The mRNA from the cells were extracted and subjected to RT-PCR using specific primer for MMP-1, MMP-2, MMP-9, MMP-12, MMP-14, and MMP-16. A representative result from one of three independent experiments is shown.

CHAPTER IV

DISCUSSION AND CONCLUSION

Atherosclerosis is one of the leading causes of mortality worldwide. High concentration of LDL cholesterol is one of the major risk factors for the pathogenesis of atherosclerosis that lead to hypertension, coronary heart disease (CHD), stroke and death by resulting in cholesterol-burdened and activated macrophages, a hallmark of atherosclerotic plaques (Anneleen Remmerie, 2018; Dimitry A. Chistiakov, 2017; Shashkin P., 2005; Xiao-Hua Yu, 2013). Reduction of plasma LDL level is the main treatment target for prevention of atherosclerosis and other associated diseases.

The reference method for quantification of LDL in blood circulation is β-quantification (Masakazu Nakamuraa, 2014). Nevertheless, this method requires ultracentrifugation, needs large sample volume, time-consuming, and expensive. Thus, this method does not suit for routine laboratory. Consequently, an inexpensive method and easy approach for estimation of LDL concentration, called Friedewald equation, was established and named according to inventor (William T. Friedewald, 1972). Nowadays, this calculation method is widely used by many laboratories throughout the world to determine plasma LDL level.

Friedewald equation estimates plasma LDL level from measurement of total cholesterol, triglyceride, and high density lipoprotein (HDL) cholesterol. However, if triglyceride level is higher than 400 mg/dl, this calculated concentration of LDL is not

accurate. Several studies have tried to modify this formula to overcome this limitation (Ana Vujovic, 2010; Anandaraja S., 2005; Puaviliai W, 2004; Richard K. D. Ephraim, 2018). Still, these modifications were complicate and not accurate. To figure out this limitation, several direct LDL measurement procedures have been developed such as homogenous methods capable of full automation which are different in detail and procedure depend on manufacturers, chemical precipitation technique, and combination between immunological precipitation and enzymatic assay (Anders Larsson, 2018; Anirban Maitra, 1997; Jayesh Prabhakar Warade, 2016; So-Young Lee, 2015).

This study, we have developed the direct plasma or serum LDL measurement method using immunologically-based technique as an alternative technique and can be developed for self-evaluation of LDL level in blood samples in the future. Since antibodies are produced in response to the presence of foreign molecules in the body, specific binding property of antibody to its specific antigen can apply as a tool in various biomedical applications and researches such as diagnosis of diseases, treatment, and used as a tracker for cell signaling studies (Araya Ranok, 2013; Panida Khunkaewla, 2007). We expected that the antibody against human LDL will specifically bind to LDL in the blood and LDL can be directly measured without other interferences such as triglyceride, a major cause of non-accuracy LDL level estimated by Friedewald equation or other indirect measurement.

Since sandwich ELISA is an immunologically-based technique that highly efficient in sample detection. It quantifies antigen between 2 layers of antibody that recognized different epitope of target protein. The first antibody called captured antibody which is highly specific to target protein can eliminate non-target protein out

and capture only our target protein when the specimen added. The second antibody called detected antibody that bind the target protein at different epitope was follow added. As the antigen concentration increases, the amount of detection antibody increases, leading to a higher measured response. Thus, the standard curve of sandwich-ELISA will show a positive slope (Karen L. Cox, 2014).

Antibodies are synthesized by plasma cells, one type of differentiated B-lymphocytes. There are 2 main types of antibody: monoclonal and polyclonal antibody (pAb) which the specific antibody comes from monoclone or polyclones of secreting cells respectively. Generally, mAb which is the antibody comes from monoclone of Ab-secreting cells can determine the epitope binding site whereas pAb cannot. Polyclonal antibody is the antibody that comes from polyclone of antibody-secreting cells, therefore the epitope binding site cannot be determined among the mixture of antibody clones. To develop the direct plasma LDL measurement based on sandwich ELISA, 2 antibodies that recognize different epitopes of human LDL are necessary tools. As mentioned above that the mAb can determine the binding epitope of the antigen, thus the mAb against human LDL was our choice to generate and use as the tool to quantify the LDL level in this study. In 1975, Kohler and Milstein developed a technique named hybridoma technique that allows the growth of clonal populations of hybrid cells between antibody-secreting cells and immortal myeloma cells. The hybridoma technique becomes a standard tool for production of mAb. In this study, mAbs against human LDL were successfully generated by standard hybridoma technique and used as a tool to develop the technique of direct plasma LDL level quantification based on sandwich ELISA. The name of these clones was shorten and re-named as hLDL-1E2, hLDL-G10, hLDL-G11, hLDL-E8, hLDL-2D8,

hLDL-B6, and hLDL-D4. Isotypic determination was performed and found that mAb clone hLDL-1E2, hLDL-G10, hLDL-G11, and hLDL-E8 belong to IgG_1 isotype. Clone hLDL-2D8 belongs to IgG_{2b} isotype. Clone hLDL-B6 and hLDL-D4 belong to IgM isotype.

Lipids are transported in circulation by forming of the soluble complex of lipoprotein particles. Several types of blood lipoproteins, composed of different apolipoproteins and lipid composition, found in our human body. The only apolipoprotein found in LDL is apoB-100 (Dennis Vance, 2002). Cross-reactivity experiment found that all of the generated mAbs to human LDL react with apoB-100 but not react with apoE. Nevertheless, apoB-100 is not presented only in LDL but also in VLDL. Thus elimination of apoB-100 containing VLDL, which can cause false positive for the quantification, has to be performed. In clinical and research laboratories usually precipitate apoB-containing lipoproteins using polyvalent anion and divalent cation. It has been reported that heparin/$MnCl_2$ was used as a precipitation reagent for apoB precipitation (Joyce Corey Gibson, 1984). However, apoE is a heparin binding protein therefore contamination of apoB-containing VLDL in the precipitant may occur. Furthermore, apoA1, the major apolipoprotein of HDL and its associated cholesterol were left in the solution. It has been reported that only LDL but not VLDL and HDL could be precipitated with heparin in the absence of additional divalent cations by reducing the plasma pH to 5.11 (Heinrich Wieland, 1983). Accordingly, to avoid contamination of other apoB-containing lipoprotein, heparin/citrate pH 5.04 was used as a precipitating reagent. The result indicated that both VLDL and HDL were not precipitated. Other plasma proteins, except LDL were

remained in the precipitant. However, those plasma proteins have no effect on our measurement because our generated mAbs specifically bind to apoB.

After the precipitation step, only LDL was directly measured by our direct plasma LDL development method based on sandwich ELISA. Two clones of mAbs-against human LDL, which recognized different epitope of human LDL were selected and used as a study tool. After switch test to find the better sensitivity signal for the measurement system, mAb hLDL-E8 was used as captured antibody while mAb hLDL-2D8 was biotinylated and used as detection antibody. To obtain the best sensitivity for measurement, each batch of mAb preparation was titrated for the optimum concentration before use. .

To ensure that the developed technique for direct plasma LDL quantification using the generated mAbs can be used, two hundred and eight specimens from SUT hospital were randomized and used for this study. Plasma LDL level was measured by our in-house ELISA (direct measurement) and the results were compared with SUT hospital report (calculated measurement). The results indicated that mean of LDL level from our in-house ELISA and SUT hospital method were 126.6±43.1 mg/dl (range 90.0 to 258.0 mg/dl) and 123.2±42.3 mg/dl (range 34.0 to 236.0 mg/dl), respectively. The result from our in-house ELISA and SUT hospital were highly correlated according to simple linear regression analysis (Pearson's correlation coefficient r = 0.8491, p-value < 0.0001). The direct measurement from our in-house ELISA was not significantly difference from SUT hospital report. However, the mean of LDL level from our in-house ELISA was a bit higher than SUT hospital.

In general, calculated LDL level using Friedewald equation is not accurate if triglyceride level is higher than 400 mg/dl (Richard K. D. Ephraim, 2018). To

investigate whether triglyceride concentration influences the LDL quantification using our developed technique, standard human triglyceride were added into specimens to a final concentration of either 300 or more than 500 mg/dl respectively before measurement. The results revealed that LDL level was not significantly different between normal samples and triglyceride added samples. Furthermore, simple linear regression analysis showed high correlation among these group samples. These results suggested that high concentration of triglyceride level has no effect on determination of plasma LDL by our developed method. In addition, plasma level of other parameters in lipid profile such as total cholesterol and HDL cholesterol were analyzed and found that these parameters have no effect on LDL level obtained by direct LDL measurement using our developed method.

In conclusion, the immunologically-based direct plasma LDL measurement method using self-generated mAbs against human LDL was successfully developed. Major difficulty of the developed method is the sample LDL precipitation step, which is very strong pH dependent and personal skill is required. Thus, improvement of the technique to suit for the routine laboratory test is needed such as reduction of time consuming or omitting of the precipitation step. However, this method can be used as an alternative useful method for clinical diagnosis of LDL and LDL-related diseases and can be developed for self-evaluation in the future.

In addition of using the generated mAbs against human LDL for as a clinical diagnosis tool for development of direct plasma LDL measurement, in this study, the mAbs were also used as a tracker for monitoring of LDL oxidation level. LDL oxidation was considered to occur in stepwise manner. The lipid part of LDL molecule was firstly modified to generate mm-LDL. Once the period of oxidation

increase, the protein component of the LDL was also modified and obtained a molecule called ox-LDL (Hiroyuki Itabe, 2011). To determine the oxidizing degree of lipid component in LDL, the standard method used for determination of the lipid peroxidation product such as malondialdehyde called TBARS assay was used (Adriana E Scoccia, 2001; Ghaffari, 2010). The TBRAS assay is a colorimetric method that determine the lipid peroxidation product by spectrophotometric measuring of the pink color of MDA-TBA complex. Once the lipid component of the LDL was oxidized, the lipid peroxidation products will be generated and the positive result of TBARS will be obtained.

Nonetheless, this technique cannot distinguish between mm-LDL and ox-LDL because the lipid component of LDL particle can be maximum oxidized without oxidation of protein component for mm-LDL while ox-LDL, the lipid component can be maximum oxidized together with oxidation of protein component. Using the TBARS assay will provide the same result of only lipid oxidation level for both types of LDL. Therefore, the generated mAbs against human LDL that specifically bind to apoB-100, the protein component of LDL by indirect ELISA, was combined to the TBARS assay to discriminate between mm-LDL and ox-LDL. The discrimination using the generated mAbs based on modification of the protein structure that leads to lowering of binding affinity of the mAbs to its antigen. So, the ox-LDL should provide lower binding activity compared to the native LDL and the mm-LDL.

The results indicated that discrimination between mm-LDL and ox-LDL was successfully done by combination of the TBARS assay and the immunologically based-indirect ELISA technique using the generated mAbs against human LDL.

Fully oxidized LDL is known as a potent atherogenic agent of the atherosclerosis progression that can cause atherosclerosis. Several studies report that macrophages can engulf the ox-LDL and become foam cell formation. The accumulation of foam cells in the arterial wall is the hallmark of atherosclerosis (Dimitry A. Chistiakov, 2017; Shashkin P., 2005; Yuri V, 2006). However, few studies on the effect of native LDL and mm-LDL associated atherosclerosis have been reported. Primary study on the effect of different types of LDL in atherosclerosis was performed. In term of foam cell formation study, native-LDL, mm-LDL, and ox-LDL could induced foam cell formation in a dose dependent manner. However, the characteristics of lipid droplets in macrophage-derived foam cells by the high oxidative degree LDL can cause the larger size and higher number of lipid droplets inside the cells more than the native LDL. As a result, we conclude that all of different types of LDL; native LDL, mm-LDL, and ox-LDL could induced foam cell formation. As atherosclerotic plaque is formed by the accumulation of the foam cell, therefore high efficiency of foam cell formation of the ox-LDL and mm-LDL indicated that altherogenicity of ox-LDL and mm-LDL are higher than native LDL. However, more experiments need to be performed to support and elucidate.

At the advanced stage of atherosclerosis, plaque was growing and the numbers of foam cells accumulate around plaque and plaque shoulder were increased. Foam cells contribute into the local inflammation through the secretion of pro-inflammatory mediators such as chemokines, cytokines, reactive oxygen species (ROS), and matrix-degrading proteases. It has been reported that stability and strength of the fibrous cap covering the plaque is the result of a dynamic process between extracellular matrix such as gelatin, fibrinogen, and collagen and their degradation by matrix

metalloproteinases (MMPs) (Hakan Orbay, 2013). After plaque rupture, a small piece of plaque or a clotting blood known as thrombus will flow into the blood circulation leading to cardiovascular diseases, cerebrovascular disease, myocardial infarction, stroke, and death. Several studies reported that lipid-loaded macrophages stimulated by ox-LDL associated with the expression of MMPs around the atherosclerotic lesion. Nowadays, MMP-2 and MMP-9 are the most studies among several types of MMPs family (Gabriela M. Sanda, 2017; Yue, 2009). However, the effect of native LDL and mm-LDL on MMPs expression is not much understood.

This study, effect of the different types of LDL on expression of several MMPs in macrophages both in the mRNA level and protein level was observed. By performing RT-PCR, we found that native-LDL, mm-LDL, and ox-LDL can induce MMP-1, MMP-2, MMP-9, MMP-12, MMP-14, and MMP-16 expression at mRNA level at 48 h. Notably, increasing the degree of oxidation increased the expression of all studied MMPs. The obvious result was observed for MMP-1, MMP-2, and MMP-9 expression. However, the incubation time for expression of each MMP may differ from each other. Therefore, the optimization of the cultivation time for each MMP expression is needed for future study.

As found that all types of LDL could induced the expression of the studied MMPs in the mRNA level, however, not all mRNA can be translated to be a functional protein. Hence, expression of the studied MMPs was also observed in the protein level. By performing the gelatin zymographic analysis, the active MMP-2 was starting to express by LDL after 12 h and by the mm-LDL and ox-LDL after 24 h. Induction of the active form of MMP-2 by either mm-LDL or ox-LDL was increased until the concentration reached to 100 μg/ml and then decreased at a final

concentration of the LDL at 200 μg/ml. However, the expression of MMP-9 induced by mm-LDL and ox-LDL was decreased when increase the incubation time in a dose dependent manner.

From these primary results, we can conclude that different types of LDL; native LDL, mm-LDL, and ox-LDL were able to induce MMPs expression both mRNA and protein level. However, each type of LDL can have a different effect on each type of MMP. From our study found that MMP-9 expression was associated with the early stage of atherosclerosis because its expression at protein level can be observed at the short time of different types of LDL incubation with PMA-derived macrophages and MMP-2 expression was associated in the late stage of atherosclerosis because its expression at protein level needs a longer tine of incubation. However, the role of MMPs in atherosclerosis progression induced by LDL, mm-LDL, and ox-LDL seems to be the stepwise signal. More study experiments need to be elucidated.

REFERENCES
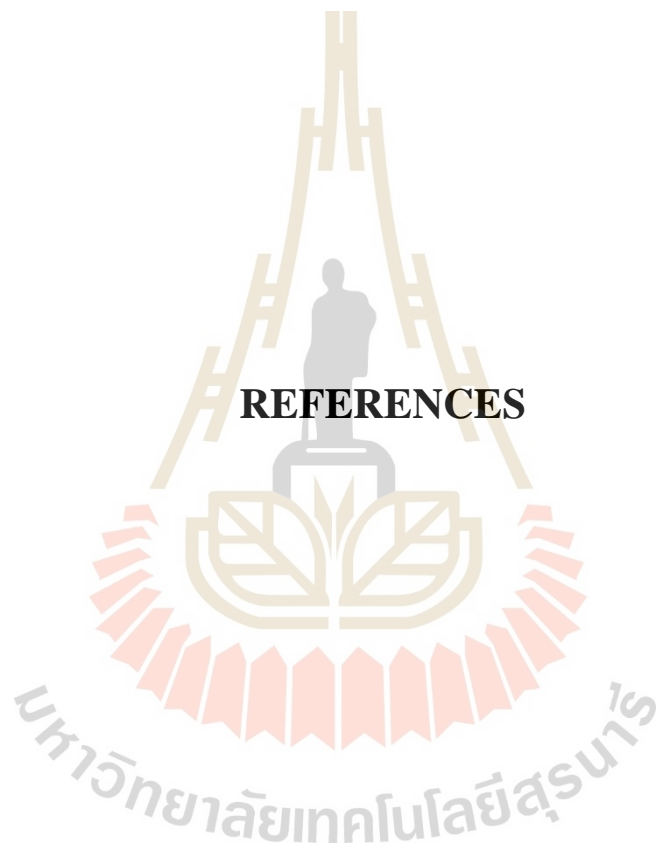
REFERENCES

Abbas, K. A., Lichtman, H. A., and Pillai, S. (2011). Cellular and molecular immunology updated: The immune system (7 ed.). Pensylvania: **Elsevier Saunders**.

Adriana E Scoccia, María Silvina Molinuevo, Antonio Desmond McCarthy, and Ana María Cortizo. (2001). A simple method to assess the oxidative susceptibility of low density lipoproteins. **BMC Clinical Pathology**. 1(1).

Aernout Luttun, Esther Lutgens, Ann Manderveld, Katleen Maris, Desire Collen, Peter Carmeliet, and Lieve Moons. (2004). Loss of matrix metalloproteinase-9 or matrix metalloproteinase-12 protects apolipoprotein E–deficient mice against atherosclerotic media destruction but differentially affects plaque growth. **Circulation**. 109: 1408-1414.

Akinori Tokito, Michihisa Jougasaki, Tomoko Ichiki, and Shuichi Hamasaki. (2013). Cardiotrophin-1 induces matrix metalloproteinase-1 in human aortic endothelial cells. **PLOS One**. 8(7).

Alex Y. Strongin, Ivan Collier, Gregory Bannikov, Barry L. Marmer, Gragory A. Grant, and Gregory I. Goldberg. (1994). Mechanism of cell surface activation of 72-kDa type IV collagenase. **Journal of Biological Chemistry**. 270(10): 5331-5338.

Ana Vujovic, Jelena Kotur-Stevuljevic, Slavica Spasic, Nada Bujisic, Jelena Martinovic, Milica Vujovic, Vesna Spasojevic-Kalimanovska, Aleksandra

Zeljkovic, and Dragoljub Pajic. (2010). Evaluation of different formulas for LDL-C calculation. **Lipids in Health and Disease**. 9(27).

Anandaraja S., Narang R., Godeswar R., Laksmy R., and Talwar K. K. (2005). Low-density lipoprotein cholesterol estimation by a new formula in Indian population. **International Journal of Cardiology**. 102: 117-120.

Anders Larsson, Emil Hagstrom, Lennart Nilsson, and Maria K. Svensson. (2018). Treatment target re-classification of subjects comparing estimation of low-density lipoprotein cholesterol by the Friedewald wquation and direct measurement of LDL-cholesterol. **Upsala Journal of Medical Sciences**. 123(2): 94-99. doi:10.1080/03009734.2018.1465496

Andrea Lichte, Hansjorg Kolkenbrock, and Harald Tschesche. (1996). The recombinant catalytic domain of membrane-type matrix metalloproteinase- 1 (MT1 -MMP) induces activation of progelatinase A and progelatinase A complexed with TIMP-2. **FEBS Letters**. 397: 227-282.

Anirban Maitra, Shaina V. Hirany, and Ishwarlal Jialal. (1997). Comparison of two assays for measuring LDL cholesterol. **Clinical Chemistry**. 43:6: 1040-1047.

Anneleen Remmerie and Charlotte L. Scott (2018). Macrophages and lipid metabolism. **Cellular Immunology**. 330: 27-42.

Apiratmateekul, N. (2007). Production of conditioned media for generation of hybridomas for monoclonal antibody production. (Master of Science), Chiang Mai University.

Araya Ranok, Panida Khunkaewla, and Wipa Suginta. (2013). Human cartilage chitinase 3-like Protein 2: cloning, expression, and production of polyclonal and monoclonal antibodies for osteoarthritis detection and identification of

potential binding partners. **Monoclonal antibodies in immunodiagnosis and immunotherapy**. 32: 317-325.

Barrington, R. (2013). Plasma lipoproteins: A primer. Retrieved from http://www.robertbarrington.net/plasma-lipoproteins-a-primer.

Beatriz Alvarez, Carmen Ruiz, Pilar Chacon, Jose Alvarez-Sabin, and Manuel Matas. (2004). Serum values of metalloproteinase-2 and metalloproteinase-9 as related to unstable plaque and inflammatory cells in patients with greater than 70% carotid artery stenosis. **Journal of Vascular Surgery**. 40: 469-475.

Brian W. Howell and Joachim Herz. (2001). The LDL receptor gene family: signaling functions during development. **Current Opinion in Neurobiology**. 11: 74-81.

Bryan G. Hughes and Richard Schulz. (2014). Targeting MMP-2 to treat ischemic heart injury. **Basic Res Cardiol**. 109: 424.

Chia-Chen Liu, Takahisa Kanekiyo, Huaxi Xu, and Guojun Bu. (2013). Apolipoprotein E and alzheimer disease: risk, mechanisms, and therapy. **Nat Rev Neurol**. 9(2): 106-118. doi:10.1038/nrneurol.2012.263.

Christian A. Gleissner, Norbert Leitinger, and Klaus Ley. (2007). Effects of native and modified low-density lipoproteins on monocyte recruitment in atherosclerosis. **Hypertension**. 50: 276-283.

David L. Nelson and Michael M. Cox. (2008). Principles of Biochemistry (4 ed.).

Dennis Vance and Jean Vance. (2002). Biochemistry of lipids, lipoproteins and membranes (4 ed.): Elsevier.

Dimitry A. Chistiakov, Alexandra A. Melnichenko, Veronika A. Myasoedova, Andrey V. Grechko, and Alexander N. Orekhov. (2017). Mechanisms of foam

cell formation in atherosclerosis. **J Mol Med**. 9*5*, 1153-1165. doi:10.1007/s00109-017-1575-8.

Eiji Matsuura, Fabiola Atzeni, Piercarlo Sarzi-Puttni, Maurizio Turiel, Luis Lopez, and Michael Nurmohamed. (2014). Is atherosclerosis is an autoimmune disease? **BMC Medicin**. 12(47).

Eric B. Springman, Eddie L. Angleton, Henning Birkedal-Hansen, and Harold E. Van Wart. (1990). Multiple modes of activation of latent human fibroblast collagenase: Evidence for the role of a Cys73 active-site zinc complex in latency and a "cysteine switch" mechanism for activation. **Proc. Natl. Acad. Sci. USA**. 87: 364-368.

Gabriela M. Sanda, Mariana Deleanu, Laura Toma, Camelia S. Stancu, Maya Simionescu, and Anca V. Sima. (2017). Oxidized LDL-exposed human macrophages display increased MMP-9 expression and secretion mediated by endoplasmic reticulum stress. **Journal of Cellular Biochemistry**. 118: 661-669.

Ghaffari, M. A. and Ghiasvand, T. (2010). Kinetic study of low density lipoprotein oxidation by copper. **Indian Journal of Clinical Biochemistry**. 25(1): 29-36.

Hakan Orbay, Hao Hong, Yin Zhang, and Weibo Cai. (2013). Positron emission tomography imaging of atherosclerosis. **Theranostics**. 3(11): 894-902.

Handberg, A., Hojlund, K., Gastaldelli, A., Flyvbjerg, A., Dekker, J. M., Petrie, J., Piatti, P., Beck-Nielsen, H., and the RISC Investigators. (2012). Plasmas CD36 is associatedwithmarkers of atherosclerosis, insulin resistance and fatty liver in a nondiabetic healthy population. **Journal of Internal Medicine**. 271: 294-304.

Harold E. Van Wart and Henning Birkedal-Hansen. (1990). The cysteine switch: A principle of regulation of metalloproteinase activity with potential applicability to the entire matrix metalloproteinase gene family. **Proc. Natl. Acad. Sci. USA**. 87: 5578-5582.

Heinrich Wieland and Dietrich Seidel. (1983). A simple specific method for precipitation of low density lipoproteins. **Journal of Lipd Research**. 24: 904-909.

Hiroharu Kataoka, Noriaki Kume, Susumu Miyamoto, Manabu Minami, Hideaki Moriwaki, Takatoshi Murase, Tatsuya Sawamura, Tomoh Masaki, Nobuo Hashimoto, and Toru Kita. (1999). Expression of lectin like oxidized low-density lipoprotein receptor-1 in human atherosclerotic lesions. **Circulation**. 99(24): 3110-3117.

Hiroyasu Uzui, Alice Harpf, Ming Liu, Terence M. Doherty, Arun Shukla, Ning-Ning Chai, Pinky V. Tripathi, Stefan Jovinge, Douglas J. Wilkin, Kamlesh Asotra, Prediman K. Shah, and Tripathi B. Rajavashisth. (2002). Increased expression of membrane type 3–matrix metalloproteinase in human atherosclerotic plaque-role of activated macrophages and inflammatory cytokines. **Circulation**. 106: 3024-3030.

Hiroyuki Itabe, Takashi Obama, and Rina Kato. (2011). The dynamics of oxidized LDL during atherogenesis. **Journal of Lipids**. doi:10.1155/2011/418313.

Hisashi Kai, Hisao Ikeda, Hideo Yasukawa, Mamiko Kai, Yukihiko Seki, Fumitaka Kuwahara, Takafumi Ueno, Kenzo Sugi, and Tsutomu Imaizumi. (1998). Peripheral blood levels of matrix metalloproteases-2 and -9 are elevated in patients with acute coronary syndromes. **J Am Coll Cardiol**. 32: 368-372.

Hoiroaki Okazaki, Masaki Igarashi, Makiko Nishi, Motohiro Sekiya, Makiko Tajima, Satoru Takase, Mikio Takanashi, Keisuke Ohta, Yoshiaki Tamura, Sachiko Okazaki, Naoya Yahagi, Ken Ohashi, Michiyo Amemiya-Kudo, Yoshimi Nakagawa, Ryozo Nagai, Takashi Kadowaki, Jun-ichi Osuga, and Shun Ishibashi. (2008). Identification of neutral cholesterol ester hydrolase, a key enzyme removing cholesterol from macrophages. **Journal of Biological Chemistry**. 283(48): 33357-33364.

Howard S. Kruth, Nancy L. Jones, Wei Huang, Bin Zhao, Itsuko Ishii, Janet Chang, Christian A. Combs, Daniela Malide, and Wei-Yang Zhang. (2005). Macropinocytosis is the endocytic pathway that mediates macrophage foam cell formation with native low density lipoprotein. **Journal of Biological Chemistry**. 280(3): 2352-2360.

Janeway, C. A., Travers, P., Walport, M., and Capra, J. D. (1999). Immunobiology: The immune system in health and disease: Current Biology Publications. New York: NY.

Jason L. Johnson, Graciela B. Sala-Newby, Yasmin Ismail, Concepcion M. Aguilera, and Andrew C. Newby. (2008). Low tissue inhibitor of metalloproteinases 3 and high matrix metalloproteinase 14 levels defines a subpopulation of highly invasive foam-cell macrophages. **Arterioscler Thromb Vasc Biol**. 28(9): 1647-1653.

Jason L. Johnson, Laurent Devel, Bertrand Czarny, Sarah J. George, Christopher L. Jackson, Vassilis Rogakos, Fabrice Beau, Athanasios Yiotakis, Andrew C. Newby, and Vincent Dive. (2011). A selective matrix metalloproteinase-12

inhibitor retards atherosclerotic plaque development in apolipoprotein E–knockout mice. **Arterioscler Thromb Vasc Biol**. 31(3): 528-535.

Jason L. Johnson, Nicholas P. Jenkins, Wei-Chun Huang, Karina Di Gregoli, Graciela B. Sala-Newby, Vincent P. W. Scholtes, Frans L. Moll, Gerard Pasterkamp, and Andrew C. Newby. (2014). Relationship of MMP-14 and TIMP-3 expression with macrophage activation and human atherosclerotic plaque vulnerability. **Mediators of Inflammation**.

Jason L. Johnson, Sarah J. George, Andrew C. Newby, and Christopher L. Jackson. (2005). Divergent effects of matrix metalloproteinases 3, 7, 9, and 12 on atherosclerotic plaque stability in mouse brachiocephalic arteries. **PNAS**. 102: 15575-15580.

Jayesh Prabhakar Warade, Hemant Dahake, and Kavitha, R. (2016). Comparison between direct estimation of LDL and Friedewald's formula. **International Archives of Integrated Medicine**. 3(2): 10-17.

Jingyan Liang, Enqi Liu, Ying Yu, Shuji Kitajima, Tomonari Koike, Yingji Jin, Masatoshi Morimoto, Kinta Hatakeyama, Yujiro Asada, Teruo Watanabe, Yasuyuki Sasaguri, Shigeyuki Watanabe, and Jianglin Fan. (2006). Macrophage metalloelastase accelerates the progression of atherosclerosis in transgenic rabbits. **Circulation**. 113: 1993-2001.

Johnson, J. L. (2017). Metalloproteinases in atherosclerosis. **European Journal of Pharmacology**. 816: 93-106.

Joyce Corey Gibson, Ardon Rubinstein, and Virgil Brown, W. (1984). Precipitation of apo E-containing lipoproteins by precipitation reagents for apolipoprotein B. **Clinical Chemistry**. 30: 1784-1788.

Karen L. Cox, Viswanath Devanarayan, Aidas Kriauciunas, Joseph Manetta, Chahrzad Montrose, and Sitta Sittampalam. (2014). Immunoassay Methods

Kenneth Feingold and Carl Grunfeld. (2018). Introduction to Lipids and Lipoproteins A. B. Feingold KR, Boyce A, et al. (Ed.) Retrieved from https://www.ncbi.nlm.nih.gov/books/NBK305896/

Kindt, Thomas J, Goldsby, Richard A Osborne, Barbara Anne, Kuby, and Janis. (2007). Kuby immunology (6 ed.). United States: New York : W.H. Freeman, c2007.

Kohler, G., and Milstein, C. (1975). Continuous cultures of fused cells secreting antibody of predefined specificity. **Nature**. 256(5517): 495-497. doi:10.1038/256495a0.

Lakshmi P. Kotra, Jason B. Cross, Yoichiro Shimura, Rafael Fridman, Bernhard H. Schlegel, and Shahriar Mobashery. (2001). Insight into the complex and dynamic process of activation of matrix metalloproteinases. **J. Am. Chem. Soc**. 123: 3108-3113.

Libby, P. (2013). Collagenases and cracks in the plaque. **The Journal of Clinical Investigation**. 1238(8): 3201-3203.

Lijnen, H. R. (2001). Plasmin and matrix metalloproteinases in vascular remodeling. **Thromb Haemost**. 86: 324-333.

Masafumi Kuzuya, Shigeru Kanda, Takeshi Sasaki, Norika Tamaya-Mori, Xian Wu Cheng, Takeshi Itoh, Shigeyoshi Itohara, and Akihisa Iguchi. (2003). Deficiency of gelatinase A suppresses smooth muscle cell invasion and development of experimental intimal hyperplasia. **Circulation**. 108: 1375-1381.

Masakazu Nakamuraa, Yuzo Kayamori, Hiroyasu Iso, Akihiko Kitamura, Masahiko Kiyama, Isao Koyama, Kunihiro Nishimura, Michikazu Nakai, Hiroyuki Noda, Mahnaz Dasti, Hubert W. Vesper, and Yoshihiro Miyamotoi. (2014). LDL cholesterol performance of beta quantification reference measurement procedure. **Clin Chim Acta**. 20: 288-293.

Newby, A. C. (2007). Role of metalloproteinases in plaque rupture. I**nternational Journal of Gerontology**. 1(3): 103-111.

Noemi Ramos-DeSimone, Elizabeth Hahn-Dantona, John Sipley, Hideaki Nagase, Deborah L. French, and James P. Quigley. (1999). Activation of matrix metalloproteinase-9 (MMP-9) via a converging plasmin/stromelysin-1 cascade enhances tumor cell invasion. **Journal of Biological Chemistry**. 274: 13066-13076.

Nooijer, d. R., Verkleij, C. J. N., Thusen, von der J. H., Jukema, J. W., Wall, van der E. E., Berkel, van Th. J. C., Baker, A. H., and Biessen, E. A. L. (2006). Lesional overexpression of matrix metalloproteinase-9 promotes intraplaque hemorrhage in advanced lesions but not at earlier stages of atherogenesis. **Arterioscler Thromb Vasc Biol**. 26: 340-346.

Panida Khunkaewla, Sawitree Chiampanichayakul, Umpa Yasamut, Supansa Pata, and Watchara Kasinrerk. (2007). Production, characterization, and functional analysis of newly established CD99 monoclonal antibodies MT99/1 and MT99/2. **Hybridoma**. 26: 241-249.

Patricia A. M. Snoek-van Beurden and Johannes W. Von den Hoff. (2005). Zymographic techniques for the analysis of matrix metalloproteinases and their inhibitors. **BioTechniques**. 38: 73-83.

Pepper, M. S. (2001). Role of the matrix metalloproteinase and plasminogen activator–plasmin systems in angiogenesis. **Arterioscler Thromb Vasc Biol**. 21: 1104-1117.

Peter J. Gough, Ivan G. Gomez, Paul T. Wille, and Elaine W. Raines. (2006). Macrophage expression of active MMP-9 induces acute plaque disruption in apoE-deficient mice. **The Journal of Clinical Investigation**. 116: 59-69.

Petri I. Makinen, Jari P. Lappalainen, Suvi E. Heinonen, Pia Leppanen, Markku T. Lahteenvuo, Jussi V. Aarnio, Janne Heikkila, Mikko P. Turunen, and Seppo Yla-Herttuala. (2010). Silencing of either SR-A or CD36 reduces atherosclerosis in hyperlipidaemic mice and reveals reciprocal upregulation of these receptors. **Cardiovascular Research**. 88: 530-538. doi:10.1093/cvr/cvq235.

Playfair, J. H. L. and Chain, B.M. (2012). Immunology at a Glance (10 ed.): Wiley-Blackwell.

Puaviliai W and Laorugpongse D. (2004). Is calculated LDL-C by using the new modified Friedewald equation better than the standard Friedewald equation? **Journal of The Medical Association of Thailand**. 87: 589-593.

Rafael Fridman, Marta Toth, Irina Chvyrkova, Samy O. Meroueh, and Shahriar Mobashery. (2003). Cell surface association of matrix metalloproteinase-9 (gelatinase B). **Cancer and Metastasis Reviews**. 22: 153-166.

Renu Virmani, Allen P. Burke, Andrew Farb, and Frank D. Kolodgie. (2005). Pathology of the Vulnerable Plaque. **Journal of the American College of Cardiology**. 47(8): C13-18.

Richard, K. D. Ephraim, E. A., Swiithin M. Swaray, Enoch Odame Anto, Prince Adoba, Bright Oppong Afranie, Emmanuella Nsenbahatu, Patrick Adu, Linda Ahenkorah Fondjo, Samuel Asamoah Sakyi, and Beatrice Amoah. (2018). Developing a modified low-density lipoprotein (M-LDL-C) Friedewald's equation as a substitute for direct LDL-C measure in a Ghanaian population: A comparative study. **Journal of Lipids**.

Seppo T. Nikkari, Kevin D. O'Brien, Marina Ferguson, Thomas Hatsukami, Howard G. Welgus , Charles E. Alpers , and Alexander W. Clowes. (1995). Interstitial collagenase (MMP-1) expression in human carotid atherosclerosis. **Circulation**. 92(6): 1393-1398.

Shashkin, P., Dragulev, B., and Ley, K. (2005). Macrophage differentiation to foam cells. **Current pharmaceutical design**. 11(23): 3061-3072.

Shun-ichiro Matsumoto, Tatsushi Kobayashi, Masao Katoh, Shigeki Saito, Yasushi Ikeda, Masato Kobori, Yasuhiko Masuho, and Teruo Watanabe. (1998). Expression and localization of matrix metalloproteinase-12 in the aorta of cholesterol-fed rabbits. **American Journal of Pathology**. 153(1): 109-119.

Shutong Yao, Nana Yang, Guohua Song, Hui Sang, Hua Tian, Cheng Miao, Ying Zhang, and Shucun Qin. (2012). Minimally modified low-density lipoprotein induces macrophage endoplasmic reticulum stress via toll-like receptor 4. **Biochimica et Biophysica Acta**. 1821: 954-963.

So-Young Lee, Sang-Keun Hahm, Jin-A Park, Sung-Kyu Choi, Ji-Young Yoon, Seon-Hee Choi, and Kyoung-So Jeon. (2015). Measuring low density lipoprotein cholesterol: Comparison of direct measurement by Hisens reagents

and Friedewald estimation. **Korean Journal of Family Medicine**. 36: 168-173. doi:10.4082.

Sukhova, G. K., Schonbeck, U., Rabkin, E., Schoen, F. J., Poole, A. R., Billinghurst, R. C., and Libby, P. (1999). Evidence for increased collagenolysis by interstitial collagenases-1 and -3 in vulnerable human atheromatous plaques. **Circulation**. 18: 2503-2509.

Tripathi B. Rajavashisth, Xiao-Ping Xu, Stefan Jovinge, Simcha Meisel, Xiao-Ou Xu, Ning-Ning Chai, Michael C. Fishbein, Sanjay Kaul, Bojan Cercek, Behrooz Sharifi, and Prediman K. Shah. (1999). Membrane type 1 matrix metalloproteinase expression in human atherosclerotic plaques evidence for activation by proinflammatory mediators. **Circulation**. 99: 3103-3109.

Uwe Schonbeck, Francois Mach, Galina K. Sukhova, Curran Murphy, Jean-Yves Bonnefoy, Rosalind P. Fabunmi, and Peter Libby. (1997). Regulation of matrix metalloproteinase expression in human vascular smooth muscle cells by T lymphocytes: a role for CD40 signaling in plaque rupture? **Circulation Research**. 81(3): 448-454.

Vera Knauper, Horst Will, Carlos Lopez-Otin, Bryan Smith, Susan J. Atkinson, Heather Stanton, Rosalind M. Hembry, and Gillian Murphy. (1996). Cellular mechanisms for human procollagenase-3 (MMP-13) activation: Evidence that MT1-MMP (MMP-14) and gelatinase A (MMP-2) are able to generate active enzyme. **Journal of Biological Chemistry**. 271: 17124-17131.

Vincent Lemaitre, Timothy K. O'Byrne, Alain C. Borczuk, Yasunori Okada, Alan R. Tall, and Jeanine D'Armiento. (2001). Apo E knockout mice expressing

human matrix metalloproteinase-1 in macrophages have less advanced atherosclerosis. **Journal of Clinical Investigation**. 107: 1227-1234.

Vincent P. W. Scholtes, Jason L. Johnson, Nicholas Jenkins, Graciela B. Sala-Newby, Jean-Paul P. M. de Vries, Gert Jan de Borst, Dominique P. V. de Kleijn, Frans L. Moll, Gerard Pasterkamp, and Andrew C. Newby. (2012). Carotid atherosclerotic plaque matrix metalloproteinase-12–positive macrophage subpopulation predicts adverse outcome after endarterectomy. **J Am Heart Assoc**. doi: 10.1161/JAHA.112.001040.

Viviane Z. Rocha and Peter Libby. (2009). Obesity, inflammation, and atherosclerosis. **Nature Reviews Cardiology**. 6: 399. doi:10.1038/nrcardio.2009.55.

Wang, Y. (2012). Structural characterization of immunoglobulin G antibodies with LC-MS based approaches. (Doctor of Philosophy), Northeastern University.

William T. Friedewald, Robert I. Levy, and Donald S. Fredickson. (1972). Estimationof the concentration of Low-Density LipoproteinCholesterol in plasma, without use of the preparative ultracentrifuge. **Clinical Chemistry**. 18(6): 499-502.

Xiao-Hua Yu, Yu-Chang Fu, Da-Wei Zhang, Kai Yin, and Chao-Ke Tang (2013). Foam cells in atherosclerosis. **Clinica Chimica Acta**. 424: 245-252.

Yue, H. H., Leng, N., Wua, Z.B., Li, H.M., Li, X.Y., Zhua, P. (2009). Expression of CD147 on phorbol-12-myris-tate-13-acetate (PMA)-treated U937 cells differentiating into foam cells. **Archives of Biochemistry and Biophysics**. 485: 30-34.

Yuri V. Bobryshev. (2006). Monocyte recruitment and foam cell formation in atherosclerosis. **Micron**. 37: 208-222. doi:10.1016/j.micron.2005.10.007.

Zorina S. Galis, Maria Muszynski, Galina K. Sukhova, Elissa Simon-Morrissey, and Peter Libby. (1994). Enhanced expression of vascular matrix metalloproteinases induced in vitro by cytokines and in regions of human atherosclerotic lesions. **Annals New York Academy of Sciences**. 748: 501-507.
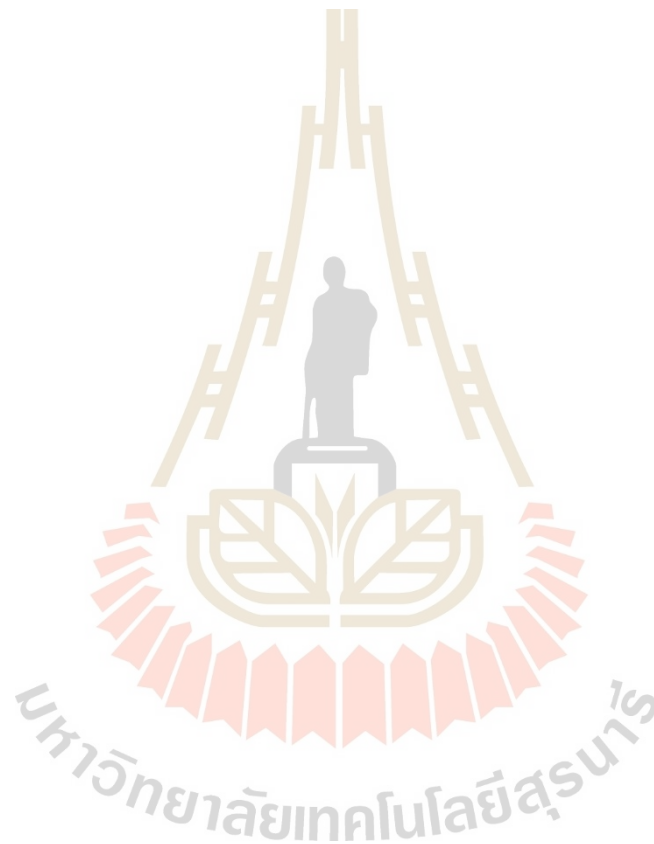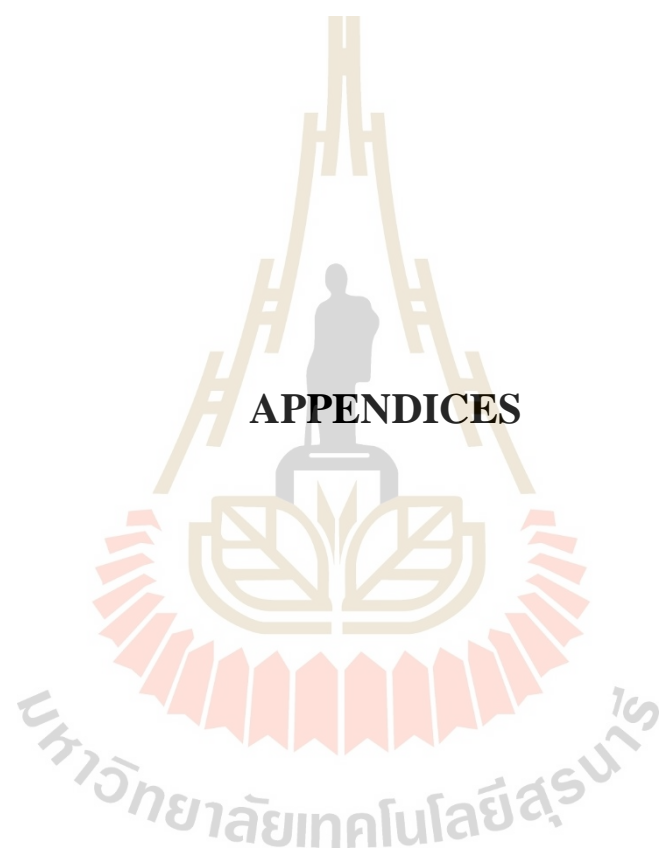
APPENDICES

APPENDIX A

LIST OF CHEMICALS, MATERIALS, ANTIBODIES, ANIMALS, AND CELL LINES USED IN THIS STUDY

Chemicals, materials, antibodies, animals, and cell lines	Source
Acrylamide	AppliChem, Damstadt, Germany
Agarose gel	Norgen, Biotek Corp., Thorold, ON, Canada
3-Aminophthalhydrazide	Fluka, Buchs, Switzerland
Ammonium chloride (NH_4Cl)	Carlo Erba, Milan, Italy
Ammonium (II) sulfate $(NH_4)_2SO_4$	Carlo Erba, Milan, Italy
Bis-acrylamide	Acros Organics, New Jersey, USA
10X BM Condimed H1	Roche Diagnostics, Mannheim, Germany
Bromphenol blue	Carlo Erba, Milan, Italy
Calcium chloride ($CaCl_2$)	Carlo Erba, Milan, Italy
Chloroform	Carlo Erba, Milan, Italy
Chromatin pre-stained protein ladder	Vivantis, Malaysia
Complete Freund's adjuvant	Sigma-Aldrich, St. Louis, MO, USA
Coomassie brilliant blue R250	AppliChem, Damstadt, Germany
Copper (II) sulfate ($CuSO_4$)	Carlo Erba, Milan, Italy

p-Coumaric acid	Fluka, Buchs, Switzerland
Dimethylsulfoxide (DMSO)	Vivantis, Malaysia
Disodium hydrogen phosphate (Na_2HPO_4)	Carlo Erba, Milan, Italy
Ethanol	Carlo Erba, Milan, Italy
Ethylenediaminetetraacetic acid - disodium salt dehydrate (EDTA)	Amersham Biosciences, Uppsala, Sweden
EZ-Link® NHS-Biotin reagents	Thermo Scientific, Rockford, USA
Female BALB/c mouse	National Laboratory Animal Center, Nakhon Pathom, Thailand
Fetal Bovine Serum (FBS)	Gibco, Gran Island, N.Y., USA
Film developer and replenisher	Carestream, Rochester, N.Y., USA
Film fixer and replenisher	Carestream, Rochester, N.Y., USA
Fungizone (Amphotericin B)	Gibco, Gran Island, N.Y., USA
gDNA Maxi Kit (Blood/Cultured cells)	Geneaid, New Taipei, Taiwan
Gelatin	Sigma-aldrich, St. Louis, MO, USA
Gentamycin	Nida Pharma Incorporation, Ayutthaya, Thailand
1% Gential Violet	United Drug, Bangkok, Thailand
Glycerol	Carlo Erba, Milan, Italy
Glycine	Vivantis, Malaysia
GoTaq® DNA Polymerase	Promega, Woods Hollow Road, Madison, USA
Gracial acetic acid	Carlo Erba, Milan, Italy
Heparin	Troikaa Pharmaceuticals, Gujarat, India

HiTrap™ IgM purification HP column	GE Healthcare, Uppsala, Sweden
HiTrap™ Protein G HP column	GE Healthcare, Uppsala, Sweden
Horseradish peroxidase conjugated – rabbit anti-mouse immunoglobulins – antibody	Dako, Glostrup, Denmark
Horseradish peroxidase conjugated – streptavidin	Invitrogen, Thermo Scientific, USA
Hydrochloric acid (HCl)	Carlo Erba, Milan, Italy
30% Hydrogen peroxide (H_2O_2)	Carlo Erba, Milan, Italy
50X Hypoxanthine Aminopterin – Thymidine (HAT)	Sigma, St. Louis, MO, USA
50X Hypoxanthine Thymidine (HT)	Sigma, St. Louis, MO, USA
Immobilin®-P transfer membrane	Millipore, Billerica MA, USA
Incomplete Freund's adjuvant	Sigma-Aldrich, St. Louis, MO, USA
Isocove's Modified Dulbecco's – Medium (IMDM)	Gibco, Gran Island, N.Y., USA
Isopropanol	Tedia, USA
Isotypic determination kit	Sigma, St. Louis, MO, USA
LightCycler® 480 SYBR Green I Master	Roche Diagnostics, Mannheim, Germany
Lipoprotein, Low Density, Human (LDL)	United States Biological, Massachusetts, USA
Malondialdehyde (MDA)	Acros Organics, New Jersey, USA
Medical X-ray Green/MXG film	Carestream, Rochester, N.Y., USA
2-Mercaptoethanol	Acros Organics, New Jersey, USA

Methanol	Carlo Erba, Milan, Italy
Mouse Myeloma cells, P3X63Ag8.653 (ATCC® CRL-1580™)	Watchara Kasinrerk's lab, Biomedical Technology Research Center, Department of Medical Technology, Faculty of Associated Medical Sciences, Chiang Mai University, Thailand
Mycoplasma specific primers	BioDesign, Thailand
Oil Red O	Amresco, Solon, Ohio, USA
Optimem® reduced serum medium	Gibco, Gran Island, N.Y., USA
Paraformaldehyde	Carlo Erba, Milan, Italy
Phorbol 12-myristate 13-acetate (PMA)	Sigma, St. Louis, MO, USA
Pierce™ BCA protein assay kit	Thermo Scientific, Rockford, USA
Polyoxyethylenes orbitan monolaurate – (Tween 20)	Scharlau Chemie, S.A., Barcelona, Spain
Polyethylene glycol (PEG)	Sigma, St. Louis, MO, USA
Potassium chloride (KCl)	Carlo Erba, Milan, Italy
Potassium hydrogen carbonate (KHCO$_3$)	Carlo Erba, Milan, Italy
Potassium hydrogen phosphate (KH$_2$PO$_4$)	Carlo Erba, Milan, Italy
Rosewell Park Memorial Institute – 1640 medium (RPMI)	Gibco, Gran Island, N.Y., USA
Serum-free media for hybridoma – culture (ISF-1)	Biochrom AG, Berlin, Germany
Skim milk	Himedia, Mumbai, India
Sodium carbonate (Na$_2$CO$_3$)	Carlo Erba, Milan, Italy

Sodium chloride (NaCl)	Carlo Erba, Milan, Italy
Sodium heparin 158 USP units – blood collection tube	Becton Dickinson, USA
Sodium hydrogen carbonate (NaHCO$_3$)	Carlo Erba, Milan, Italy
Sodium hydrogen phosphate (NaH$_2$PO$_4$)	Carlo Erba, Milan, Italy
Sodium hydroxide (NaOH)	Carlo Erba, Milan, Italy
Sodium laurylsulfate (SDS)	Carlo Erba, Milan, Italy
Spectrum™ Spectra/Por™ dialysis – membrane 12,000 to 14,000 dalton – MWCO	Fisher Scientific, Sweden
SYBR Safe DNA Gel Stain	Thermo Fisher Scientific, Massachusettes, USA
3, 3', 5, 5;-Tetramethylbenzidine – substrate (TMB)	Merck, Darmstadt, Germany
N, N, N', N'-Tetramethyl – ethylenediamine (TEMED)	AppliChem, Damstadt, Germany
Thiobarbituric acid (TBA)	Acros Organics, New Jersey, USA
THP1, Human monocytic cell lines	Watchara Kasinrerk's lab, Biomedical Technology Research Center, Department of Medical Technology, Faculty of Associated Medical Sciences, Chiang Mai University, Thailand
10 cm diameter tissue culture dish	SPL Life Science, Gyeonggi-do, Korea
Tris (hydroxymethyl) aminomethane	Vivantis, Malaysia

Tris (hydroxymethyl) aminomethane – hydrochloride	Acros Organics, New Jersey, USA
Tri-sodium citrate	Carlo Erba, Milan, Italy
Triton X-100®	USB Corporation, Cleveland, OH, USA
Trizol™ reagent	Invitrogen, Thermo Scientific, USA
0.4% Trypan blue	Gibco, Gran Island, N.Y., USA
U937, Human monocytic cell lines	Watchara Kasinrerk's lab, Biomedical Technology Research Center, Department of Medical Technology, Faculty of Associated Medical Sciences, Chiang Mai University, Thailand
Very low density lipoprotein, human – (VLDL)	Abcam, England
Viva cDNA synthesis kit	Vivantis, Selangor Darul Ehsan, Malaysia
6-wells tissue culture plate	SPL Life Science, Gyeonggi-do, Korea
12-wells tissue culture plate	SPL Life Science, Gyeonggi-do, Korea
96-wells ELISA plate	Nunc, Denmark
Whatman filter paper – (diameter 90 mm, 0.45 µm pore size)	GE Healthcare, Uppsala, Sweden

APPENDIX B

LIST OF INSTRUMENT USED IN THIS STUDY

Instruments	Source
AKTA start protein purification system	GE Healthcare, Uppsala, Sweden
Automatic high pressure autoclave – Hirayama	Artisan Technology Group, USA
Autopipettes for tissue culture	Thermo Scientific, USA
Autopipettes – Research plus	Eppendorf, Germany
Biohazard safety cabinet class II	ESCO, Singapore
Brushless microcentrifuge	Denvile Scientific, Canada
CO_2 incubator – Forma series II water jacket	Thermo Scientific, USA
Electrophoresis and electrotransfer unit	Cosmo Bio, Tokyo, Japan
Fluorescent inverted light microscope – IX51	Olympus, Japan
Gene Amp PCR System – 9700	Applied Biosystems, Singapore
Hemacytometer – Neubauer improved bright line	Marien Feld, Germany
Himac compact refrigerated centrifuge – RXII series	Hitachi, Japan
Hypercassette for Western Blot	Amersham, Buckinghamshire, England

Inverted light microscope – CKX41	Olympus, Japan
LightCycler®480 Real-Time PCR system	Roche Diagnostics, Mannheim, Germany
Light microscope – CX21	Olympus, Japan
Microplate spectrophotometer	BIO-RAD, USA
Multichannel pipette – ACURA855	Socorex, Switzerland
Multichannel pipette for tissue culture	Biohit, Finland
Nanodrop spectrophotometer – ND 1000	Thermo Scientific, USA
pH meter	Satorius, Germany
Rapid-Flow sterile disposable bottle top filters with PES membrane - Nalgene	Thermo Fisher Scientific, Rochester, N.Y., USA
Refrigrated microcentrifuge – 5415R	Eppendorf, Germany
Rocking shaker, Rockel II model 260350	Boekel Scientific, Pensylvania
Rotator	Fine PCR, Korea
Sodium Dodecyl Sulfate – Poly Acrylamide Gel Electrophoresis (SDS-PAGE) apparatus	BIO-RAD, USA
Spectronic spectrophotometer – Genesys 20	Thermo Fisher Scientific, USA
Trans-blot semi-dry transfer cell	BIO-RAD, USA
Ultra-sonicator	Crest, Pensylvania
Versatile refrigerated centrifuge – CT15RT	Techcomp, Kowloon, Hong Kong

APPENDIX C

REAGENTS AND BUFFER PREPARATION

1. Reagents for human blood cells and cell lines culture

1.1 Incomplete Isocove's modified dulbecco's (IMDM) medium

IMDM powder	1 pack
NaHCO$_3$	3.024 g
Gentamycin (40 mg/ml)	1 ml

Dissolve in deionized water and adjust volume to 1,000 ml

Filtrate through 0.2 μm membrane filter

Add Fungizone (250 μg/ml)   1 ml

Determine the sterility before use and store at 4°C

1.2 Complete IMDM medium

Incomplete IMDM medium	90 ml
Heat inactivated fetal bovine serum	10 ml

Determine the sterility before use and store at 4°C

1.3 0.6% 2-Mercaptoethanol (2-ME)

Incomplete IMDM medium	5 ml
2-Mercaptoethanol	30 μl

Aliquot to 50 μl/tube and store at -20°C

1.4 HAT (Hypoxanthine-Aminopterin-Thymidine) medium

Incomplete IMDM medium	78 ml
Heat inactivated FBS	10 ml
BM condimed H1	10 ml
0.6% 2-ME	30 µl
50X HAT	2 ml

Determine the sterility before use and store at 4°C

1.5 HT (Hypoxanthine-Thymidine) medium

Incomplete IMDM medium	118 ml
Heat inactivated FBS	15 ml
BM condimed H1	15 ml
0.6% 2-ME	30 µl
50x HT	2 ml

Determine the sterility before use and store at 4°C

1.6 Hypotonic solution for red blood cells lysing (0.084% NH_4Cl)

NH_4Cl	0.829 g
$KHCO_3$	0.1 g
EDTA	0.0037 g
Deionized water	90 ml

Adjust pH to 7.2 with HCl

Adjust volume to 100 ml by deionized water

Filtrate through 0.2 µm membrane filter

1.7 Turk's solution

Glacial acetic acid   3 ml

1% Gential violet   1 ml

Adjust volume to 100 ml by deionized water

Filtrate through 0.45 µm filter paper

1.8 Freezing medium (10% DMSO in 25% FBS-IMDM)

Incomplete IMDM medium   65 ml

Heat inactivated FBS   25 ml

DMSO   10 ml

Filtrate through 0.2 µm membrane filter

Determine the sterility before use and store at 4°C

1.9 Incomplete RPMI-1640 medium

RPMI powder   1 pack

NaHCO$_3$ 2 g

Gentamycin (40 mg/ml)   1 ml

Dissolve in deionized water and adjust volume to 1,000 ml

Filtrate through 0.2 µm membrane filter

Add Fungizone (250 µg/ml)   1 ml

Determine the sterility before use and store at 4°C

1.10 Complete RPMI-1640 medium

IncompleteRPMI-1640 medium 90 ml

Heat inactivated fetal bovine serum 10 ml

Determine the sterility before use and store at 4°C

1.11 Optimem$^®$ reduced serum medium

Optimem$^®$ powder 1 pack

NaHCO$_3$ 2.4 g

Gentamycin (40 mg/ml) 1 ml

Dissolve in deionized water and adjust volume to 1,000 ml

Filtrate through 0.2 μm membrane filter

Add Fungizone (250 μg/ml) 1 ml

Determine the sterility before use and store at 4°C

2. Reagents for Enzyme-linked immunosorbent assay (ELISA)

2.1 Coating buffer (0.1 M carbonate-bicarbonate buffer pH 9.6)

Na$_2$CO$_3$ 1.06 g

NaHCO$_3$ 1.26 g

H$_2$O 200 ml

Mix and adjust pH to 9.6 with concentrated HCl

Adjust final volume to 250 ml with deionized water

Store at 4°C

2.2 0.05% Tween-PBS

PBS pH 7.2	500 ml
Tween 20	250 µl

Mix and store at RT

2.3 Blocking solution (2% skim milk-PBS)

Skim milk	2 g
PBS pH 7.2	100 ml

Freshly prepare before use

2.4 Stop reaction solution (1N HCl)

Concentrated HCl	8.3 ml
H_2O	91.7 ml

Slowly dropwise HCl to H_2O

Store at RT

2.5 10X Phosphate buffer saline (PBS) pH 7.2

NaCl	80 g
KCl	2 g
Na_2HPO_4	11.5 g
KH_2PO_4	2 g
H_2O	700 ml

Adjust pH to 7.2 with NaOH or HCl

Adjust volume with H_2O to	1,000 ml

2.6 1X PBS pH 7.2

10x PBS pH 7.2	100 ml
H_2O	900 ml

Store at RT

3. Reagents for Sodium Dodecyl Sulfate – Poly Acrylamide Gel Electrophoresis (SDS-PAGE)

3.1 1.5 M Tris-HCl pH 8.8

Tris-base	9.08 g
H_2O	20 ml
Adjust pH to 8.8 with HCl	
Adjust volume with H_2O to	50 ml

Store at 4°C

3.2 0.5 M Tris-HCl pH 6.8

Tris-base	3 g
H_2O	25 ml
Adjust pH to 6.8 with HCl	
Adjust volume with H_2O to	50 ml

Store at 4°C

3.3 30% Monomer (30.8% acrylamide, 2.7% bis-acrylamide)

Acrylamide	15 g
Bis-acrylamide	0.4 g

H$_2$O to	50 ml

Filtrate through 0.45 µm filter paper

Store in dark at 4°C

3.4 10X Running buffer

Glycine	144.13 g
Tris-base	30.28 g
SDS	10 g
H$_2$O to	1,000 ml

Store at RT

3.5 1X Running buffer

10X Running buffer	100 ml
H$_2$O	900 ml

Store at RT

3.6 10% Ammonium persulfate (APS)

Ammonium persulfate	0.05 g
H$_2$O	0.5 ml

Mix well, aliquot to 100 µl/tube, and store at -20°C

3.7 10% Sodium dodecyl sulfate (SDS)

SDS	0.1 g
H_2O	1 ml

Mix well, aliquot to 150 µl/tube, and store at -20^oC

3.8 Stacking gel (4% gel, 0.125 M Tris pH 6.8)

H_2O	1.5 ml
0.5 M Tris-HCl pH 6.8	625 µl
Acrylamide/bis (30.8%/2.7%)	332.5 µl
10% SDS	25 µl
10% APS	12.5 µl
TEMED	5 µl
Total volume	2.5 ml

3.9 Resolving gel (10% gel, 0.375 M Tris pH 8.8)

H_2O	4 ml
1.5 M Tris-HCl pH 8.8	2.5 ml
Acrylamide/bis (30.8%/2.7%)	3.3 ml
10% SDS	100 µl
10% APS	50 µl
TEMED	10 µl
Total	10 ml

3.10 10X non-reducing buffer (NRB)

H_2O	1.25 ml
1 M Tris-HCl pH 6.8	0.625 ml
Glycerol	1 ml
10% SDS	2 ml
1% Bromophenol blue	125 μl

Aliquot to 300 μl/tube and keep at -20°C

3.11 5X reducing buffer (RB)

10X NRB	250 μl
2-ME	25 μl
H_2O	225 μl

Aliquot to 100 μl/tube and keep at -20°C

3.12 0.025% Coomassie brilliant blue R250 (40% methanol; 7% acetic acid)

Coomassie brilliant blue R250	0.25 g
Methanol	400 ml
Glacial acetic acid	70 ml
Add H_2O to	1,000 ml

Mix well until dissolve and store at RT

3.13 De-staining gel solution I (40% methanol, 7% acetic acid)

Methanol	400 ml
Glacial acetic acid	70 ml
Add H$_2$O to	1,000 ml

Mix well until dissolve and store at RT

3.14 De-staining gel solution II (5% methanol, 7% acetic acid)

Methanol	50 ml
Glacial acetic acid	70 ml
Add H$_2$O to	1,000 ml

Mix well until dissolve and store at RT

4. Reagents for Western blot

4.1 Towbin buffer (25 mM Tris; 192 mM Glycine; 20%Methanol)

Tris-base	3.03 g
Glycine	14.4 g
Methanol	200 ml
Adjust volume with H$_2$O to	1,000 ml

Mix well until dissolve and store at RT

4.2 5% Skim milk

Skim milk	2.5 g
1X PBS pH 7.2	50 ml

Mix well until dissolve (Freshly prepare before use)

4.3 0.1% Tween-PBS

Tween 20   0.5 ml

1x PBS pH 7.2   500 ml

Mix well and store at RT

4.4 Chemiluminescent substrate

    4.4.1 Luminol

    3-Aminophthalhydrazide   0.02214 g

    DMSO   500 μl

    Mix well until dissolve by vortexing

    Add 0.1 M Tris-HCl pH 8.8 to   50 ml

    90 mM p-coumaric acid   220 μl

    Store in dark at $4^{o}C$

        4.4.1.1 0.1 M Tris-HCl pH 8.8

        1.5 M Tris-HCl pH 8.8   10 ml

        H_2O 140 ml

        Mix well and store at $4^{o}C$

        4.4.1.2 90 mM p-coumaric acid

        p-coumaric acid   0.0369 g

        DMSO   2.5 ml

        Mix well until dissolve and aliquot into 230 μl per tube

        Store at $-20^{o}C$

4.4.2 Hydrogen peroxide (H_2O_2)

6% H_2O_2	153 µl
0.1 M Tris-HCl pH 8.8 to	50 ml

Store at RT

4.5 Film developing solution

Stock solution (Carestream, U.S.A.)	100 ml
H_2O	400 ml

Store in dark at RT (be able to reuse until the color changes to dark tan)

4.6 Film fixative solution

Stock solution (Carestream, U.S.A.)	100 ml
H_2O	400 ml

Store in dark at RT (be able to reuse until the color is getting brown)

5. Reagents for immunoglobulin G purification

5.1 Binding buffer (20 mM Sodium phosphate; pH 7.0)

1M Na_2HPO_4	11.56 ml
1M NaH_2PO4	8.4 ml
H_2O	800 ml

Adjust pH to 7.0 with 1N HCl

Adjust volume with H_2O to	1,000 ml

Filtrate through 0.45 µm Whatman filter paper (GE Healthcare, Uppsala, Sweden) and degas by sonication before use

5.1.1 1M Na_2HPO_4

Na_2HPO_4	2.84 g
H_2O	20 ml

5.1.2 1M NaH_2PO_4

NaH_2PO_4	2.76 g
H_2O	20 ml

5.2 Elution buffer (0.1M Glycine pH 2.7)

Glycine	0.7506 g
H_2O	50 ml

Adjust pH to 2.7 with 1N HCl

Adjust volume with H_2O to	100 ml

Filtrate through 0.45 µm Whatman filter paper (GE Healthcare, Uppsala, Sweden) and degas by sonication before use

Store at RT

5.3 Neutralizing buffer (1M Tris-HCl pH 9.0)

Tris-base	6.05 g
H_2O	20 ml

Adjust pH to 9.0 with 1N HCl

Adjust volume with H_2O to	50 ml

Store at RT

5.4 20% Ethanol

Absolute ethanol	200 ml
H_2O	800 ml

Filtrate through 0.45 µm Whatman filter paper (GE Healthcare, Uppsala, Sweden) and degas by sonication before use

Store at RT

6. Reagents for immunoglobulin M purification

6.1 Binding buffer (20 mM Sodium phosphate, 0.8 M $(NH_4)_2SO_4$, pH 7.5)

$NaH_2PO_4.H_2O$	2.76 g
$(NH_4)_2SO_4$	105.71 g
H_2O	800 ml
Adjust pH to 7.5	
Adjust volume with H_2O to	1,000 ml

Filtrate through 0.45 µm Whatman filter paper (GE Healthcare, Uppsala, Sweden) and degas by sonication before use

Store at RT

6.2 Elution buffer (20 mM Sodium phosphate pH 7.5)

$NaH_2PO_4.H_2O$	2.76 g
H_2O	800 ml
Adjust pH to 7.5	
Adjust volume with H_2O to	1,000 ml

Filtrate through 0.45 μm Whatman filter paper (GE Healthcare, Uppsala, Sweden) and degas by sonication before use

Store at RT

6.3 Regeneration buffer (20 mM Sodium phosphate, 30% Isopropanol)

$NaH_2PO_4.H_2O$	2.76 g
Isopropanol	300 ml
H_2O	500 ml
Adjust pH to 7.5	
Adjust volume with H_2O to	1,000 ml

Filtrate through 0.45 μm Whatman filter paper (GE Healthcare, Uppsala, Sweden) and degas by sonication before use

Store at RT

7. Reagent for LDL precipitation using heparin/citrate pH 5.04

7.1 Heparin citrate pH 5.04

Trisodium citrate	1.882 g
Heparin (5000 IU/ml)	1 ml
Adjust pH to 5.04	
Adjust volume with H_2O to	100 ml

Store at RT

8. Reagents for gelatin zymography

8.1 Resolving gel (7.5% SDS-PAGE contains 0.2% gelatin)

0.5 % gelatin	4 ml
H_2O	840 µl
1.5 M Tris-HCl pH 8.8	2.5 ml
Acrylamide/bis (30.8/2.7)	2.5 ml
10% SDS	100 µl
10% APS	50 µl
TEMED	10 µl
Total	10 ml

8.2 0.5% Gelatin

Gelatin	0.1 g
H_2O	20 ml

Heat at $60^{o}C$ for 20 min

Cool down at temperature before used

8.3 Stacking gel (4% gel, 0.125 M Tris pH 6.8)

H_2O	1.5 ml
0.5 M Tris-HCl pH 6.8	625 µl
Acrylamide/bis (30.8%/2.7%)	332.5 µl
10% SDS	25 µl
10% APS	12.5 µl
TEMED	5 µl

Total volume	2.5 ml

8.4 Re-nature buffer (2.5% V/V Triton X-100[®])

Triton X-100[®]	2.5 ml
Add H_2O to	100 ml

Store at RT

8.5 Activation buffer (50 mM Tris-HCl, 0.15 M NaCl, and 10 mM CaCl₂)

Tris-HCl	7.878 g
NaCl	8.766 g
$CaCl_2$	1.11 g
Dissolve in H_2O and add H_2O to	1,000 ml

Store at RT

9. Reagents for agarose gel electrophoresis

9.1 50X TAE buffer (0.04 M Tris-base, 0.002 M EDTA, and 0.02 M Acetic acid)

Tris-base	242 g
Disodium EDTA	18.61 g
Glacial acetic acid	57.1 ml
Add H_2O to	1,000 ml

Store at RT

9.2 1X TAE buffer

50X TAE buffer	20 ml
H_2O	980 ml

Store at RT

9.3 1% Agarose gel

Agarose	0.3 g
Add 1X TAE buffer to	30 ml

Melt until agarose well dissolve using microwave

Cool down at RT

Add SYBR green	1 μl

Pour the mixture into the gel cassette, place the combs, and let the gel polymerize at RT

10. Reagents for LDL oxidation

10.1 Stock $CuSO_4$ solution (1M $CuSO_4$)

$CuSO_4$	0.16 g
1X PBS pH 7.2	1 ml

Dissolve by vortexing

10.2 Working $CuSO_4$ solution (100 μM $CuSO_4$)

1 M $CuSO_4$	0.5 μl
1X PBS pH 7.2 to	5 ml

Freshly prepare before use

11. Reagents for Thiobarbituric Acid Reactive Substances (TBARS) assay

11.1 25% Acetic acid

Gracial acetic acid	25 ml
H_2O to	100 ml

Store at RT

11.2 1% Thiobarbituric acid (TBA)

TBA	0.1 g
H_2O to	10 ml

Freshly prepare before use

12. Reagents for Oil Red O staining

12.1 1% Paraformaldehyde

Paraformaldehyde	1 g
1X PBS pH 7.2	80 ml

Heat at $56^{o}C$ until dissolve

Add 1 drop of 1N NaOH

Add 1X PBS pH 7.2 to	100 ml

Filtrate through 0.45 μm filter paper and store at RT

12.2 0.1% Paraformaldehyde

1% Paraformaldehyde	1 ml
1X PBS pH 7.2	9 ml

Store at RT

12.3 60% Isopropanol

Isopropanol	60 ml
H_2O	40 ml

Store at RT

12.4 0.5% Oil Red O stock solution

Oil Red O	0.5 g
Isopropanol to	100 ml

Filtrate through 0.45 µm filter paper and store at RT
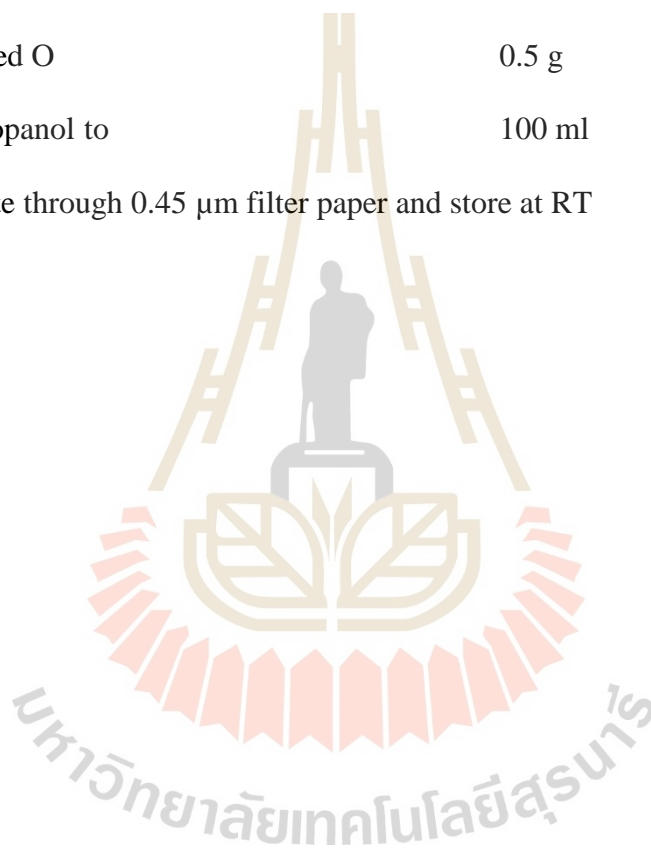
CURRICULUM VITAE

PERSONAL DATA:

Name	:	Miss Kanokwan Lowhalidanon
Date of birth	:	May 8, 1989
Nationality	:	Thai
Current address	:	School of Chemistry,
		Institute of Science,
		Suranaree University of Technology
		Nakhon Ratchasima, 30000,
		Thailand,
		Tel. +66-884936395, +66-44223954
		E-mail: k.lowhalidanon@gmail.com

SCHOLARSHIP:

2011	:	Student fee exemption scholarship from One Research One Graduate student (OROG) Grant, Suranaree University of Technology